Discovery and characterization of an anti-inflammatory lipid derived from *Mycobacterium vaccae*

By

David G. Smith

B.S., The Ohio State University, 2010

A thesis submitted to the

Faculty of the Graduate School

of the University of Colorado in partial fulfillment

of the requirement for the degree of

Doctor of Philosophy

Department of Chemistry and Biochemistry

2017

This thesis entitled:

Discovery and characterization of an anti-inflammatory lipid derived from *Mycobacterium vaccae*

written by David G. Smith

has been approved by the Department of Chemistry and Biochemistry

_____

Christopher A. Lowry, PhD

_____

Dylan J. Taatjes, PhD

Date_____

The final copy of this thesis has been examined by the signatories, and we find that both the content and the form meet acceptable presentation standards of scholarly work in the above-mentioned discipline.

Smith, Gregory David (PhD, Chemistry and Biochemistry)

Discovery and characterization of an anti-inflammatory lipid derived from *Mycobacterium vaccae*

Thesis directed by Christopher A. Lowry, PhD.

In modern urban environments there is an increased prevalence of allergies, asthma, inflammatory bowel diseases (IBD), and anxiety disorders. The underlying cause for these disorders, as postulated by the Hygiene Hypothesis, is chronic inflammation, and the imbalance in the immune system is caused by a lack of interaction with microbes that have been removed from the urban space and lifestyle. One such microbe is the environmental saprophyte, *Mycobacterium vaccae*. In animal models, immunization with *M. vaccae* protects against the development of these prevalent inflammatory disorders. This immunoregulatory effect has been shown to occur due to the expansion of regulatory T cells, but it is still unclear how *M. vaccae* is interacting with the immune cells.

To better understand the mechanisms of immune suppression, we screened secreted molecules and whole cell preparations for anti-inflammatory properties. We were able to isolate and determine the structure of a single fatty acid, 10(*Z*)-hexadecenoic acid. The fatty acid was an effective immunosuppressant both *in vivo* in a murine model of allergic asthma, and *ex vivo*, as observed by decreased release of proinflammatory cytokines, like interleukin-5 from splenocytes.

We next investigated how the anti-inflammatory effects are achieved using macrophages as a model system. The mRNA transcriptional profile of macrophages treated with 10(*Z*)-

hexadecenoic acid suggested that peroxisome proliferator-activated receptor (PPAR)α was mediating the effects. It was subsequently confirmed, using transfection assays, that 10(*Z*)-hexadecenoic acid increases PPARα signaling. Furthermore, PPARα was demonstrated to be necessary for the anti-inflammatory effects, as a PPARα antagonist blocked the effects of 10(*Z*)-hexadecenoic acid, and 10(*Z*)-hexadecenoic acid had no effect in macrophages isolated from PPARα$^{-/-}$ mice.

Collectively, these data define 10(*Z*)-hexadecenoic acid as an immunosuppressant metabolite that may contribute to the immunomodulatory effects of *M. vaccae* immunization. Furthermore, to our knowledge, 10(*Z*)-hexadecenoic acid is not synthesized *de novo* in mammals, and its biosynthesis appears to be unique to mycobacteria.. This is also the first instance where a *Mycobacterium* or *Mycobacterium*-derived molecule has been shown to have anti-inflammatory effects mediated through PPARα.

Acknowledgements

I am grateful to many people for the opportunity to train as a scientist. Throughout my life, my family has been extremely supportive of my academic career. My mother has been a huge inspiration and has always been there through the emotional ride of this process. Even during my graduate career, I sought her writing advice. My father is also instrumental in where I am today. Since my childhood, he strived to make science fun and interesting and is the reason I love problem solving. Lastly, my wife, Monica, has been absolutely necessary through my training. She has made me a more passionate, driven, proud person. I know I can always rely on her support.

I am thankful to Chris for allowing me to train in his lab—which was especially generous since it is a lab outside the department. I am continually impressed with the breadth of Chris' knowledge. He is creative and truly inspirational. My research has taken me in a lot of challenging directions, and Chris was there leading and learning with me. The science has been a lot of fun, which has made everything so much more rewarding. When the science wasn't super fun, or I had my moments of fear and anxiety, he always knew what to say or do to make me feel better. He has cultivated the greatest lab environment I have ever experienced. I am thankful for all the past and current lab members and am very fortunate to have found such great friendships among them.

I would also like to thank all my other committee members: Dylan Taatjes, Hubert Yin, Xuedong Liu, and Robin Dowell. I faltered and struggled some my first year, so I am very grateful that they accepted the responsibility of guiding me. They have all taught me so much.

The course of this PhD has had me scrambling all over campus. At various points I have received help, resources, or guidance from the Fleshner lab, Seals lab, Palmer lab, Jinsen Chen, Annette Erbse, and Jamie Kershner. Robin Dowell and Mary Allen have been very generous with their time and literally taught me everything I know about RNA-seq. Mary was with me at the lab bench watching every single pipette transfer. She showed me all the tips and tricks that are not included in the protocols. During the buggy process of analyzing the data, she and Robin were always around to get their hands dirty too.

I owe so much to all the talented collaborators I have been able to work with. Xiang Wang's lab seeded most of this work by synthesizing our lipid. From Jon Clardy's group, Alexandra was an excellent partner to have while screening mycobacteria. I would also like to thank Del Besra's lab and Laura Rosa Brunet's lab for their excellent collaborations. Del and his student, Petr Illarionov, were invaluable for synthesizing the lipids, and László Nagy for running the PPAR reporter gene assays, and thanks to Laura's student, Roberta Martinelli, who ran the *in vivo* mouse allergy models.

Finally, I would like to thank the funding sources that made this work possible including gifts through the CU Foundation. I'm also grateful for the various awards and competitions offered by the University of Colorado Boulder, which have afforded me to purchase necessary reagents and equipment.

Table of Contents

Chapter 1: Introduction 1

1.1 The Hygiene Hypothesis 1

1.1.1 The “Old Friends” Hypothesis 3

1.1.2 Immunoregulatory mechanisms of “Old Friends” 4

1.2 *Mycobacterium vaccae* 7

1.3 LPS signaling in macrophages 9

Chapter 2. Suppression of airway allergic inflammation by a novel bacterially-derived lipid isolated from *Mycobacterium vaccae* 12

2.1 Introduction 12

2.1.1 The hygiene hypothesis and inflammatory disease 12

2.1.2 The mycobacterial cell wall and therapeutic applications 13

2.2 Materials and methods 18

2.2.1 Animals 18

2.2.2 Mycobacterium vaccae 18

2.2.3 Isolation of the lipids 19

2.2.4 Synthesis of triacylglycerol 20

2.2.5 Synthesis of 10(*Z*)-hexadecenoic acid; (10*Z*)-hexadec-10-enoic acid (CAS No. 2511-97-9) 22

2.2.6 Thp1 cell assay 24

2.2.7 Murine model of allergic pulmonary inflammation: prevention studies 24

2.2.8 Murine model of allergic pulmonary inflammation: treatment studies 25

2.2.9 Ex vivo splenocyte culture 25

2.2.10 Murine peritoneal macrophage isolation and screening 26

2.2.11 Dynamic light scattering of lipid micelles 27

2.2.12 Lipid extraction 27

2.2.13 Cytokine measurements 28

2.2.14 Cytotoxicity assay 28

2.2.15 Ligands 28

2.2.16 Statistical analysis 29

2.3 Results 29

2.3.1 Pretreatment with an aqueous methanol extraction of *M. vaccae* reduces allergic pulmonary inflammation 31

2.3.2 Specific fractions of the mycobacterial extract are anti-inflammatory *in vitro* 32

2.3.3 The anti-inflammatory component of the fraction is a triglyceride 34

2.3.4 The triglyceride, 1,2,3-tri[*Z*-10-hexadecenoyl]glycerol, has therapeutic potential in a mouse model of pulmonary allergic inflammation 35

2.3.5 The free fatty acid, 10(*Z*)-hexadecenoic acid, has therapeutic potential in a mouse model of pulmonary allergic inflammation 39

2.3.6 Physical properties of 10(*Z*)-hexadecenoic acid 40

2.3.7 10(*Z*)-hexadecenoic acid prevents LPS-induced secretion of IL-6 in macrophages 42

2.4 Discussion 45

Chapter 3. Anti-inflammatory effects of 10(*Z*)-hexadecenoic acid are dependent on PPARα 51

3.1 Introduction 51

3.1.1 Bioactive lipids and lipid receptors 51

3.2 Materials and methods 55

3.2.1 Animals 55

3.2.2 10(*Z*)-hexadecenoic acid 55

3.2.3 Macrophage stimulation assay 56

3.2.4 Cytokine ELISA 57

3.2.5 RNA extraction and library preparation 57
3.2.6 Sequencing 58
3.2.7 RNA read processing, mapping, and differential expression 58
3.2.8 Pathway analysis 59
3.2.9 Transfections and reporter gene assays 59
3.2.10 Pharmacologic inhibition of PPARs 59
3.2.11 Statistical analysis 60
3.3 Results 60
3.3.1 10(*Z*)-hexadecenoic acid suppresses LPS-induced inflammation 60
3.3.2 10(*Z*)-hexadecenoic acid activates PPARα 72
3.3.3 Anti-inflammatory effects of 10(*Z*)-hexadecenoic acid are dependent on PPARα 74
3.4 Discussion 78
Bibliography 85
Appendix 1. *In vitro* cell-based assay for identification of anti-inflammatory *M. vaccae*-derived small molecules 102
A1.1 Introduction 102
A1.1.1 Natural product chemistry 102
A1.1.2 *M. vaccae* 103
A1.2 Materials and methods 104
A1.2.1 Animals 104
A1.2.2 Growing M. vaccae 104
A1.2.3 Extraction and separation of culture supernatants 105
A1.2.4 Macrophage bioassay 105
A1.3 Results 106

A1.3.1 Advanced screening 106
A1.4 Discussion 110
Appendix 2: Evolution of nonpathogenic Mycobacterium: A Pan-genomic study 113
Appendix 3: RNA-Seq supplemental material 125

List of Figures

Figure 1.1 Increased prevalence of inflammatory disease. 2

Figure 1.2 Co-evolved mechanisms of immune suppression. 5

Figure 1.3 Graphical scheme of TLR4 signaling. 11

Figure 2.1 Arrangement and composition of mycobacterial cell wall and lipid structures. 16

Figure 2.2 Structures associated with the synthesis of the triacylglycerol, 1,2,3-tri[*Z*-10-hexadecenoyl]glycerol, isolated from extracts of *M. vaccae*. 22

Figure 2.3 Diagrammatic illustrations of experimental designs. 31

Figure 2.4 *M. vaccae* and *M. vaccae* fraction 148.2 reduce bronchopulmonary inflammation. .. 33

Figure 2.5 Synthetic triglyceride, 1,2,3-tri[*Z*-10-hexadecenoyl]glycerol, reduces bronchopulmonary inflammation. 37

Figure 2.6 Synthetic triglyceride 1,2,3-tri[*Z*-10-hexadecenoyl]glycerol has an anti-inflammatory effect on immune cells recovered by bronchoalveolar lavage (BAL) fluid and splenocytes. 38

Figure 2.7 *In vivo* screening of synthetic acyl chain length and isomer variations. 39

Figure 2.8 Critical micelle concentrations of 10(*Z*)-hexadecenoic acid. 41

Figure 2.9 Thin layer chromatography of macrophages treated with 10(*Z*)-hexadecenoic acid. . 42

Figure 2.10 Anti-inflammatory effects of 10(*Z*)-hexadecenoic acid in freshly-isolated murine peritoneal macrophages. 44

Figure 2.11 Macrophage cell viability assay. 45

Figure 3.1 Differential expression of 10(*Z*)-hexadecenoic acid-treated and vehicle-treated cells in the presence of LPS. 64

Figure 3.2 Summary of GSEA results enriched for LPS-stimulated macrophages pretreated with 10(*Z*)-hexadecenoic acid. 68

Figure 3.3 Summary of GSEA results enriched for vehicle (“DMEM”) pretreatment of LPS-stimulated macrophages. 70

Figure 3.4 Network visualizations of related gene set enrichments. 72

Figure 3.5 Analysis of the effects of M. vaccae-derived lipids on PPARα, PPARγ, PPARδ, and RARα signaling in transfection assays using COS-1 cells. 74

Figure 3.6 PPARα antagonist blocks anti-inflammatory effects of 10(Z)-hexadecenoic acid. 76

Figure 3.7 PPARα is necessary for anti-inflammatory effects of 10(*Z*)-hexadecenoic acid. 78

Figure A1.1 Anti-inflammatory activity of fractionated *M. vaccae* extractions..... 108

Figure A1.2 Anti-inflammatory activity of fractionated *M. vaccae* E3 fraction. 108

Figure A2.1 Pangenome size. 117

Figure A2.2 Phylogenetic clustering of *Mycobacterium* genomes based on proteome..... 118

Figure A2.3 Genome synteny among mycobacteria..... 121

Figure A2.4 Circular plot of genomic islands in *M. vaccae*. 124

List of Tables

Table 2.1. Characterization of the cellular infiltrate in the lungs of allergic mice challenged intratracheally with ovalbumin in *Experiment 2*. 32

Table 3.1. Proinflammatory cytokine and chemokine ligand mRNAs downregulated by preincubation of freshly isolated murine peritoneal macrophages with 10(*Z*)-hexadecenoic acid prior to stimulation with lipopolysaccharide 63

Table 3.2. Top 10 differentially expressed genes of freshly isolated murine peritoneal macrophages preincubated with 10(*Z*)-hexadecenoic acid prior to stimulation with lipopolysaccharide 65

Table 3.3. Selective PPAR antagonists and agonists. 75

Table A1.1. Masses and possible structures of fractions 25, 28, and 30 of EtOAc 3 109

Table A2.1. Summary of the 30 genomes used in the analysis 113

Table A3.1. Rank ordered list of most significant ($q < 0.1$) differentially expressed genes. 125

Table A3.2. Top scoring KEGG pathways enriched for differential expressed genes ($q < 0.1$). 128

Table A3.3. KEGG pathways and GO biological process with associated genes that are significantly downregulated in LPS-stimulated murine macrophages preincubated with 10(*Z*)-hexadecenoic acid. 130

List of Abbreviations

AA	arachidonic acid
AP-1	activator protein 1
APC	antigenantigen-presenting cell
CLA	conjugated linoleic acid
DC	dendritic cells
DLS	dynamic light scattering
FA	fatty acid
GPCR	G protein-coupled receptor
IBD	inflammatory bowel disease
IFNα	interferon α
IKK	inhibitor of κB kinase
IRAK	interleukin-1 receptor-associated kinase
IRF	IFN regulatory factor
IκB	inhibitor of κB
LCFA	longlong-chain fatty acid
LPS	lipopolysaccharide
MAPK	mitogen-activated protein kinase
MyD88	myeloid differentiation factor 88
NF-κB	nuclear factor κB
PPAR	peroxisome proliferator-activated receptor
SCFA	shortshort-chain fatty acid
STAT	signal transducer and activator of transcription
TAG	triacylglycerol
TAK1	transforming growth factor β-activated kinase 1
Th1	helper T cell type 1
Th17	helper T cell type 17
Th2	helper T cell type 2
TNF	tumor necrosis factor
Treg	regulatory T cell
TRIF	TIR-domain-containing adaptor protein inducing IFNβ
PRR	pattern recognition receptor
DC-SIGN	dendritic cell-specific intercellular adhesion molecule 3-grabbing non-integrin
IL	interleukin
s.c.	subcutaneous
TLR	toll-like receptor
mAGP	mycolylarabinogalactanmycolyl-arabinogalactan-peptidoglycan complex
PIM	phosphatidylmannosides
LM	lipomannan
LAM	lipoarabinomannan
manLAM	mannose capped LAM
BAL	bronchoalveolar lavage

Chapter 1: Introduction

1.1 The Hygiene Hypothesis

The Hygiene Hypothesis was first proposed in the late 1980s to explain the rise in allergic conditions (Strachan, 2000). Chronic inflammatory conditions, like allergies, are primarily driven by hyperactive helper T cell type 1 (Th1), helper T cell type 2 (Th2), and/or helper T cell type 17 (Th17). Epidemiological studies on the modern ways of life proposed that modern hygiene requirements were reducing contact with pathogens that prime immune responses. At that time, it was believed that a lack of Th1 stimulation would result in a compensatory increase in Th2 activity following exposure to more innocuous stimuli, as seen with allergic disorders. However, Th1-mediated disorders were also exploding in prevalence in the same countries in which allergy was on the rise (Bach, 2002b). Moreover, allergies are most common in inner cities, which was the most common setting for infections (i.e. Th1 stimulation)(Riedler et al., 2001). Most follow-up studies have failed to show an association between childhood infection and increased allergic conditions in the modern world(Benn et al., 2004; Bremner et al., 2008; Matricardi and Ronchetti, 2001).

Investigators have seen several categories of chronic inflammatory disorders become much more prevalent in developed countries (Bach, 2002a). The rising Th2-driven disorders include allergic disorders (asthma, hay fever), and Th1/Th17-driven disorders including some autoimmune diseases (for example, type 1 diabetes and multiple sclerosis) (Bach, 2002a) and inflammatory bowel diseases (IBD; ulcerative colitis and Crohn's disease) (Sawczenko et al., 2001). Several of these disorders have increased an average of 2- to 3- fold in industrialized

nations between 1950 and the present(Beasley et al., 1998; Eder et al., 2006; Gillespie et al., 2004; Sawczenko et al., 2001; Upton, 2000).

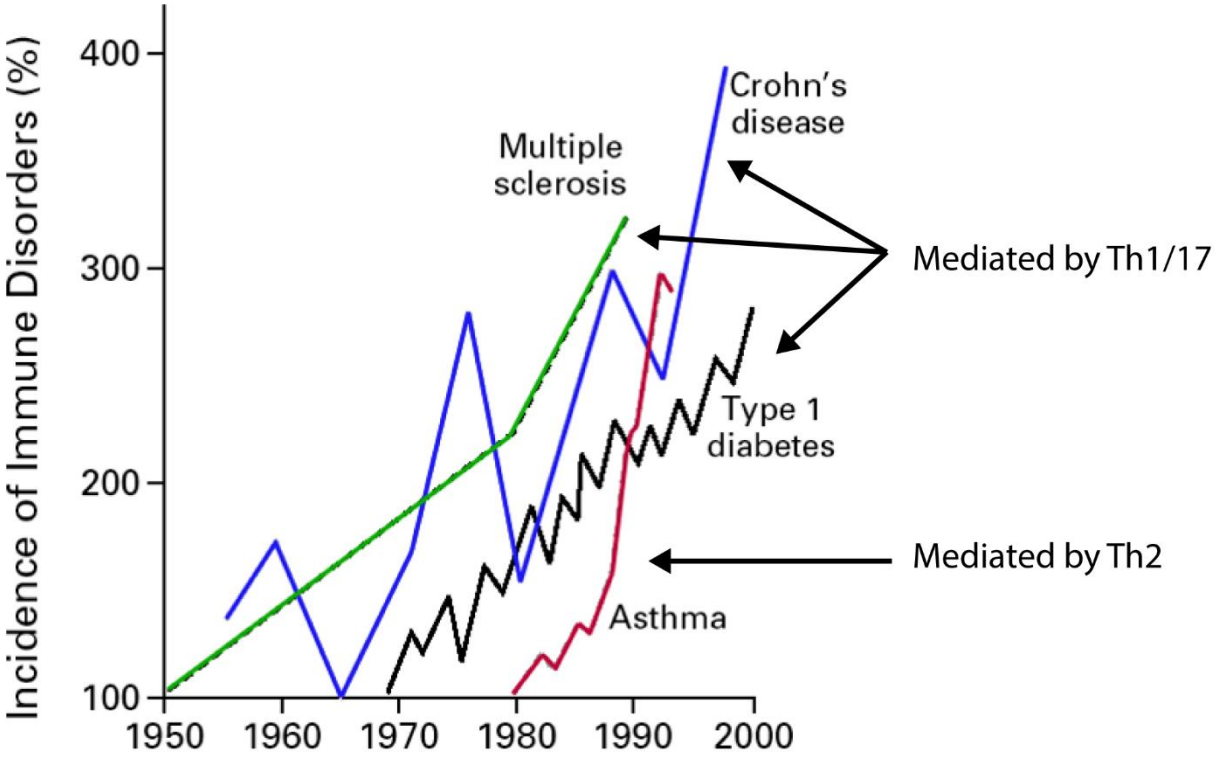

Figure 1.1 Increased prevalence of inflammatory disease.
The incidence of immune disorders in developed countries (United States and France) has increased over the past 50 years. Reproduced with permission from (Bach, 2002b), Copyright Massachusetts Medical Society.

The Hygiene Hypothesis suggests that some of this increased prevalence is the result of defective regulation of the immune system. Instead of microbes that drive Th1 responses, these conditions are likely resulting from diminished exposure to specific classes of microorganisms. Subsequent studies correlated protection from low-grade inflammatory disorders with exposure to cowsheds(Riedler et al., 2001), endotoxin(Braun-Fahrländer et al., 2002), helminths(Yazdanbakhsh et al., 2002) and lactobacilli(Bjorksten et al., 1999), thereby consolidating the view that microorganisms or their components were a crucial factor.

1.1.1 The "Old Friends" Hypothesis

The "Old Friends" hypothesis was proposed to emphasize that we no longer believe that exposure to childhood infections or outright pathogens per se is beneficial but rather that lack of exposure to symbiotic organisms, as well as the Old Infections, is harmful (Rook et al., 2004). Indeed, hygiene is important for the prevention of serious infections. In support of this hypothesis, germ-free mice, devoid of microorganisms, develop increased susceptibility to allergy (Cahenzli et al., 2013; Herbst et al., 2011; McCoy et al., 2006). Instead of a targeted expansion of any single helper T cell, there needs to be a balance of helper T cells and the cells that regulate inflammation, regulatory T cells (Treg). The "Old Friends" consist of a group of microorganisms that are necessary to maintain that balance, and they include (1) the symbiotic microbiota residing in the cutaneous and mucosal surfaces (e.g., surfaces of the upper airways, lungs, and gastrointestinal tract); (2) pathogens associated with the "Old Infections" (for example, helminths) that were present throughout life in evolving human hunter-gatherer populations; and (3) organisms from the natural environment with which humans were inevitably in daily contact through inhalation or ingestion (and so had to be tolerated by the immune system) (Rook et al.). One of the classic examples of the "Old Infections" is *H. pylori*, which is potently immunoregulatory and consequently has protective effects in allergy and chronic inflammatory disorders (Arnold et al., 2011, 2012). Environmental microorganisms have been referred to as "pseudocommensals" because they would have been present in large numbers throughout mammalian evolution, even if they do not colonize the gut(Rook and Lowry, 2009; Rook et al., 2004). Our understanding of the "Old Friends" hypothesis has been informed by studies using heat-inactivated and viable environmental bacteria, particularly soil-derived bacteria belonging to the genus *Mycobacterium*, which can be viewed as a case study of the

potential for environmental microorganisms to influence immunoregulatory circuits and prevent inflammatory disease (Zuany-Amorim et al., 2002a).

It was hypothesized that these organisms took on the role of training the immune system in tolerance because they themselves needed to be tolerated, either because they were harmless but ubiquitous in the external environment or because they provided essential services for their hosts, as is the case with probiotic gut flora (Collins and Bercik, 2009), or because, although not harmless, they are not eradicable by inflammatory processes, which therefore inflict tissue damage (Rook, 2009; Rook and Rosa Brunet, 2002).

1.1.2 Immunoregulatory mechanisms of "Old Friends"

The central idea of the "Old Friends" hypothesis was that, rather than provoking aggressive immune responses, these organisms cause maturation of regulatory dendritic cells (DCreg). These cells are similar to classical dendritic cells (DC), which present microbial antigens, but DCreg also secrete anti-inflammatory cytokines, like interleukin (IL)-10 and transforming growth factor beta (TGF-β)(King et al., 1993; Smits et al., 2005). When DCreg encounter T cells, they select for Treg differentiation rather than Th1 or Th2 cells(van der Kleij et al., 2002; Smits et al., 2005). This continuous background activation of regulatory DC (DCreg) and subsequent activation of Treg specific for the "Old Friends" themselves, resulted in constant background bystander suppression of inflammatory responses. Secondly, these DCreg inevitably sample self, gut contents and allergens, and so induce Treg cells specific for suppressing three groups of chronic inflammatory disorders (Th1-, Th2-, and Th17-driven). This hypothetical model is supported by clinical trials and experimental models in which exposure to "Old Friends" has treated allergy (Gutzwiller et al., 2007; Wilson et al., 2005; Zuany-Amorim et al.,

2002a), autoimmunity (Zaccone et al., 2009), or intestinal inflammation (Summers, 2005). Within this general scheme, there is a diverse and expanding set of mechanisms that "Old Friends" use to suppress inappropriate inflammation.

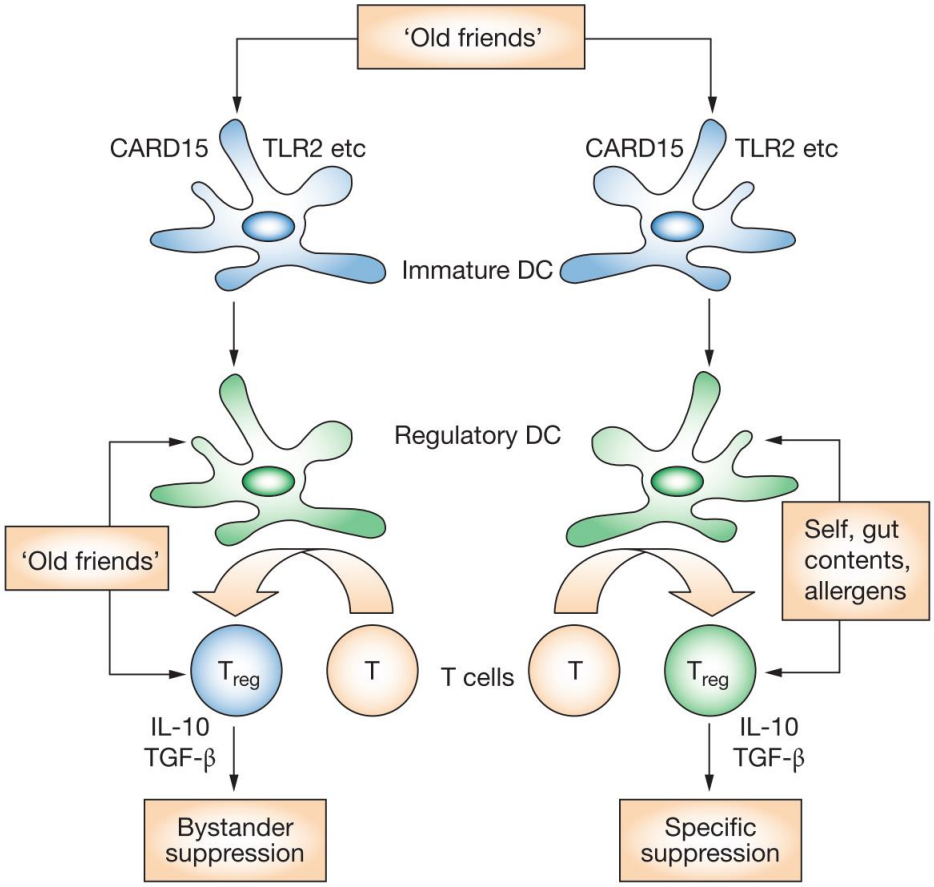

Figure 1.2 Co-evolved mechanisms of immune suppression.
'Old Friends' promote differentiation of regulatory DCs, which drive production of regulatory T cells. These endogenous mechanisms are thought to be involved in prevention of inflammatory disease, including autoimmune disorders and allergic disorders. Reproduced with permission from (Guarner et al., 2006), Copyright Macmillan Publishers Ltd.

A number of bacterial antigens have been identified that increase immunoregulatory circuits, predominantly by interactions with the pattern recognition receptor (PRR) dendritic cell-specific intercellular adhesion molecule 3-grabbing non-integrin DC-SIGN on DCs. DC-SIGN ligation

interferes with toll-like receptor-mediated inflammatory responses, resulting in decreases in nuclear factor kappa-light-chain-enhancer of activated B cell (NF-κB) signaling, decreases in IL-6, tumor necrosis factor (TNF), and IL-12, concurrently with increases in IL-10(Vergne et al., 2014). Activation of DC-SIGN in DCs may be a common mechanism through which bacterial antigens derived from the "Old Friends" gain entry into immune cells and ultimately bias T cell differentiation toward a Treg phenotype(Bergman et al., 2004; van Kooyk and Geijtenbeek, 2003; Vergne et al., 2014).

DCs and other antigen-presenting cells (APC), like macrophages, typically reside in the tissue surrounding the gastrointestinal tract or airways, which are the points of passage for "Old Friends". A separate step is necessary for APCs to make direct contact with the "Old Friends". This function is performed in part by microfold or membranous cells (M cells), which have been documented as entry sites for *M. tuberculosis* in mice (Teitelbaum et al., 1999). Similar reports have been made for M cell recognition of mycobacteria in the gastrointestinal tract (Fujimura, 1986). Once the microbe reaches an APC, it can subvert inflammatory responses with glycosylated or fucosylated antigens on the cell surface, which are recognized by the PRRs, like DC-SIGN (van Liempt et al., 2006).

Immune suppression can also be achieved through small molecules secreted by "Old Friends". Mycobacteria and other environmental bacteria are capable of tryptophan biosynthesis and metabolism, which allows them to generate tryptophan metabolites that activate the aryl hydrocarbon receptor. This results in immunoregulation and mucosal protection from damage (Zelante et al., 2013). Activation of aryl hydrocarbon receptor can either induce functional Treg

cells that suppress inflammation or enhance Th17 cell differentiation and increase inflammation, depending on the specific nature of the agonist (Mezrich et al., 2010; Quintana et al., 2008).

Short-chain fatty acids (SCFAs), including acetate, propionate, and butyrate, are produced by bacteria in the gut during fermentation of insoluble fiber from dietary plant matter (Sonnenburg et al., 2014). Of particular interest here, SCFAs have anti-inflammatory effects by regulating the release of cytokines and chemokines from immune cells(Cavaglieri et al., 2003; Meijerink et al., 2010; Tedelind et al., 2007). Importantly, propionate and acetate can directly induce colonic Tregs and their suppressive capacity via activation of G protein-coupled receptor (GPCR) 43, encoded by the free fatty acid receptor 2 gene (*Ffar2*) (Arpaia et al., 2013; Smith et al., 2013). This is one of the primary routes by which *Clostridia* affect Treg populations(Zeng and Chi, 2015). Furthermore, butyrate, which is also a metabolite of *Clostridia* species, potentiates DCs to induce Treg through inhibition of histone deacetylase (HDAC) and may induce epigenetic changes(Zeng and Chi, 2015).

1.2 *Mycobacterium vaccae*

M. vaccae is an environmental saprophyte, which is also distinguished from more notorious mycobacteria for being non-pathogenic. Among related pathogenic species is *M. tuberculosis*, the causative agent of tuberculosis. *M. tuberculosis* is able to be such a successful pathogen in part because it exhibits some of the immune subversion strategies of the "Old Friends". The infection is characterized by a decrease in Th1 and increase in Th2 responses(Ashenafi et al., 2014). Importantly, the low levels of Th1 activity prevent clearance of the bacterium. In early attempts of vaccination with attenuated strains of *M. tuberculosis*, researchers observed the balance of Th1/Th2 cells shift more towards Th1(Hernandez-Pando et al., 1997). This generated

interest to test other mycobacterial species as potential vaccines, such as *M. vaccae*, which was able to induce a shift towards a Th1 phenotype, the results varied depending on dosage and population(Hernandez-Pando et al., 1997; Stanford, 1999). Aside from the mixed efficacy as a vaccine, the bacterium's effects on the balance of Th1/Th2 cells inspired investigation in animal models of other Th2-mediated disorders.

In mice rendered allergic to ovalbumin (OVA), subcutaneous (s.c.) treatment with heat-killed *M. vaccae* prevented the development of allergen-induced bronchial inflammation as well as airway hyperresponsiveness(Zuany-Amorim et al., 2002b). Furthermore, the protective effects were independent of the Th1 cytokine, interferon gamma (IFN-γ). In a follow-up study the authors demonstrated that the characteristic influx of eosinophils following allergen challenge could be prevented with the adoptive transfer of splenocytes from *M. vaccae*-treated mice(Zuany-Amorim et al., 2002a). This specific inhibition was mediated through IL-10 and TGF-β, as antibodies against these cytokines reversed the effects. Thus, Treg generated by mycobacteria treatment may have an essential role in restoring the balance of the immune system. This potential mediating role of Tregs also has been observed in a stress-induced model of colitis, where the protective effects of *M. vaccae* can be reversed with pretreatment with anti-CD25 antibody. CD25 is a marker of CD4+FoxP3+ Treg (Reber et al., 2016). Lastly, treatment with heat-killed *M. vaccae* has been shown to induce the development of $CD11c^{+}$ APCs, which also have markedly increased expression of IL-10 and TGF-β (Adams et al., 2004). Together, these results suggest *M. vaccae* can generate regulatory APCs capable of inducing the production of allergen-specific Tregs that exert global immune stabilizing effects.

The role of APCs is likely to be the linchpin of *M. vaccae*-mediated immune suppression. Treatment with *M. vaccae* reduces the number of IL-4+ T cells in co-cultures of DCs and naïve CD4+ T cells compared to unstimulated cultures (Le Bert et al., 2011a). Furthermore, this effect was DC-dependent, and, through transcriptional profiling, it was determined that DC priming to inhibit Th2 responses is achieved through early activation of the cAMP response element-binding protein (CREB) pathway(Le Bert et al., 2011a).

1.3 LPS signaling in macrophages

Toll-like receptors (TLRs) are a group of receptors expressed on the surface of cells involved in the innate immune system. TLRs are strongly conserved, with most mammalian species containing between ten to fifteen TLRs (Janeway and Medzhitov, 2002). The function of these receptors is to recognize pathogen-associated molecular patterns (PAMPs), which are molecules broadly produced among pathogens and are often lipids, polysaccharides, or DNA. Each receptor is specialized for at least one PAMP, for example, TLR4 is activated by the characteristic endotoxin of gram-negative bacteria, lipopolysaccharide (LPS). There is a diverse set of PAMPs that stimulate TLRs, but the resulting signal transduction pathway and transcriptional response are very similar.

The cellular response to microbial PAMPs requires formation of a larger receptor complex that starts with the homo- or heterodimerization of TLRs. On the cytosolic side, TLRs interact with a family of five adaptor proteins, myeloid differentiation factor 88 (MyD88), MyD88-adaptor-like, TIR-domain-containing adaptor protein inducing IFNβ (TRIF), TRIF-related adaptor molecule, and sterile-alpha and armadillo-motif containing protein (O'Neill and Bowie, 2007). Depending on the TLR, signal transduction starts with either MyD88 or TRIF,

with the exception of the LPS sensor, TLR4, which signals through both (Hu et al., 2015). The downstream transcriptional response to TLR activation is mediated through activation of three major transcription factors: nuclear factor κB (NF-κB), activator protein 1 (AP-1), and interferon regulatory factors (IRFs) (Fig. 1.3). Upon the initial ligand binding event on TLR4, MyD88 accumulates at the intracellular domain, which recruits interleukin-1 receptor-associated kinases (IRAKs) 1,2 and 4 (Lin et al., 2010). The IRAK complex recruits TNF associated factor (TRAF) 6 leading to polyubiquitination of TRAF6 and IRAK 1/2 (Ferrao et al., 2012). The polyubiquitin chains allow transforming growth factor β-activated kinase 1 (TAK1) to dock to the complex and phosphorylate inhibitor of κB kinase (IKK) (Ferrao et al., 2012). The activated IKK, phosphorylates inhibitor of κB (IκB), leading to its degradation and liberation of NFκB (Napetschnig and Wu, 2013). NFκB controls transcription of many proinflammatory cytokines such as TNF, IL-1β, IL-6, and chemokines such as monocyte chemoattractant protein 1 and macrophage inflammatory protein 3α (Napetschnig and Wu, 2013). TAK1 also initiates a second kinase cascade through activation of extracellular-signal related kinase, c-jun N terminal kinase and p38. These kinases lead to the downstream activation of AP-1, which controls transcription of a distinct set of proinflammatory molecules (Vandevenne et al., 2010).

The second adaptor protein of TLR4, TRIF, initiates an overlapping but unique proinflammatory response from MyD88. The role of TRIF was first discovered from MyD88-deficient macrophages, which were still able to mount a proinflammatory response to LPS, albeit attenuated and delayed (Kawai et al., 1999). The delayed onset is thought to be due to receptor interacting proteins 1/3, which directly associate with TRIF (Barton and Medzhitov, 2004). TRIF also associates with IRF-3 and IRF7, which are then activated by either of two kinases, TANK-

binding kinase-1 or IKKε (Han et al., 2004). This leads to a type 1 IFN response driven by IFNα and IFNβ.

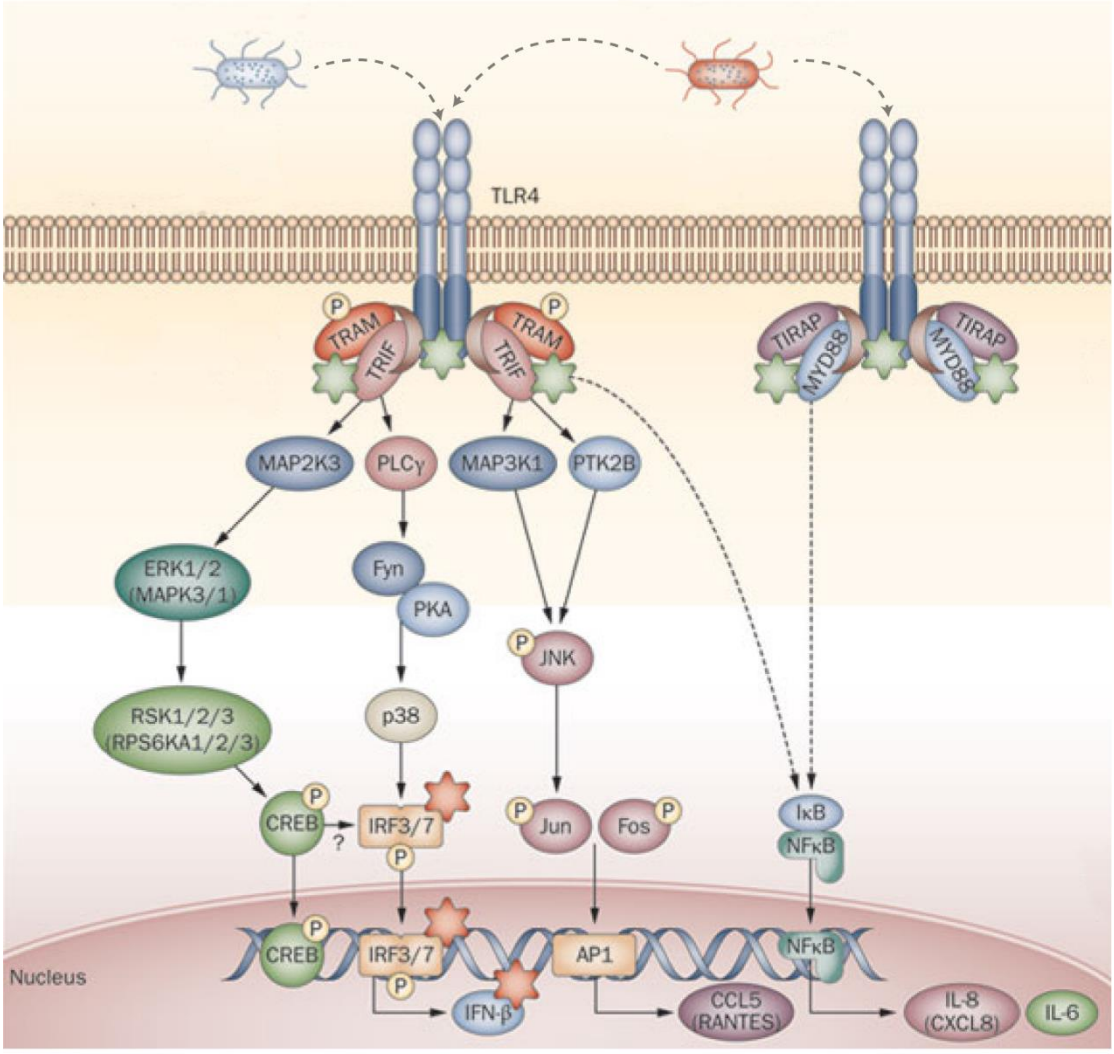

Figure 1.3 Graphical scheme of TLR4 signaling.
Reproduced with permission from (Ragnarsdottir et al., 2011), Copyright Macmillan Publishing Ltd.

Chapter 2. Suppression of airway allergic inflammation by a novel bacterially-derived lipid isolated from *Mycobacterium vaccae*

Acknowledgments: This work has been completed in collaboration with Roberta Martinelli, Gurdyal S. Besra, Petr A. Illarionov, Istvan Szatmari, Peter Brazda, Jon R.F. Hunt, Wenqing Xu, Xiang Wang, László Nagy, Graham A.W. Rook, and Laura Rosa Brunet. Gurdyal Besra and Petr Illarionov isolated and synthesized the triacylglycerol of 10(*Z*)-hexadecnoic acid. They also completed the gas chromatography and NMR structural characterization of the molecule. Wenqing Xu and Xiang Wang developed the synthesis and produced the free fatty acid form of 10(*Z*)-hexadecnoichexadecenoic acid. *In vivo* screening and experimentation was performed by Roberta Martinelli, Jon Hunt, and Laura Rosa Brunet. The manuscript was prepared with help from Roberta Martinelli, Gurdyal S. Besra, László Nagy, Graham A.W. Rook, and Laura Rosa Brunet.

Note: Text from this manuscript has been adapted from a manuscript submitted to and being reviewed by PLOS Biology.

2.1 Introduction

2.1.1 The hygiene hypothesis and inflammatory disease

Evidence suggests that common, harmless microorganisms, collectively referred to as "Old Friends", to which humans have been exposed throughout evolution, drive immunoregulatory mechanisms that inhibit inappropriate immune responses by the host (Okada et al., 2010; Rook, 2009, 2010; Rook and Rosa Brunet, 2002). These microorganisms include lactobacilli, which are routinely found in fermented food, saprophytic mycobacteria, which are ubiquitous in water, mud, soil, and decaying organic matter, and "Old infections", which include *Helicobacter* species and some helminths (Rook, 2009). We propose that exposure to these Old Friends allows the immune system of the host to distinguish between virulent pathogens and harmless organisms through a variety of mechanisms, including the induction of specific subsets of antigen presenting cells such as dendritic cells and modulation of innate immunity (Le Bert et al., 2011b; Garn et al., 2016; Lowry et al., 2016). In their absence, the host may develop

unwarranted and increasingly dysregulated immune responses to allergens, to self-antigens or to gut microbiota. Indeed, a simultaneous increase in allergies, autoimmune diseases and inflammatory bowel diseases has been observed in modern living conditions, where exposure to Old Friends has decreased dramatically due to changes in lifestyle (Bloomfield et al., 2016; Lowry et al., 2016; Lyte and Cryan, 2014; Rook, 2010; Stamper et al., 2016). Chronic low-grade inflammation has also been linked to mental health disorders such as depression, posttraumatic stress disorder (PTSD), and autism spectrum disorder (Hoisington et al., 2015; Lowry et al., 2016). Experimental data are accumulating to support this hypothesis. We have been particularly interested in a saprophytic mycobacterium, *Mycobacterium vaccae* (National Collection Type Culture (NCTC) 11659), which has shown encouraging therapeutic potential in diseases of immunodysregulation (Gutzwiller et al., 2007; Rook et al., 2007), as well as immunoregulatory and stress protective effects in murine models (Adams et al., 2004;Lowry et al., 2007;Reber et al., 2016;Zuany-Amorim et al., 2002).

2.1.2 The mycobacterial cell wall and therapeutic applications

Mycobacteria are characterized by an unusual cell wall rich in lipids. The core of the cell wall is a complex structure comprised of peptidoglycans (long polymers of the repeating disaccharide N-acetyl glucosamine–N-acetyl muramic acid that are linked via peptide bridges), covalently attached to arabinogalactans, which are in turn attached to mycolic acids formed from two fatty acids, a saturated shorter C20–C26 α-branch that is connected to a C60–C90 meromycolate branch (Brennan, 2003; Kieser and Rubin, 2014a). This structure is called the mycolylarabinogalactan-peptidoglycan complex (mAGP). The outer layer is composed of free lipids, with longer and shorter fatty acids to complement the shorter and the longer chains of the

mAGP (Brennan, 2003). Interspersed in this layer are cell wall glycerophospholipids and glycolipids, which include the phosphatidylmannosides (PIMs), the phthiocerol, lipomannan (LM), lipoarabinomannan (LAM), trehalose mono- and dimycolates, sulfolipids, lipooligosaccharides, and phenolic glycolipids (Jackson, 2014). When the cell wall is disrupted the free lipids and the lipoproteins are solubilized, while the mAGP remains in the insoluble residue. It has been proposed that whereas soluble lipids act in signaling processes, the insoluble core is essential for mycobacterial viability (Marrakchi et al., 2014). The suggested role of free lipids in the induction of immune responses has elicited substantial interest (van der Kleij and Yazdanbakhsh, 2003).

Between the rapid- (e.g. *M. vaccae*) and slow-growing (e.g. *M. tuberculosis*) mycobacteria, there are notable structural differences in the extractable lipids. *M. tuberculosis* produces a mannose-capped LAM (manLAM) that enhances virulence, whereas nonpathogenic mycobacteria produce an inositol phosphate-capped LAM (Appelmelk et al., 2008). The polar lipids within the cell envelope are often necessary for the unique functions of the various mycobacteria clades. For example, species within the *M. tuberculosis* complex produce unique lipooligosaccharides that assist in protein release and virulence (Van Der Woude et al., 2012). Compared to the pathogenic species, there is a lack of structural and functional detail regarding nonpathogenic cell envelope lipids. Underneath the cell envelope is the plasma membrane, where there is little difference in lipid composition between rapid- and slow-growing mycobacteria (Minikkin, 1982). The plasma membrane is predominately composed of PIMs with C16 and/or C18 acyl chains. Lastly, all mycobacteria produce neutral lipids, which are primarily stored as lipid bodies in the cytoplasm (Bansal-Mutalik and Nikaido, 2014). Depending on environmental

conditions and metabolic state, neutral lipids comprise 30-60% of the total lipid content, with triacylglyercides (TAG) being 84-86% of all neutral lipids (Nandedkar, 1983; Reed et al., 2007). TAGs are an important energy source, and in some cases the main energy source, of mycobacteria, but they are also an important carbon source for the biosynthesis of many of the polar lipids mentioned above (Herker and Ott, 2012; Wheeler and Ratledge, 1988).

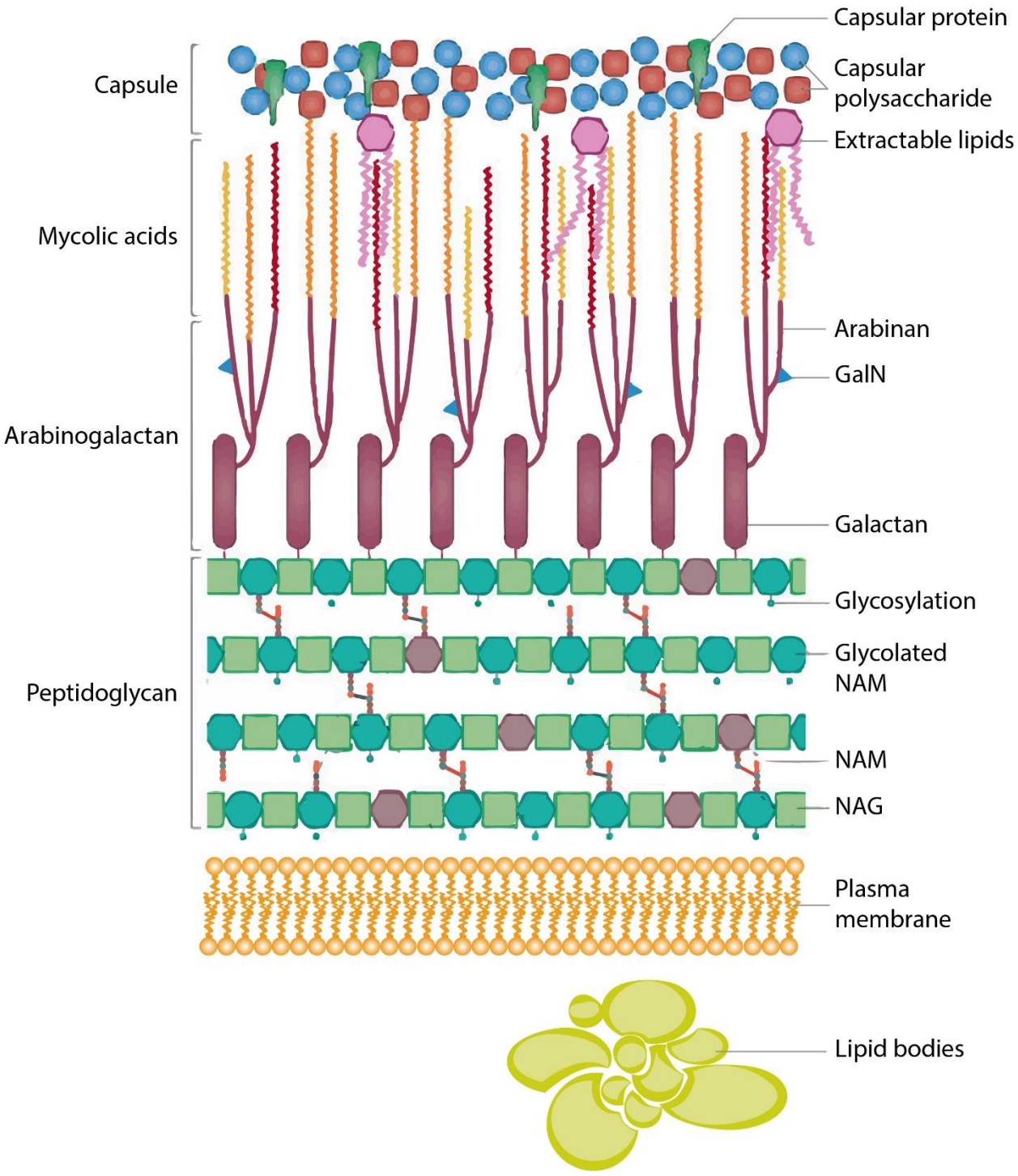

Figure 2.1 Arrangement and composition of mycobacterial cell wall and lipid structures.
The cell wall and plasma membrane are generally conserved among all mycobacteria with the exception of the capsule, which is only produced by pathogenic species. Reproduced with permission from (Kieser and Rubin, 2014b), copyright Macmillan Publishers Ltd. Abbreviations: NAG, N-acetyl glucosamine; NAM, N-acetyl muramic acid; GalN, non-N-acetylated galactosamine.

Strong regulatory mechanisms operate during both chronic infections with pathogens and chronic exposure to harmless organisms. These mechanisms limit immune-mediated pathology during infections and prevent repeated and inappropriate immune responses to organisms that pose no threat to the host. The identification of specific molecules that promote immunoregulation may provide novel therapeutic avenues for the treatment of diseases of immunodysregulation such as allergies, autoimmune diseases, inflammatory bowel diseases, and stress-related psychiatric disorders including major depressive disorder and PTSD, where chronic, low-grade inflammation has been identified as a risk factor (Lowry et al., 2016). We have previously shown that treatment with a heat-killed preparation of the saprophytic mycobacterium, *M. vaccae*, prevents murine allergic pulmonary inflammation by inducing $CD4^{+}CD45RB^{low}$ Tregs (Zuany-Amorim et al., 2002a). These cells are allergen-specific and upon passive transfer can protect recipient allergic mice from airway inflammation by significantly reducing eosinophilia in the lungs. In addition, treatment with *M. vaccae* induces a population of pulmonary $CD11c^{+}$ antigen-presenting cells, which are characterized by increased expression of IL-10, transforming growth factor beta (TGF-β) and IFNα (Adams et al., 2004). Furthermore, at least *in vitro*, priming of human DCs with *M. vaccae* induces strong inhibition of Th2 responses (Le Bert et al., 2011). Because lipids are an important constituent of the mycobacterial cell wall and have been shown to modulate immune responses, we investigated whether lipids extracted from *M. vaccae* may provide therapeutic benefits in a mouse model of pulmonary allergic inflammation. Here we found that a triacylglycerol lipid constituent of *M. vaccae* and its synthetic free fatty acid form have therapeutic potential as they are active in limiting symptoms of pulmonary allergic inflammation. We successfully synthesized these lipids and showed that their synthetic forms maintained therapeutic activity. Furthermore, the synthetic

free fatty acid inhibited proinflammatory signaling of activated macrophages *ex vivo*. This is the first report to show that a synthetic *M. vaccae*-derived lipid suppresses allergic airway inflammation *in vivo*.

2.2 Materials and methods

2.2.1 Animals

For studies involving isolation of bacterially-derived small molecules, and *in vivo* studies, adult female BALB/c mice, 6-8 weeks old (Harlan, Abingdon, UK), were housed under standard conditions with food and water available *ad libitum*. With regard to the potential therapeutic application of this research, female mice were chosen for these preliminary experiments. For studies involving *ex vivo* studies of freshly isolated peritoneal macrophages, adult male BALB/c mice (BALB/cAnHsd; Cat. No. 047; Harlan, Indianapolis, IN, USA), 6-8 weeks old, were used and housed under standard conditions with food and water available *ad libitum*.

For studies involving isolation of bacterially-derived small molecules, and *in vivo* studies, all experimental protocols complied with the Home Office 1986 Animals Scientific Act. For studies involving *ex vivo* studies of freshly isolated peritoneal macrophages, all experimental protocols were consistent with the National Institutes of Health Guide for the Care and Use of Laboratory Animals, Eighth Edition (The National Academies Press, 2011) and the Institutional Animal Care and Use Committee at the University of Colorado Boulder approved all procedures. All possible efforts were made to minimize the number of animals used and their suffering.

2.2.2 Mycobacterium vaccae

Isolation of bacterially-derived small molecules from *M. vaccae* was conducted using sterile paste derived from freshly grown stocks. For *in vivo* studies, sterile vials of heat-killed whole

cell *M. vaccae* suspension (10 mg/ml; strain NCTC 11659) were supplied by SR Pharma (London, UK). For studies involving *ex vivo* studies of freshly isolated peritoneal macrophages, the same material was provided by Bio Elpida (Lyon, France; batch ENG#1).

2.2.3 Isolation of the lipids

Wet cells (200 g of paste of sterile heat-killed whole cell *M. vaccae*) were extracted using 440 mL of petroleum ether, 400 mL of methanol, and 40 mL 0.3% aqueous sodium chloride overnight with gentle agitation. The mixture was then left to stand and the upper organic petroleum-ether supernatant fraction was separated by careful aspiration. The lower aqueous phase was extracted again using petroleum ether (400 mL) as described above. The petroleum-ether extracts were combined and dried to yield the apolar lipids. The lower aqueous phase was then extracted using chloroform/methanol/water (90:100:30; 520 mL) with gentle agitation, overnight. The resulting lipid extract was separated by vacuum filtration and the residual biomass extracted using chloroform/methanol/water (50:100:40; 170 mL) overnight with gentle agitation twice. The three polar lipid extractions were combined and chloroform (290 mL) and 0.3 % aqueous sodium chloride (290 mL) were added. The entire mixture was briefly shaken, allowed to settle and the upper phase was carefully removed and discarded. The lower organic layer was dried to yield the polar lipids. The polar lipids were resuspended in a minimum volume of chloroform (20 mL) and added to chilled acetone (1.5 L) and left at 4 °C, overnight. The resulting precipitate (lipid fraction 147) was separated by centrifugation from the acetone soluble lipids (220 mg) designated lipid fraction 148. Fraction 148 was further fractioned using column chromatography using increasing amounts of methanol in chloroform to afford seven lipidic fractions. These were screened for their immunomodulatory potential as described below. While

a number of fractions were deemed interesting, fraction 148.2 (82 mg) was further analyzed. The resulting fraction was deemed pure by thin-layer chromatography (TLC) using chloroform as an eluant following charring with a heat gun after spraying with 5% ethanolic molybdophosphoric acid. Through a combination of high resolution mass spectrometry (HRMS), 1-dimensional (1D) (^{1}H and ^{13}C), and two-dimensional (2D) (correlation spectroscopy (COSY) and ^{1}H/^{13}C heternonuclear multiple bond correlation (HMBC)) nuclear magnetic resonance (NMR) spectroscopy, and gas chromatography-mass spectrometry (GC-MS) analyses, the structure of the triglyceride was completely determined.

2.2.4 Synthesis of triacylglycerol

The synthesis of triacylglycerol was based on the method of Besra and colleagues (Besra et al., 1993). Briefly, the acetylenic carboxylic acid (**1**) and trimethylsilyl chloride (0.1 equivalent) in anhydrous methanol were mixed at room temperature for 12 hours. The reaction was evaporated to dryness to yield the pure methyl ester product (**2**) as confirmed by thin layer chromatography (TLC) and ^{1}H/^{13}C-NMR analysis and was used directly in the next step without further purification. The carboxylic acid methyl ester (**2**) was dissolved in diethyl ether and 2 equivalents of lithium aluminum hydride were added and the reaction was stirred at room temperature for 4 hours. The reaction was quenched with glacial acetic acid and the acetylenic alcohol product (**3**) was extracted with diethyl ether and water. The ethereal layer was recovered and washed with water and then brine, then concentrated to dryness. To a solution of the acetylenic alcohol (**3**) (1 equivalent) in hexamethylphosphoramide (HMPA), n-butyl lithium (2 equivalents) was added at 0 °C under nitrogen over a period of 30 min. The reaction was stirred at 0 °C for 20 min. 1-iodopentane (1.4 equivalent) was added and the reaction mixture was left to

warm to ambient temperature and stirred for 20 hours. The reaction was quenched with the addition of saturated aqueous ammonium chloride and the product (**4**) was extracted with diethyl-ether. The product (**4**) was concentrated and purified by column chromatography using a petroleum ether-ethyl acetate gradient, monitored by TLC and characterized by $^{1}H/^{13}C$-NMR. A suspension of Lindlar's catalyst in dry benzene was saturated with hydrogen gas and cooled to 10 °C. Then a solution of (**4**) in benzene and quinoline was added under a stream of nitrogen. The reaction mixture was stirred for 1 hour at 10 °C. The reaction mixture was filtered, concentrated and the product (**5**) was purified by column chromatography using a petroleum ether-ethyl acetate gradient, monitored by TLC and characterized by $^{1}H/^{13}C$-NMR. A solution of (**5**) in dichloromethane (1 volume) was added to a stirring solution of pyridinium dichromate (4 equivalents) in dimethylformamide (DMF, 10 volumes). The reaction mixture was stirred for 2 days at room temperature. Water was added and the product (**6**) was extracted into dichloromethane, washed with brine and concentrated. The product (**6**) was purified by column chromatography and characterized by MS and $^{1}H/^{13}C$-NMR. The starting acid (**6**) was dissolved in dichloromethane/DMF and oxalyl chloride was added; the reaction mixture was then stirred at room temperature for 1 hour. The reaction mixture was evaporated and the crude acid chloride (**7**) was used in the next step. Glycerol (1 equivalent) in pyridine was added to the acid chloride (**7**) (3.3. equivalents) and the reaction mixture was left to stir overnight. Dichloromethane and water were added to the reaction mixture and the product was recovered in the organic layer and concentrated. The synthetic triacylglycerol was purified by column chromatography using increasing methanol in chloroform, monitored by TLC and characterized by MS, and $^{1}H/^{13}C$-NMR analyses. All indicated structures are shown in Fig. 2.2.

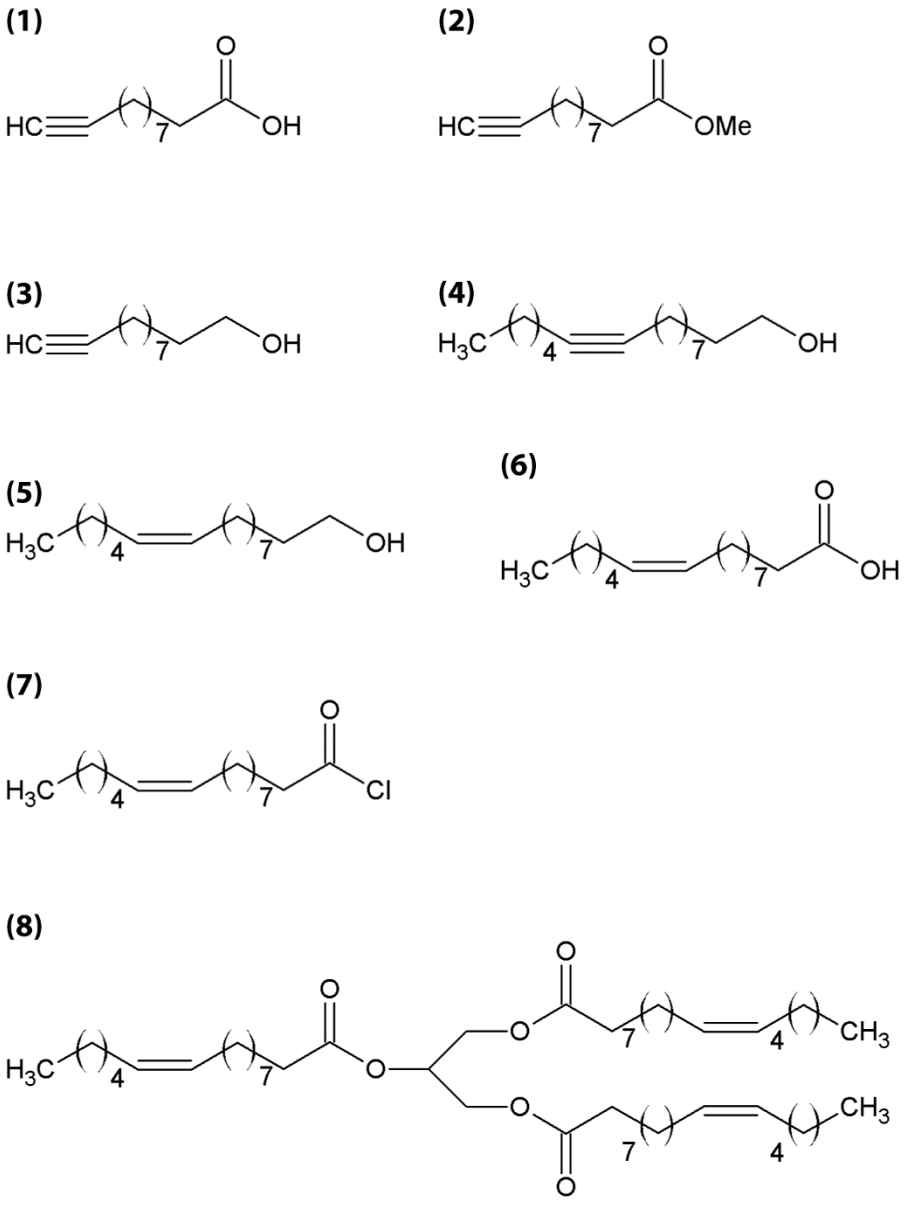

Figure 2.2 Structures associated with the synthesis of the triacylglycerol, 1,2,3-tri[*Z*-10-hexadecenoyl]glycerol, isolated from extracts of *M. vaccae*.

2.2.5 Synthesis of 10(*Z*)-hexadecenoic acid; (10*Z*)-hexadec-10-enoic acid (CAS No. 2511-97-9)

Unless otherwise noted, reagents were obtained commercially and used without further purification. Dichloromethane (CH_2Cl_2) was distilled over calcium hydride (CaH_2) under a nitrogen atmosphere. Tetrahydrofuran (THF; $(CH_2)_4O$) was distilled from sodium-benzophenone

under a nitrogen atmosphere. Thin-layer chromatography analysis of reaction mixtures was performed on Dynamic Adsorbents, Inc., silica gel F-254 TLC plates. Flash chromatography was carried out on Zeoprep 60 ECO silica gel. ^{1}H spectra were recorded with a Varian INOVA 500 spectrometer. Compounds were detected by monitoring UV absorbance at 254 nm.

To a 5 mL sealed tube containing 1-heptene (0.50 mL, 3.55 mmol), methyl 10-undecenoate (0.080 mL, 0.36 mmol) and 0.35 mL THF was added to a Grubbs Z-selective metathesis catalyst (2.2 mg, 3.48 µmol, Sigma-Aldrich, Cat. No. 771082). The reaction was stirred at 45 ^{o}C for 8 h before cooling to room temperature. The slurry was filtrated through a short plug of silica gel and concentrated. The obtained oil was dissolved in 1.0 mL THF. The solution was cooled to 0 ^{o}C, then 9-borabicyclo[3.3.1]nonane (9-BBN) solution in THF (1.28 mL, 0.50 M, 0.64 mmol) was added. After 2 h stirring at 0 ^{o}C, the reaction was quenched with 60 µL EtOH, then 1.5 mL pH 7 potassium phosphate buffer and 1.5 mL 30% H_2O_2. The mixture was stirred at room temperature for 12 h, then extracted with 5 mL EtOAc three times. The combined organic layers were washed with 4 mL saturated $Na_2S_2O_3$ and 3 mL brine, then dried over Na_2SO_4, filtered and concentrated. To the crude oil in 1.0 mL THF was added LiOH monohydrate (38 mg, 0.90 mmol) in 1.0 mL water. After 2 h, the reaction solution was cooled to 0 ^{o}C before addition of 0.91 mL 1.0 N HCl. After being concentrated under reduced pressure, the aqueous solution was saturated with NaCl and extracted with 3 mL dichloromethane three times. The combined organic layers were dried over Na_2SO_4, filtered and concentrated. Purification by flash chromatography (2:1:1 hexanes/dichloromethane/diethyl ether) provided (10Z)-hexadec-10-enoic acid (0.022 g, 90%) as a colorless oil. ^{1}H NMR (500 MHz, $CDCl_3$): δ 5.48 – 5.22 (m,

2H), 2.35 (t, J = 7.5 Hz, 2H), 2.01 (q, J = 6.6 Hz, 4H), 1.63 (p, J = 7.4 Hz, 2H), 1.35 – 1.15 (m, 16H), 0.88 (t, J = 6.9 Hz, 3H).

2.2.6 Thp1 cell assay

Thp1 cells were used as an immunological screen to characterize properties of the isolated lipid fractions of *M. vaccae* in terms of IL-12p40 and IL-10 secretion. Thp1 cells (ATCC, Teddington, UK) were differentiated overnight with 1.2% DMSO (Cat. No. D-5879; Sigma-Aldrich, Gillingham, UK) in culture media containing RPMI 1640 medium containing 20 mM Hepes buffer without L-glutamine (Cat. No. 42402-016; Gibco BRL, Grand Island, NY, USA), containing 10% fetal calf serum (Cat. No. 10106-169; Gibco BRLBRL), and 2 mM L-glutamine (Cat. No. 25030-024; Gibco BRL). Cells were washed, counted and resuspended at a concentration of $2x10^6$/ml. Cells were stimulated *in vitro* with isolated lipid fractions of *M. vaccae* at 37 °C and 5% CO_2. Supernatants were collected after 24 or 48 hours and cytokine concentrations were measured using commercially available ELISA kits (R&D Systems, Abingdon, UK). For experimental timeline, see Fig. 2.3A.

2.2.7 Murine model of allergic pulmonary inflammation: prevention studies

Mice were treated subcutaneously on day –21 with either whole cell heat-killed *M. vaccae* (0.1 mg in 100 µl of sterile saline), *M. vaccae* lipid preparation (1 or 5 µg in 100 µl of buffer) or with sterile buffer alone. On days 0 and 12, mice were sensitized by intraperitoneal (i.p.) injection of 10 µg chicken egg ovalbumin (Grade V, Sigma-Aldrich, UK) in 100 µl of alum gel (AMS, Abingdon, UK). On days 19 and 21, mice were challenged intratracheally (i.t.) with 50 µl of 10 µg/ml ovalbumin in sterile saline solution (Fig. 2.3B-D).

2.2.8 Murine model of allergic pulmonary inflammation: treatment studies

In separate studies, 3 weeks prior to treatment with *M. vaccae* (0.1 mg in 100 µl of sterile saline), 1,2,3-tri[*Z*-10-hexadecenoyl]glycerol (5 µg in 100 µl of buffer, s.c.; Fig. 2.3E), 10(*Z*)-hexadecenoic acid (5 µg or 1 µg in 100 µl buffer, s.c.; Fig. 2.3F) or with sterile buffer alone, animals received two ovalbumin and alum injections 12 days apart (on days 0 and 12) to determine the therapeutic potential of treatment with *M. vaccae* and its lipid components, 1,2,3-tri[*Z*-10-hexadecenoyl]glycerol and 10(*Z*)-hexadecenoic acid (Fig. 2.3E,F). *M. vaccae*, its lipid components, or vehicle was injected on day 21. Mice were immunized again with ovalbumin and alum injections on days 42 and 54 and challenged with ovalbumin intratracheally (i.t.) with 50 µl of 10 µg/ml ovalbumin in sterile saline solution on days 61 and 62. Mice were euthanized 24 hours after the second i.t. antigen challenge by i.p. injection of sodium pentobarbital (240 mg/kg, Animal Care, York, UK). The trachea was cannulated and the BAL fluid was collected by washing three times with 0.3 ml of RPMI supplemented with 50 U/ml penicillin and 50 µg/ml streptomycin (Invitrogen). The number of cells recovered was determined using a Neubauer chamber. Differential cell counts for each BAL sample were obtained from slide cytospin (Cytospin 3, Shandon Scientific, Cheshire, UK) stained with Wright-Giemsa (Sigma-Aldrich). A differential count of 200 cells was performed using standard histological criteria. The remaining BAL fluid was centrifuged and the supernatant stored at –20 °C for cytokine analysis. Concentrations of IL-5 and IL-10 were measured using commercially available ELISA kits.

2.2.9 Ex vivo splenocyte culture

Spleens from mice from each treatment group were pooled and a single cell suspension was prepared. Erythrocytes were removed by hypotonic lysis. Cells were washed and resuspended in

culture media containing RPMI, 10% fetal calf serum, 2 mM glutamine, 50 U/ml penicillin and 50 µg/ml streptomycin. Splenocytes ($10x10^6$/ml) were stimulated ex vivo with phosphate-buffered saline (PBS; Invitrogen), ovalbumin (50 µg/ml) for antigen-specific stimulation, and with plate-bound anti-CD3 (0.5 µg/ml, Pharmingen, Oxford, UK) for polyclonal activation of T cells. Supernatants were collected 72 hours later for analysis of cytokine concentrations. Concentrations of IL-5 and IL-10 were measured using commercially available ELISA kits.

2.2.10 Murine peritoneal macrophage isolation and screening

Murine peritoneal macrophages were isolated as previously described (Zhang et al., 2008) and used to determine the effects of 10(*Z*)-hexadecenoic acid on lipopolysaccharide-induced IL-6 secretion (Fig. 2.3G). Briefly, mice received one 1 ml i.p. injection of 3% thioglycollate medium (Cat. No. 9000-294, VWR, Radnor, PA, USA). Ninety-six hours later, macrophages were collected in DPBS (Cat. No. 14190136, Invitrogen, Carlsbad, CA, USA). Cells were centrifuged and resuspended in DMEM/F-12 (Cat. No. 10565018, Invitrogen) supplemented to be 10% (v/v) fetal bovine serum (Cat. No. 16000036, Invitrogen) and 1% penicillin/streptomycin (Cat.No. 15140148, Invitrogen). One mouse yielded enough cells for one experimental replicate. $1x10^5$ cells/well were allowed to adhere for 1.5 h before being washed with DPBS. 10(*Z*)-hexadecenoic acid was dissolved in DMEM/F-12 with 0.5% (v/v) dimethyl sulfoxide (Cat. No. D8418, Sigma-Aldrich). The macrophages were incubated with either 10(*Z*)-hexadecenoic acid (0.4 µM, 4 µM, 20 µM, 100 µM, 500 µM, 1000 µM) or DMEM/F-12 for 1 h before being stimulated with either 1 µg/ml lipopolysaccharide (serotype 0127:B8, Sigma-Aldrich, St. Louis, MO, USA) or DMEM/F-12. Culture supernatants were collected at 6, 12, and 24 h post-stimulation.

2.2.11 Dynamic light scattering of lipid micelles

Prior to sample preparation, all reagents were sterile filtered through a 0.1 µm centrifugal filter (Cat. No. UFC30VV25, Millipore Corp.). 10(*Z*)-hexadecenoic acid was prepared in DMEM/F-12, 0.2% DMSO for a concentration of 1 mM then sterile filtered again through a 0.1 µm centrifugal filter. Dilutions were made with dust-free 10(*Z*)-hexadecenoic acid. The presence of micelles in the lipid preparations (1 mM, 500 µM, 200 µM, 100 µM, 50 µM, 25 µM, 10 µM, 1 µM) was determined from side scatter intensity as measured through DLS (Titan DynaPro, Wyatt Technologies). Data was recorded at 40% power and analysed in Dynamics V6.3.40 (Wyatt Technologies). For the DMEM/F-12, the refractive index was set at 1.3, and viscosity was set to 0.78. Scatter intensities were collected at 21°C and 37°C. The data was modelled using a 4-paramter logistic.

2.2.12 Lipid extraction

Freshly isolated murine peritoneal macrophages were treated and stimulated as previously described. The total lipid content of the macrophages was extracted as previously described (Bligh and Dyer, 1959). The extraction procedure was performed at the indicated time points after addition of either 10(*Z*)-hexadecenoic acid or LPS. Briefly, cell culture supernatants were aspirated and set aside. The macrophage monolayers were washed three times with DBPS, followed by addition of 300 µl of methanol-chloroform (2:1). The cells were scraped from the wells to create a single cell suspension. One hundred µl of chloroform was added to the suspension, and the mixture was homogenized with a handheld homogenizer (Tissuemiser, Fisher Scientific). One hundred µl of water was added, and the mixture was homogenized again. The alcoholic and organic layers were allowed to separate, and the alcoholic layer was aspirated.

The chloroform was evaporated off in a rotovap (Cat. No. SVC-100H, Savant), and the resulting lipid residue was dissolved in hexanes. The extraction procedure was also performed with the cell culture supernatants. The lipid content was separated on silica gel 60 F_{254} coated thin layer chromatography plates using a hexanes-ethyl acetate (3:1) mobile phase. Lipids were visualized in an iodine chamber.

2.2.13 Cytokine measurements

Cell culture supernatants from freshly isolated peritoneal macrophages were diluted 1:200, and IL-6 was measured using sandwiched ELISA (Cat. No. 431304, Biolegend, San Diego, CA, USA). All samples were measured in duplicate.

2.2.14 Cytotoxicity assay

Cytotoxicity was determined using the sulforhodamine B (SRB) colorimetric assay, as previously described (Vichai and Kirtikara, 2006). Briefly, without removing the culture media, cells were fixed by adding cold trichloroacetic acid and incubated at 4 °C for 1 h. The plates were washed with slow-running tap water and set out to dry overnight. Then, 0.057% SRB (Cat. No. AC333130050, Fisher, Pittsburgh, PA, USA), solubilized in 10 mM Tris (Cat. No. BP153, Fisher), was added to each well. After 30 min, plates were washed with 1% acetic acid and set out to dry overnight. SRB was measured at 490 nm on a Synergy HT microplate reader (Part Number 7091000, Biotek, Winooski, VT, USA). Cell viability was expressed as the ratio of experimental and control growth.

2.2.15 Ligands

Rosiglitazone, troglitazone, and WY14643 were obtained from Alexis Biochemicals (San Diego, CA, USA); ATRA and AM580 were obtained from Sigma-Aldrich. In addition, GW9662 was a gift from T.M. Willson (GlaxoSmithKline, Brentford, United Kingdom).

2.2.16 Statistical analysis

Results are represented as means ± SEM or means + SEM. Data were subjected to a normality test and one-way ANOVA or Student's *t*-tests were performed as appropriate. A two-tailed p value ≤ 0.05 was considered significant.

2.3 Results

The fractionation of *M. vaccae* NCTC 11659 with a number of solvents resulted in the isolation of several lipid fractions with different characteristics. Preliminary work identified lipids present in the aqueous methanol fraction, such as phospholipids, polar and neutral glycolipids and glycosylphosphatidylinositols, but not those in the petrol fraction, such as phthiocerols, dimicocerosates and mycolic acids, to be of considerable interest (data not shown).

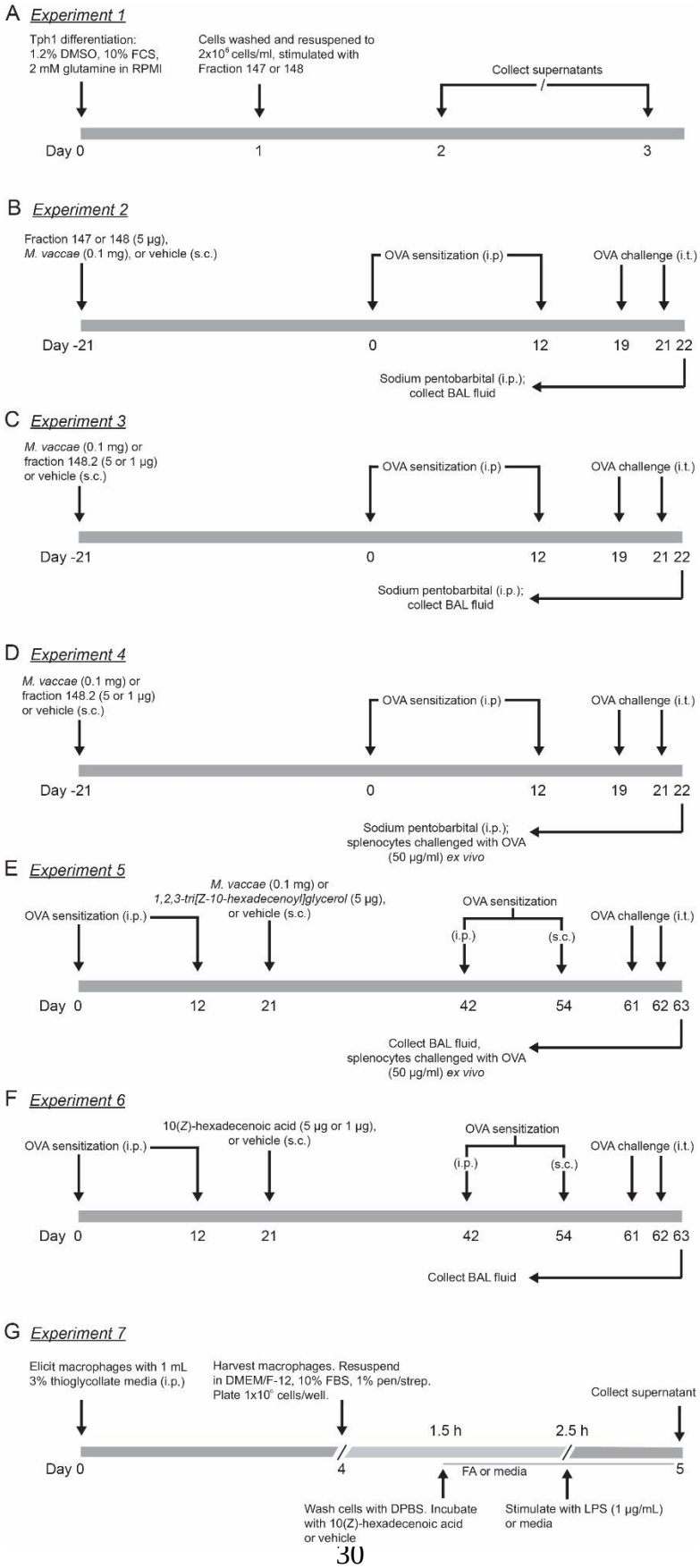
A Experiment 1
Tph1 differentiation: 1.2% DMSO, 10% FCS, 2 mM glutamine in RPMI
Cells washed and resuspened to 2x10^6 cells/ml, stimulated with Fraction 147 or 148
Collect supernatants
Day 0
1
2
3
B Experiment 2
Fraction 147 or 148 (5 µg), M. vaccae (0.1 mg), or vehicle (s.c.)
OVA sensitization (i.p)
OVA challenge (i.t.)
Day -21
0
12
19
21 22
Sodium pentobarbital (i.p.); collect BAL fluid
C Experiment 3
M. vaccae (0.1 mg) or fraction 148.2 (5 or 1 µg) or vehicle (s.c.)
OVA sensitization (i.p)
OVA challenge (i.t.)
Day -21
0
12
19
21 22
Sodium pentobarbital (i.p.); collect BAL fluid
D Experiment 4
M. vaccae (0.1 mg) or fraction 148.2 (5 or 1 µg) or vehicle (s.c.)
OVA sensitization (i.p)
OVA challenge (i.t.)
Day -21
0
12
19
21 22
Sodium pentobarbital (i.p.); splenocytes challenged with OVA (50 µg/ml) ex vivo
E Experiment 5
OVA sensitization (i.p.)
M. vaccae (0.1 mg) or 1,2,3-tri[Z-10-hexadecenoyl]glycerol (5 µg), or vehicle (s.c.)
OVA sensitization
(i.p.)
(s.c.)
OVA challenge (i.t.)
Day 0
12
21
42
54
61
62 63
Collect BAL fluid, splenocytes challenged with OVA (50 µg/ml) ex vivo
F Experiment 6
OVA sensitization (i.p.)
10(Z)-hexadecenoic acid (5 µg or 1 µg), or vehicle (s.c.)
OVA sensitization
(i.p.)
(s.c.)
OVA challenge (i.t.)
Day 0
12
21
42
54
61
62 63
Collect BAL fluid
G Experiment 7
Elicit macrophages with 1 mL 3% thioglycollate media (i.p.)
Harvest macrophages. Resuspend in DMEM/F-12, 10% FBS, 1% pen/strep. Plate 1x10^6 cells/well.
Collect supernatant
1.5 h
2.5 h
Day 0
4
FA or media
5
Wash cells with DPBS. Incubate with 10(Z)-hexadecenoic acid or vehicle
Stimulate with LPS (1 µg/mL) or media

Figure 2.3 Diagrammatic illustrations of experimental designs.
Abbreviations: BAL, bronchoalveolar lavage; i.p., intraperitoneal; i.t., intratracheal; OVA, chicken egg ovalbumin; s.c., subcutaneous; DMEM, Dulbecco's Modified Eagle Medium; LPS, lipopolysaccharide; FBS, fetal bovine serum; DPBS, Dulbecco's Phosphate-Buffered Saline.

2.3.1 Pretreatment with an aqueous methanol extraction of *M. vaccae* reduces allergic pulmonary inflammation

Upon further fractionation of the aqueous methanol fraction, we separated the phospholipid, polar glycolipid and glycosylphosphatidylinositol components (fraction 147) from the neutral glycolipid components (fraction 148). In *Experiment 1*, we assessed the immunomodulatory properties of these two fractions *in vitro* using Thp1 cells, a human monocytic cell line, exposed overnight to these preparations (for experimental timeline, see Fig. 2.3A). We found that Thp1 cells stimulated with fraction 147 preferentially produce IL-12p40. In contrast, when they were stimulated with fraction 148 they showed reduced IL-12p40 secretion and an increase in IL-10 levels (data not shown). Intrigued by these findings, in *Experiment 2* we treated mice, subsequently rendered allergic by immunization with ovalbumin and alum on Days 0 and 12, with either a heat-killed preparation of *M. vaccae* (NCTC 11659; 0.1 mg, s.c.) or fraction 147 or 148, (5 µg; s.c.), on Day –21 and determined their respective potential in limiting allergic pulmonary inflammation, measured on Day 22 following intratracheal (i.t.) ovalbumin challenge on Days 19 and 21 (for experimental timeline, see Fig. 2.3B). Pulmonary allergic inflammation is associated with a large influx of cells, particularly eosinophils, in the airway. We found that mice treated with either a heat-killed preparation of *M. vaccae* NCTC 11659 or fraction 148 showed a significant reduction in both the total cellular infiltrate and in the number of eosinophils recovered in the bronchoalveolar lavage (BAL) fluid (Table 2.1). The decrease in eosinophils was not associated with an increase in other inflammatory cells. In fact, macrophages ($p < 0.05$) were also reduced at the site of inflammation, while there were no effects on numbers

of neutrophils (Table 2.1). This reduction in disease severity was not observed in allergic mice treated with fraction 147. These results suggest that, not only do fractions 147 and 148 have different immunological properties, but also that fraction 148 prevents pulmonary allergic inflammation in a mouse model.

Table 2.1. Characterization of the cellular infiltrate in the lungs of allergic mice challenged intratracheally with ovalbumin in *Experiment 2*.

	Cells x 10^5/ml			
	Vehicle (s.c.)	M. vaccae NCTC 11659 (0.1 mg, s.c.)	Fraction 147 (5 µg, s.c.)	Fraction 148 (5 µg, s.c.)
Total cellular infiltrate	2.14 ± 0.2	0.65 ± 0.1*	1.73 ± 0.36	0.55 ± 0.1*
Eosinophils	0.41 ± 0.1	0.17 ± 0.01*	0.49 ± 0.2	0.12 ± 0.01*
Neutrophils	0.12 ± 0.04	0.03 ± 0.02	0.07 ± 0.02	0.02 ± 0.02
Macrophages	1.57 ± 0.1	0.45 ± 0.1*	1.15 ± 0.2	0.42 ± 0.1*

*denotes $p < 0.05$ compared with vehicle-treated, ovalbumin-challenged mice, using ANOVA and Bonferroni-corrected pairwise comparisons. These results are representative of at least two separate experiments ($n = 8$ per group).

2.3.2 Specific fractions of the mycobacterial extract are anti-inflammatory *in vitro*

Fraction 148 was further fractionated by column chromatography using a chloroform-methanol gradient. Based on previous results we screened seven subfractions of fraction 148 using Thp1 cells for a cytokine profile associated with low IL-12p40 and increased IL-10 levels (data not shown). Following these criteria, three subfractions were identified as having interesting features, and fraction 148.2 was used in further experiments. We found in *Experiment 3* (for experimental timeline, see Fig. 2.3C) that mice treated with either *M. vaccae* NCTC 11659 (0.1 mg, s.c.) or two different doses of fraction 148.2 (5 µg and 1 µg, s.c.) showed a reduction in both the total cellular infiltrate and the number of eosinophils and/or macrophages recovered in the BAL fluid (Fig. 2.3C and 2.4). In addition, in *Experiment 4* (for experimental timeline, see

Fig. 2.3D), we studied the effects of *M. vaccae* NCTC 11659 (0.1 mg, s.c.) and fraction 148.2 (5 or 1 µg, s.c.) on IL-10 secretion from splenocytes stimulated with allergen (50 µg/ml) *ex vivo*. Splenocytes from mice treated with *M. vaccae* NCTC 11659 and mice treated with fraction 148.2 produced increased levels of IL-10 following *in vitro* allergen (ovalbumin) stimulation (*M. vaccae* NCTC 11659, 234 ± 47 pg/ml; 1 µg fraction 148.2, 227 ± 20 pg/ml; 5µg fraction 148.2, 291 ± 16 pg/ml), compared to levels from splenocytes of mice treated with vehicle alone (179 ± 37 pg/ml). These results suggest that components of fraction 148.2 maintain the induction, measured *ex vivo* in splenocytes, of a cytokine profile associated with prevention of pulmonary allergic inflammation in a mouse model.

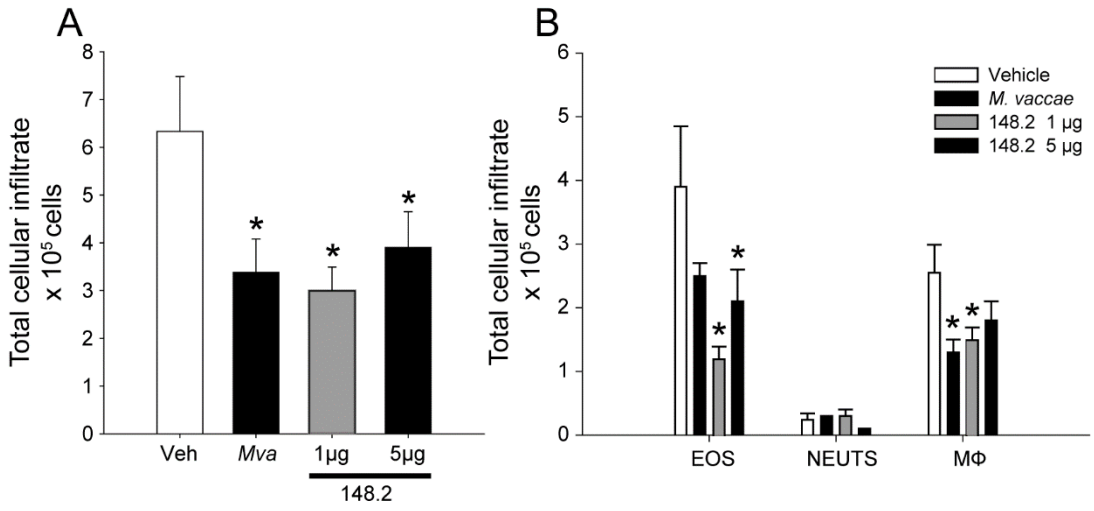

Figure 2.4 *M. vaccae* and *M. vaccae* fraction 148.2 reduce bronchopulmonary inflammation. Treatment with a heat-killed preparation of *M. vaccae* or lipid fraction 148.2 of *M. vaccae* reduced the severity of pulmonary allergic inflammation. (A) Compared to vehicle-treated control mice, subcutaneous treatment with whole heat-killed *M. vaccae* or lipid fraction 148.2 reduced the total number of cells recovered in the bronchoalveolar lavage (BAL) fluid of allergic mice challenged with ovalbumin. Allergic mice were treated with vehicle (white bars) or with 0.1 mg of a heat-killed preparation of *M. vaccae* (NCTC 11659; *Mva*; black bars) or with one of two doses of lipid fraction 148.2 (1 µg; 5 µg; gray bars). (B) Compared to vehicle-treated control mice, mice treated with *M. vaccae* or one of two doses of lipid fraction 148.2 had reduced numbers of eosinophils (EOS) and macrophages (MΦ) recovered in the BAL fluid of allergic mice challenged with ovalbumin. Data are expressed as mean + SEM of 6-8 mice per group. These results are representative of two separate experiments. *$p < 0.05$ relative to vehicle-treated controls as determined by ANOVA analysis followed by Fishers Least Significant Difference (LSD) tests.

Abbreviations: EOS, eosinophils; MΦ, macrophages; *Mva*, heat-killed preparation of *M. vaccae* (NCTC 11659); NEUTS, neutrophils.

2.3.3 The anti-inflammatory component of the fraction is a triglyceride

By performing a series of analytic chemistry experiments including high resolution mass spectrometry (HRMS), 1-dimensional (1D) (^{1}H and ^{13}C) and two-dimensional (2D) (correlation spectroscopy (COSY) and $^{1}H/^{13}C$ heteronuclear multiple bond correlation (HMBC) nuclear magnetic resonance (NMR) spectroscopy, and gas chromatography-mass spectrometry (GC-MS) analyses, we concluded that fraction 148.2 is a triacylglycerol. From the ^{1}H signals we identified a glycerol backbone at 4.20 ppm (4H) and 5.25 ppm (1H). We also obtained a complex signal at 5.32 ppm (3.3H, CH=CH), 2.3 ppm (6H, $CO\text{-}CH_2$), 2.0 ppm (8H, $CH_2CH{=}CHCH_2$) and 1.6 ppm (8H, $CO\text{-}CH_2CH_2$). Further analysis of fatty acid characteristics revealed that fraction 148.2 contained predominantly C16 and C18:1 and a smaller proportion of C18 and C16:1. The proton integration from the 1H NMR spectra indicated a degree of heterogeneity in terms of the number of acyl chains (i.e. double bonds) and the small coupling constant indicating cis fatty acids. Fatty acid analysis by GC/MS analysis of fatty acid methyl esters (FAMEs) gave predominately C16 and C18:1 FAMEs, and a smaller proportion of C18 and C16:1 FAMEs. Positive electro-spray mass spectrometry analysis of the intact lipid showed dominant sodiated molecular species at m/z 825 (C16:1 x 3), m/z 827 (C16:1 x 2, C16), m/z 853 (C18:1 x1, C16:1 x 2), m/z 857 (C18:1, C16 x 2), m/z 881 (C18:1 x 2, C16:1), m/z 883 (C18:1 x 2, C16), m/z 909 (C18:1 x3), m/z 911 (C18:1 x 2, C18), and a series of ions at m/z 827, 855, 857, 883, 911 and 913 representing saturation of fatty acids. The position of the double bond in the unsaturated FAMEs was determined through alkylthiolation and GC/MS analysis of the FAMEs and the presence of key cleavage ions (Francis, 1981). The following M = 390, G = 217, G-32 = 185 and F = 173 cleavage ions were observed for the C18:1 FAME indicating that the location of the cis double

bond was at C9,C10. The following M = 362, G = 231, G-32 = 199 and F = 131 cleavage ions were observed for the C16:1 FAME indicating that the location of the cis double bond was at C10,C11. The latter is a rather unusual lipid and appears to be restricted to *Mycobacteria* spp. (Fig. 2.2), (**8**)), although lactobacilli have been shown to have capacity to synthesize, from γ–linolenic acid, C18:1 fatty acids with a double bond at position 10,11 (Ogawa et al., 2005).

2.3.4 The triglyceride, 1,2,3-tri[*Z*-10-hexadecenoyl]glycerol, has therapeutic potential in a mouse model of pulmonary allergic inflammation

Because of its uniqueness we investigated in *Experiment 5* whether treatment with 1,2,3-tri[*Z*-10-hexadecenoyl]glycerol alone retains the therapeutic activity initially observed for treatment with whole *M. vaccae* NCTC 11659 or fraction 148.2. To this end, we synthesized the C16:1 triacylglycerol with a double bond at position 10,11 of each acyl chain (hereafter referred to as 1,2,3-tri[*Z*-10-hexadecenoyl]glycerol) and determined its therapeutic potential in a mouse model of allergic pulmonary inflammation (for experimental timeline, see Fig. 2.3E). We found that mice treated with either *M. vaccae* NCTC 11659 (0.1 mg, s.c.) or 1,2,3-tri[*Z*-10-hexadecenoyl]glycerol (5 µg, s.c.) showed a reduction in both the total cellular infiltrate and in the number of eosinophils recovered in the BAL fluid (Fig. 2.5). Once again the reduction in eosinophilia was not accompanied by an increase in T helper cell type (Th1)-mediated inflammation as the numbers of macrophages were not increased. The reduction in the numbers of eosinophils was comparable to that seen following treatment with heat-killed whole cell *M. vaccae* NCTC 11659 (Fig. 2.5). In addition, we observed a decrease in IL-5 concentrations and an increase in IL-10 concentrations in the BAL fluid of mice treated with 1,2,3-tri[*Z*-10-

hexadecenoyl]glycerol (5 μg) compared to those measured in the BAL fluid of mice treated with vehicle (Fig. 2.6A). Levels of IFNγ were below detection in the BAL fluid of allergic mice regardless of treatment. We measured cytokines in the supernatant of *ex vivo* splenocyte culture following allergen stimulation. We found an increase in IL-10 in the supernatant of splenocytes of mice treated with 1,2,3-tri[*Z*-10-hexadecenoyl]glycerol (5 μg) compared to those in the supernatant of splenocytes of mice treated with buffer (Fig. 2.6B). These results are the first to show therapeutic activity of a synthetic lipid, 1,2,3-tri[*Z*-10-hexadecenoyl]glycerol, of *M. vaccae* NCTC 11659 in a mouse model of pulmonary allergic inflammation.

To elucidate the physiological role of chain length and double bond position, the therapeutic potential of several other synthetic triglycerides was determined (Fig. 2.7A-F). We observed similar levels of cellular infiltration after allergic challenge whether mice were treated with 1,2,3-tri[*Z*-10-hexadecenoyl]glycerol, 1,2,3-tri[*Z*-10-undecenoyl]glycerol, or 1,2,3-tri[*Z*-10-octadecenoyl]glycerol (Fig. 2.4C). This result indicates that the therapeutic activity is not dependent on the acyl chain length. When mice are treated with 1,2,3-tri[*Z*-9-octadecenoyl]glycerol or 1,2,3-tri[*Z*-11-hexadecenoyl]glycerol, the total cellular infiltrate more resembles the buffer control, which indicates that the position of the double bond is most critical for the therapeutic effect (Fig. 2.7D-E). Furthermore, only the position appears to be important, as the *cis* and *trans* stereoisomers at the C10 position are equally effective (Fig. 2.7F).

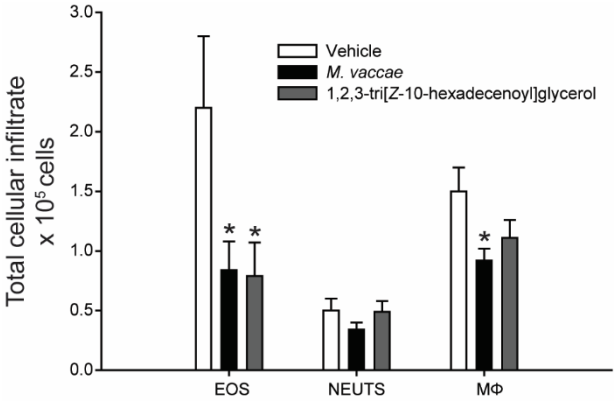

Figure 2.5 Synthetic triglyceride, 1,2,3-tri[*Z*-10-hexadecenoyl]glycerol, reduces bronchopulmonary inflammation.

Treatment with a synthetic triglyceride originally isolated and purified from *M. vaccae* reduces the severity of pulmonary allergic inflammation. Allergic mice were treated with vehicle (white bars), with 0.1 mg of heat-killed *M. vaccae* (NCTC 11659; black bars) or with a 5 µg dose of the synthetic triglyceride 1,2,3-tri[*Z*-10-hexadecenoyl]glycerol (gray bars). Compared to control mice, subcutaneous treatment with heat-killed whole cell *M. vaccae* reduced the numbers of eosinophils (EOS) and macrophages (MΦ) recovered in the bronchoalveolar lavage (BAL) fluid of allergic mice challenged with ovalbumin, while synthetic triglyceride 1,2,3-tri[*Z*-10-hexadecenoyl]glycerol reduced the numbers of eosinophils (EOS) recovered in the BAL fluid of these mice. Data are expressed as mean + SEM of 6-8 mice per group. These results are representative of two separate experiments. *$p < 0.05$ when compared to treatment with vehicle as determined by ANOVA analysis followed by Fishers Least Significant Difference (LSD) tests. Abbreviations: EOS, eosinophils; MΦ, macrophages; NEUTS, neutrophils.

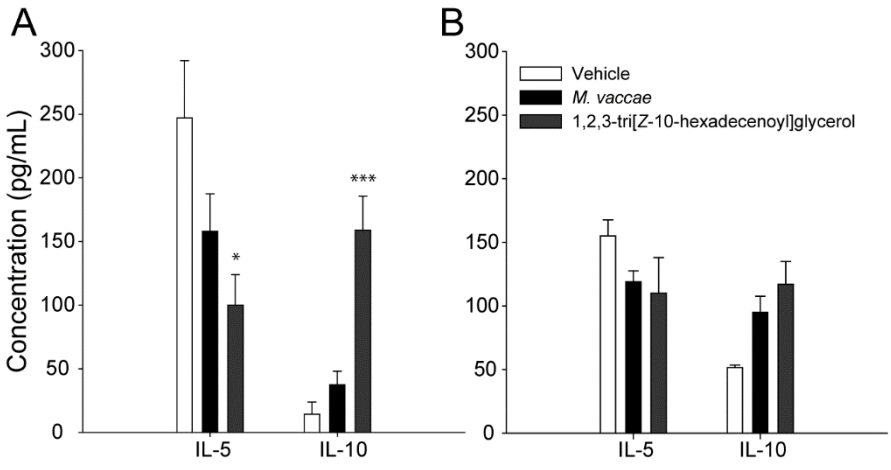

Figure 2.6 Synthetic triglyceride 1,2,3-tri[*Z*-10-hexadecenoyl]glycerol has an anti-inflammatory effect on immune cells recovered by bronchoalveolar lavage (BAL) fluid and splenocytes.
Treatment with a synthetic lipid originally obtained from *M. vaccae* altered the cytokine profile of allergic mice. (A) Levels of interleukin (IL) 5 and IL-10 were measured in the bronchoalveolar lavage (BAL) fluid of allergic mice treated with buffer (white bars), with 0.1 mg of a heat-killed preparation of whole cell *M. vaccae* (NCTC 11659; black bars) or with a 5 µg dose of the synthetic triglyceride 1,2,3-tri[*Z*-10-hexadecenoyl]glycerol (gray bars). Treatment with 1,2,3-tri[*Z*-10-hexadecenoyl]glycerol reduced IL-5 levels and increased IL-10 levels. (B) Levels of IL-5 and IL-10 were measured in the supernatant of splenocytes stimulated *in vitro* with ovalbumin. Splenocytes of mice treated with *M. vaccae* or 1,2,3-tri[*Z*-10-hexadecenoyl]glycerol produced more IL-10 than vehicle treated mice. Data are expressed as mean + SEM from pooled spleens of 6-8 mice per group. $*p < 0.05$ and $***p < 0.001$ relative to vehicle-treated controls as determined by ANOVA analysis followed by Dunnett's multiple comparison tests. These results are representative of two separate experiments.

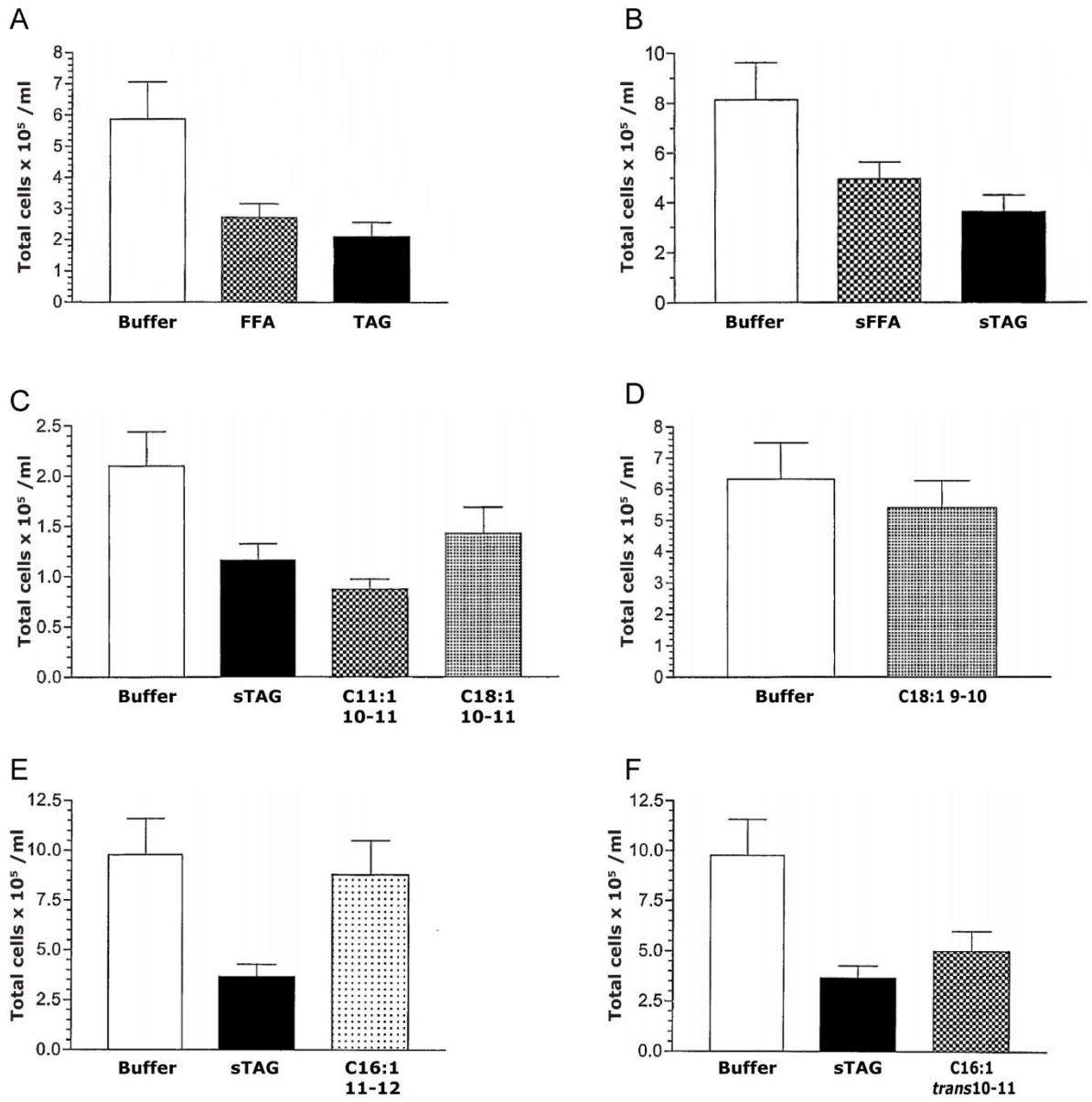

Figure 2.7 *In vivo* screening of synthetic acyl chain length and isomer variations.
The inflammatory response was measured as the total cellular infiltrate recovered from BAL fluid upon allergic challenge. (A) Three weeks prior to allergic challenge, mice were treated with either buffer, a mixture of C18 and C16 FFAs, (FFA), or a mixture of TAGs with C18 and C16 acyl chains. (TAG). (B) The treatment protocol was repeated using either buffer, a synthetic C16:1 10-11 FFA (sFFA), or synthetic triglyceride 1,2,3-tri[*Z*-10-hexadecenoyl]glycerol (sTAG). (C-F) Other synthetic triglyceride isomers with the indicated acyl chain structures were separately tested.

2.3.5 The free fatty acid, 10(*Z*)-hexadecenoic acid, has therapeutic potential in a mouse model of pulmonary allergic inflammation

To determine if the triglyceride structure was necessary for therapeutic function of 1,2,3-tri[*Z*-10-hexadecenoyl]glycerol, in *Experiment* 6 (for experimental timeline, see Fig. 2.3F) the free fatty acid, 10(*Z*)-hexadecenoic acid, was also synthesized. In the mouse model of allergic pulmonary inflammation, the free fatty acid (5 µg or 1 µg, s.c.) resulted in a significant reduction of both eosinophilia and total cellular infiltrate (data not shown). Furthermore, 10(*Z*)-hexadecenoic acid treatment did not induce increases in macrophages or neutrophils. Also similar to 1,2,3-tri[*Z*-10-hexadecenoyl]glycerol, we observed a decrease in IL-5 concentrations and an increase in IL-10 concentrations in the BAL fluid of 10(*Z*)-hexadecenoic acid-treated mice (5 µg)(data not shown). From these results, we concluded the anti-inflammatory effects of 1,2,3-tri[*Z*-10-hexadecenoyl]glycerol are not due to the molecule's multivalency, but rather the acyl chains.

2.3.6 Physical properties of 10(*Z*)-hexadecenoic acid

As a fatty acid, we expected 10(*Z*)-hexadecenoic acid to form micelles, so we used DLS to determine the critical micelle concentration. The formation of micelles could influence the effective concentration for immune suppression or influence how the lipid is transported across the plasma membrane. Scattering intensities of 10(*Z*)-hexadecenoic acid suspensions ranging from 1 µM to 1 mM, with and without LPS (0.5 mg/ml), were collected at 21°C and 37°C (Fig. 2.8). Intense, spurious signals were observed at 10(*Z*)-hexadecenoic acid concentrations above 200 µM, which is an indication that the lipid may be precipitating. The same unreliable signal was observed with the LPS samples.

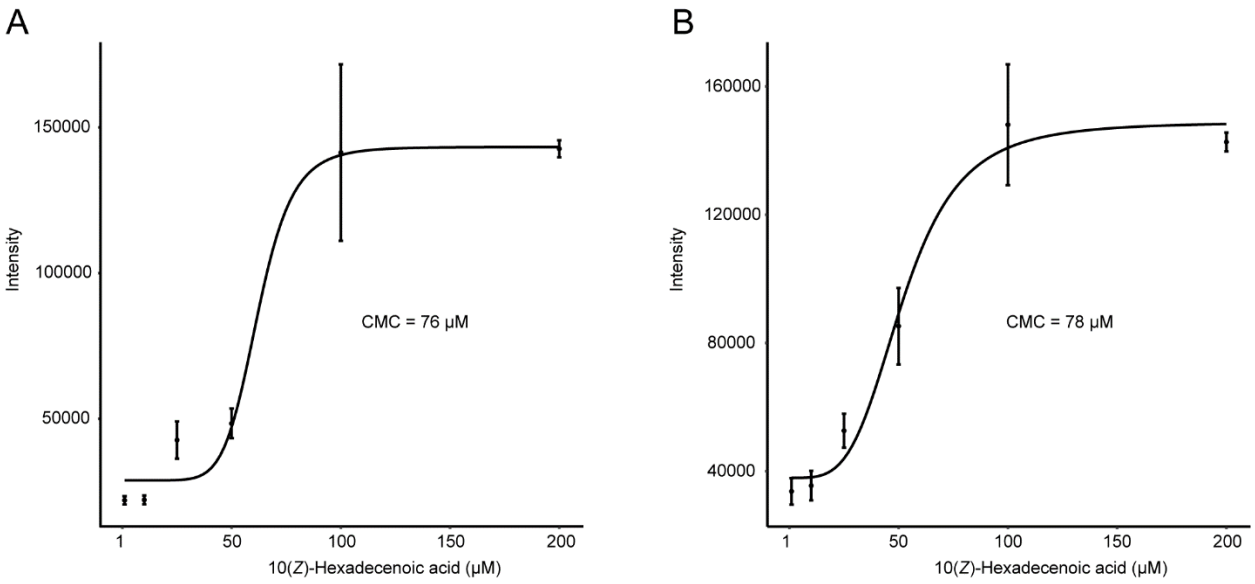

Figure 2.8 Critical micelle concentrations of 10(*Z*)-hexadecenoic acid.
Scatter intensity of lipid suspensions was measured using dynamic light scattering (DLS). Scatter intensities were collected at 40% laser power and measured at 21°C (A) and 37°C (B). The intensities were modeled using a 4-parameter logistic, and the CMC was calculated as the intersection of the of the maximum bound of the model and the slope of the inflection point.

We next tested whether 10(*Z*)-hexadecenoic acid could be detected in macrophages. Murine peritoneal macrophages were exposed to 200 µM lipid or DMEM/F-12 vehicle for 1 h, followed by addition of LPS (1 µg/ml) or DMEM/F-12 vehicle. Total lipid content of the cells and supernatant were collected at the indicated time points after addition of either 10(*Z*)-hexadecenoic acid or LPS, and lipids were visualized in an iodine chamber (Fig. 2.9). 10(*Z*)-hexadecenoic acid could be separated from other host cellular lipids using a hexanes-ethyl acetate (3:1) mobile phase. The reference 10(*Z*)-hexadecenoic acid sample was prepared from 0.16 µmol extracted into 100 µl of hexanes, which is the molar equivalent of 10(*Z*)-hexadecenoic acid used in the macrophage assay. The FFA is stored in DMEM/F-12 containing 0.2% DMSO, so the equivalent volume of vehicle to reference was extracted into 100 µl of hexanes. 10(*Z*)-hexadecenoic acid was detected in the supernatant of treated cells at all time points, but there

was no apparent difference between of the LPS-stimulated and unstimulated groups. 10(*Z*)-hexadecenoic acid was not detected in the macrophages. This may be due to the rapid metabolism of unsaturated fatty acids.

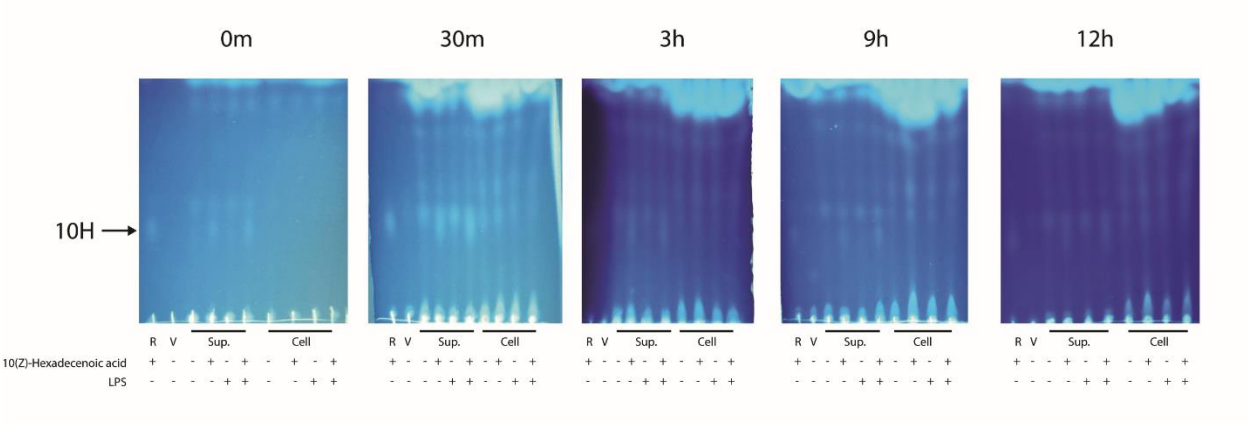

Figure 2.9 Thin layer chromatography of macrophages treated with 10(*Z*)-hexadecenoic acid. Murine peritoneal macrophages were treated with either 10(*Z*)-hexadecenoic acid or DMEM/F12 and stimulated with LPS or unstimulated. The reference sample (denoted "R") is 10(*Z*)-hexadecenoic acid resuspended in DMEM/12, and vehicle sample (denoted "V") is DMEM/12. Entire lipid content was extracted from culture supernatants ("Sup.") and the macrophage monolayer ("Cell"). Extractions were performed 0m, 30m, 3h, 9h, and 12h after addition of 10(*Z*)-hexadecenoic acid. Images were inverted to highlight the lipid separations.

2.3.7 10(*Z*)-hexadecenoic acid prevents LPS-induced secretion of IL-6 in macrophages

In *Experiment 7* (for experimental timeline, see Fig. 2.3G), we wanted to resolve if 10(*Z*)-hexadecenoic acid has a direct effect on immune cells. We chose to carry out this study on macrophages for their ubiquity and diverse role in immune processes. To simulate inflammation, freshly isolated mouse peritoneal macrophages were challenged with lipopolysaccharide (LPS; 1 µg/mL) *ex vivo*. Macrophages that were cultured in the presence of 0.4 µM up to 1 mM 10(*Z*)-hexadecenoic acid for 1 h prior to LPS treatment secreted less IL-6 compared to macrophages cultured with media alone (Fig. 2.10A-C). This difference was observable as early as 6 h after

LPS challenge, and was sustained for at least 24 h. The effect also appeared to be concentration and time dependent. The lowest concentration of 10(*Z*)-hexadecenoic acid (0.4 µM) was ineffective at 6 h, but reduced IL-6 secretion to 40% of control levels at 24 h. This time and concentration dependence may indicate that a receptor-mediated transcriptional change is occurring. In contrast to the effects of 10(*Z*)-hexadecenoic acid on LPS-induced IL-6 secretion, it had no effect of IL-6 secretion by itself (IL-6 was undetectable in all conditions; Fig. 2.10D). We also measured the concentration of IL-10 in culture supernatants of cells treated with 10(*Z*)-hexadecenoic acid or vehicle and stimulated with LPS or left unstimulated and found no measurable release of IL-10 in any group. Cell viability was measured to dispel the possibility that senescence or cell death was contributing to reduced IL-6 secretion. Using a high concentration (1 mM) of 10(*Z*)-hexadecenoic acid, less than 40% of macrophages were viable at most time points. However, macrophages cultured with all other concentrations of 10(*Z*)-hexadecenoic acid were as viable as or more viable than media controls (Fig. 2.11).

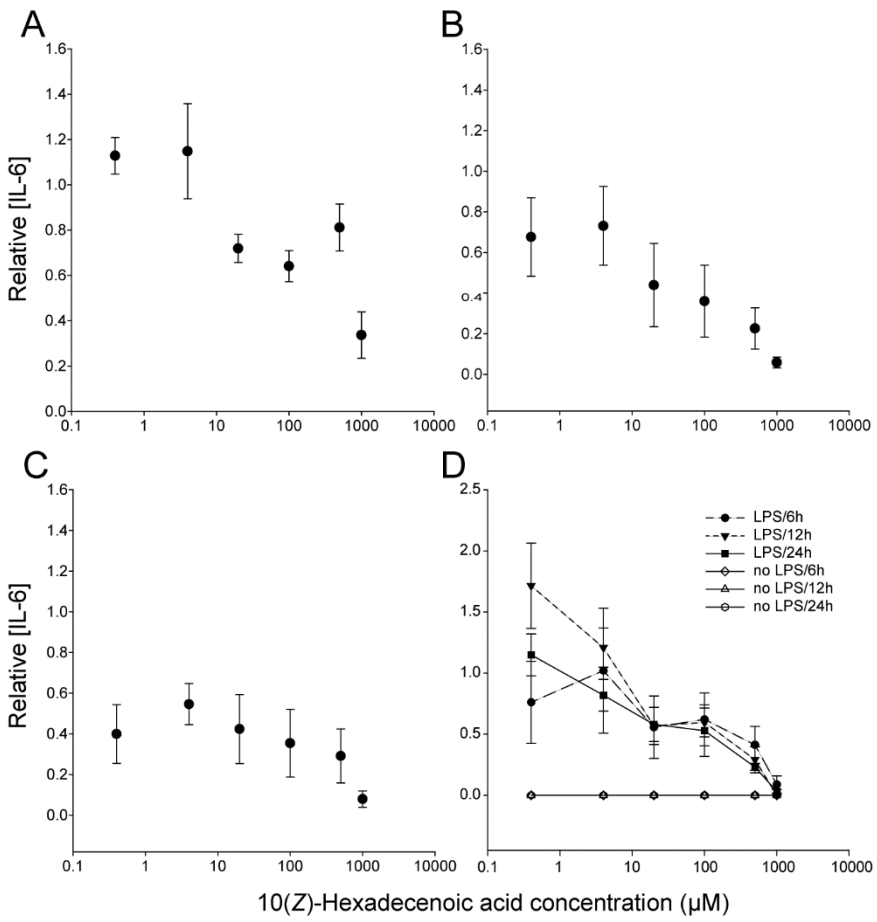

Figure 2.10 Anti-inflammatory effects of 10(*Z*)-hexadecenoic acid in freshly-isolated murine peritoneal macrophages.
Freshly isolated murine peritoneal macrophages were incubated for 1 h with synthetic 10(*Z*)-hexadecenoic acid (0.4 μM, 4 μM, 20 μM, 100 μM, 500 μM, 1000 μM), then challenged with 1 μg/mL lipopolysaccharide (LPS). Cell supernatants were collected at (A) 6 h, (B) 12 h, and (C) 24 h after LPS challenge. (D) The same experiment was repeated, but macrophages were challenged with either LPS or DMEM (as control). There was no detectable IL-6 in the cultures that did not receive LPS. Interleukin (IL) 6 concentrations in the supernatant were determined using ELISA and reported relative to media-only controls (n = 6 replicates for A-C and n = 4 for D, with each replicate using different freshly isolated peritoneal macrophages; each sample was run in duplicate). Data are expressed as mean ± SEM.

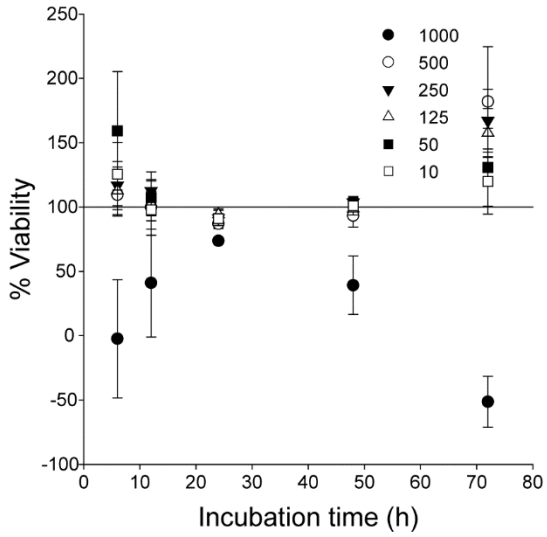

Figure 2.11 Macrophage cell viability assay.
Sulforhodamine B (SRB) was used to assess cytotoxic effects of various concentrations of synthetic 10(*Z*)-hexadecenoic acid (10 µM, 50 µM, 125 µM, 250 µM, 500 µM, 1000 µM) after 0, 6, 12, 24, 48, and 72 h of incubation with freshly isolated murine peritoneal macrophages. Percent control growth is expressed as % viability and is a ratio of the amount of growth that occurred with treatment over the amount of growth that occurred in media. One hundred percent indicates no differences in cell growth between treatment and media, whereas values below 100% indicate that growth was impaired with treatment. Data are expressed as mean ± SEM of 3-7 mice per condition.

2.4 Discussion

In this study we identified a novel lipid extract, derived from *M. vaccae*, containing a C16 monounsaturated fatty acid with the double bond in the 10 to 11 position, with unique therapeutic actions in a mouse model of allergic pulmonary inflammation. We show that treatment with a single dose of this lipid extract significantly reduced the characteristic features of pulmonary allergic inflammation such as total cellular infiltrate and eosinophilia in the lungs measured 6 weeks following treatment. We successfully synthesized 1,2,3-tri[*Z*-10-hexadecenoyl]glycerol and show that this synthetic triacylglycerol recapitulates the therapeutic activity of the lipid extract. The beneficial effects of the novel triacyglycerol, as well as the free fatty acid form, 10(*Z*)-hexadecenoic acid, as exemplified by the decrease in T helper cell type 2 (Th2) responses such as pulmonary eosinophilia, are not dependent on an increase in Th1-

mediated inflammation as neither neutrophils nor macrophages in the BAL fluid were increased. Instead, we observed an increase in the production of IL-10 both at the site of inflammation in the airways and in splenocytes stimulated with allergen *ex vivo*. Elevated levels of IL-10 have been shown previously to be associated with the beneficial effects of treatment with heat-killed whole cell *M. vaccae* NCTC 11659 (Hunt et al., 2005; Reber et al., 2016; Zuany-Amorim et al., 2002a). This is the first report to show that a lipid extract from *M. vaccae* NCTC 11659 has therapeutic activities *in vivo*. In addition, we demonstrated that 1,2,3-tri[*Z*-10-hexadecenoyl]glycerol and the synthetic free fatty acid, 10(*Z*)-hexadecenoic acid, potently suppressed LPS-induced secretion of IL-6 from freshly isolated murine peritoneal macrophages, with suppression of IL-6 secretion 24 h following LPS challenge, using a 400 nM concentration, the lowest concentration tested.

Recent work has suggested that peculiar lipid molecules of microbial origin may be ideally suited to induce Treg cells and initiate immunoregulatory mechanisms. Not surprisingly, some of these molecules are derived from long-lived pathogenic organisms, which induce chronic infection in the host, and therefore need to prevent severe immunopathology to ensure pathogen survival and transmission. For example, schistosomes, filarial worms and Leishmania protozoa have all been shown to induce increased levels of IL-10 and TGF-β in the host (Peters and Sacks, 2006; Schnoeller et al., 2008; Wilson et al., 2007). These infections are characterized by cellular hyporesponsiveness, i.e. a low proliferative response in peripheral blood mononuclear cells (PBMCs), and the induction of Treg cells (Belkaid et al., 2002; Doetze et al., 2000; Osborne and Devaney, 1999). We believe that harmless microorganisms, such as environmental saprophytes, have developed a similar talent for inducing immunoregulation. To avoid developing

unwarranted and costly immune responses to ubiquitous Old Friends, the host may have taken clues from specific molecules to recognize these organisms as harmless. For example, *M. vaccae* has been shown to induce $CD4^{+}CD45RB^{low}$ Treg cells during pulmonary allergic inflammation, which act through the production of IL-10 and TGF-β (Zuany-Amorim et al., 2002a). In this study we identified a lipid component, in its native and synthetic forms, of *M. vaccae* with interesting therapeutic properties in a mouse model of pulmonary allergic inflammation. Treatment is associated with increased levels of IL-10. Further research is required to elucidate mechanisms of action. Moreover, here we show that 10(*Z*)-hexadecenoic acid suppresses LPS-induced IL-6 release from freshly isolated peritoneal macrophages, raising the interesting possibility that macrophages may be an important mechanism through which this bacterially-derived lipid modulates immune function.

Bacterially-derived lipids may be particularly relevant for immunomodulation at the mucosal surface. Human intestinal macrophages display profound inflammation anergy (an inability to respond to an inflammatory stimulus with an inflammatory response), despite the fact that they retain phagocytic and bacteriocidal activity (Smith et al., 2005; Smythies et al., 2005). Specifically, intestinal macrophages fail to produce proinflammatory cytokines, including IL-1, IL-6, IL-12, chemokine (C-C motif) ligand 5 (CCL5), and tumor necrosis factor (TNF), in response to diverse inflammatory stimuli (Smythies et al., 2005). This effect in part is due to downregulation of adapter proteins MyD88 and toll-like receptor adaptor molecule 1 (Ticam1), which together mediate all toll-like receptor (TLR) MyD88-dependent and independent NF-κB signaling (Smythies et al., 2010). Downregulation of these inflammatory mechanisms is due in part to TGF-β derived from intestinal extracellular matrix (Smythies et al., 2010). Consequently,

Old Friends that induce TGF-β, such as *M. vaccae* (Zuany-Amorim et al., 2002a), have potential to suppress inflammatory responses in macrophages. A number of intracellular negative regulators of TLR signaling have been described, including PPARα (Xu et al., 2007) and PPARγ (Shibolet and Podolsky, 2007).

In a similar vein, lung-resident tissue macrophages induce antigen-specific $Foxp3^+$ Treg and promote airway tolerance (Duan and Croft, 2014; Soroosh et al., 2013; Strickland et al., 1996). Transfer of antigen-exposed macrophages to naïve mice is sufficient to suppress asthmatic lung inflammation and expand $Foxp3^+$ Treg populations (Soroosh et al., 2013). This mechanism is considered a steady-state phenomenon, as airway challenge with pattern recognition receptor ligands, like LPS, results in an inflammatory response (Soroosh et al., 2013). Another aspect of airway tolerance that is attributable to macrophages is their ability to induce T cell anergy or suppress DCs (Duan and Croft, 2014). Taken together, there are diverse roles for tissue macrophages, but it is clear that they are a critical interface of microbial inputs and immune tolerance.

Total concentrations of nonesterified fatty acids in human serum can exceed 1 mM and the more abundant of the individual fatty acids can account for 20-40% of this total (Jüngling and Kammermeier, 1988). Based on this justification, previous analysis of endogenous ligands in competition binding assays has been conducted at 30 μM concentrations, while transfection assays have been conducted using 30 μM (Forman et al., 1997) or 100 μM concentrations (Kliewer et al., 1997), which are in line with our finding using 10(*Z*)-hexadecenoic acid in functional assays in freshly isolated peritoneal macrophages (0.4 μM, 4 μM, 20 μM, 100 μM, 500 μM, 1000 μM). Concentrations of 10(*Z*)-hexadecenoic acid may well reach much higher

concentrations in target cells, such as macrophages and dendritic cells. Mycobacteria are intracellular parasites and are rapidly (within hours) translocated across the gut or lung mucosal lining by microfold cells (M cells), where they are phagocytosed by macrophages (Fujimura, 1986; Teitelbaum et al., 1999).

Mycobacteria are unique in that they accumulate triacylglycerols as intracellular lipophilic inclusions. For example, *M. smegmatis* accumulates triacylglycerols and the acyl chain composition varies depending on the growth medium (Garton et al., 2002). Monounsaturated fatty acids, $C_{16:1}$ hexadecenoic acid and $C_{18:1}$ octadecenoic acid were found to be high when bacteria were grown in nutrient rich Middlebrook 7H9 broth, relative to low-nitrogen Youmans' broth, but highest when bacteria were grown in Youmans' broth with monounsaturated oleic acid ((9*Z*)-octadec-9-enoic acid) supplementation. Thus, it is possible that mycobacteria synthesize and store triacylglycerols using environmental fatty acids as substrates, potentially for export to the cell envelope and release. If so, it may be possible to modify the immunoregulatory and anti-inflammatory potential of mycobacteria through modification of growth conditions.

Of potential importance, conjugated linoleic acids are bacterial metabolites. For example, specific members of the genus *Lactobacillus*, including *Lactobacillus reuteri*, and *L. plantarum*, mediate the conversion of dietary linoleic acid into immunomodulatory conjugated linoleic acids (Lee et al., 2003a; Ogawa et al., 2005). Most of the conjugated linoleic acid produced is located in the extracellular space (~98%) (Lee et al., 2003a; Roman-Nunez et al., 2007), suggesting that bacterially-derived conjugated linoleic acids may be metabolic signaling molecules that modulate the host immune response. These bacterially-derived fatty acid metabolites include 10-hydroxy-*cis*-12-octadecenoic acid (HYA), *cis*-9,*trans*-11-linoleic acid, *trans*-9,*cis*-11-linoleic

acid, and *cis*-10,*trans*-12-linoleic acid (Lee et al., 2003b; Miyamoto et al., 2015), among many others (Ogawa et al., 2005). Perhaps the closest analogue of 10(*Z*)-hexadecenoic acid identified here is trans-10-octadecenoic acid, produced by *L. plantaurm* from linoleic acid (Kishino et al., 2013) or γ-linolenic acid (Ogawa et al., 2005).

In addition to the effects of bacterially derived conjugated linoleic acids on macrophages, described above, conjugated linoleic acid suppresses NF-κB signaling and IL-12 production in dendritic cells through IL-10 production (Loscher et al., 2005). Exposure of murine dendritic cells to conjugated linoleic acid suppresses their ability to promote differentiation of naïve T cells into Th1 and/or Th17 cells *in vitro* following their adoptive transfer *in vivo* (Draper et al., 2014), and can increase the frequency of Treg in mesenteric lymph nodes (Evans et al., 2010). Future studies should investigate the effects of 10(*Z*)-hexadecenoic acid on inflammatory signaling in macrophages, dendritic cells, as well as on T cell differentiation.

Chapter 3. Anti-inflammatory effects of 10(*Z*)-hexadecenoic acid are dependent on PPARα

Acknowledgements: This work was completed in collaboration with Wenqing Xu, Xiang Wang, Petr A. Illarionov, Istvan Szatmari, Peter Brazda, and László Nagy. Wenqing Xu and Xiang Wang developed the synthesis and produced the free fatty acid form of 10(*Z*)-hexadecnoichexadecenoic acid. Petr Illarionov and László Nagy designed the PPAR reporter assay experiment, which was carried out by Istvan Szatmari and Peter Brazda.

3.1 Introduction

In previous work, we have shown that a heat-killed preparation of *M. vaccae* reduces airway inflammation in a murine model of allergic inflammation (Zuany-Amorim et al., 2002b). This was evidenced by reduced proliferation of eosinophils, neutrophils, and macrophages in the airways following allergen challenge, and by decreased IL-5 and increased IL-10 secretion from splenocytes, challenged with allergen *ex vivo*. Pretreatment with the heat-killed preparation of *M. vaccae* induced an immunoregulatory phenotype. Screening of lipid extracts of *M. vaccae* identified a novel lipid, 10(*Z*)-hexadecenoic acid, which appears to be unique to mycobacteria, that recapitulates the effects of whole, heat-killed *M. vaccae* on airway inflammation in mice. In addition, 10(*Z*)-hexadecenoic acid was shown to suppress LPS-stimulated IL-6 secretion from freshly isolated murine peritoneal macrophages. However, the mechanisms through which 10(*Z*)-hexadecenoic acid suppresses inflammation are not known.

3.1.1 Bioactive lipids and lipid receptors

In every domain of life, lipids are indispensable for cell structure, but they are also important intracellular and intercellular signaling molecules. In lipid biology, like polypeptide biogenesis, some of the molecular building blocks can only be obtained from the environment. There are only two essential fatty acids, which are the polyunsaturated fatty acids (PUFAs), linoleic acid (an ω-3 FA) and α-linoleic acid (an ω-6 FA). 10(*Z*)-hexadecenoic acid is an ω-6

fatty acid. These PUFAs and other dietary PUFAs are the primary source for lipid hormones that modulate immune responses. Arachidonic acid (AA; a polyunsaturated ω-6 fatty acid), which is derived from α-linoleic acid and represents 20% of FAs in the plasma membrane, is an archetypal immunomodulatory lipid. It is the progenitor of eicosanoids, leukotrienes, lipoxins, and epoxyeicosatrienoic acid. Impressively, these AA metabolites contribute to inflammatory processes, anti-inflammatory processes, pro-resolution, differentiation, and chemotaxis (Dennis and Norris, 2015). Furthermore, these modified PUFAs are secreted from cells and signal through surface receptors, so, given the evolutionary reliance on exogenous lipids for immune regulation and the patterns of unsaturation, these molecules and respective receptors are potentially relevant to understanding mycobacterial lipids.

A number of transcription factors have been identified that are potential mediators of the anti-inflammatory effects of 10(*Z*)-hexadecenoic acid in macrophages. One of these is a family of lipid sensing receptors, the peroxisome proliferator-activated receptor (PPAR) family. These receptors respond to a diverse population of lipids and are contextualized by their tissue-specific expression. Three isoforms of PPAR exist; PPARα is expressed in liver, heart, kidney, and muscle tissue. PPARγ is more ubiquitous and expressed in the heart, muscle, colon, kidney, pancreas, and spleen, whereas PPARδ is expressed in the brain and skin. All three isoforms are expressed in adipocytes, where PPARα and PPARδ regulate fatty acid oxidation, and PPARγ controls fatty acid storage (Chawla, 2010). The three isoforms are also expressed by macrophages and DCs, and in this context, they function to inhibit inflammation. The dietary lipid, conjugated linoleic acid (CLA), has been shown to have anti-inflammatory effects mediated through the PPARγ isoform, whereby receptor activation inhibits TNF expression in

LPS-stimulated peripheral blood mononuclear cells (Kim et al., 2011). CLA, like 10(*Z*)-hexadecenoic acid, is unsaturated at C10-11, but CLA exists as a *trans* isomer, whereas 10(*Z*)-hexadecenoic acid is a more effective immunoregulatory molecule as a *cis* isomer at C10.

Additionally, mammalian cells express a number of orphan G protein-coupled receptors (GPCRs) that have yet to be characterized. To date, 4 GPCRs have been deorphanized as free fatty acid receptors (FFARs). FFAR2/3 are exclusive for short chain fatty acids (SCFAs), such as propionate, and FFAR1/4 are promiscuous receptors for long chain FAs (LCFAs). FFAR4, in particular, is a candidate receptor for 10(*Z*)-hexadecenoic acid, which has been shown to regulate inflammation through a β-arrestin, TAB-1 pathway (Oh et al., 2010). Furthermore, FFAR1/4 are receptors for exogenous ω-3 and ω-6 FAs (Alvarez-Curto and Milligan, 2016).

Of the receptors discussed, the AA derivative receptors and FFAR are expressed on the surface of cells, and PPARs are expressed in the cytosol. The localization of 10(*Z*)-hexadecenoic acid is important to understand the mode of action. We had previously shown that the lipid forms microvesicles at concentrations above 100 μM, though this concentration is not necessary for anti-inflammatory effects. Mycobacteria have been reported to shed microvesicles that contain monoacyl and diacyl phosphatidylinositol dimannosides regardless of pathogenicity (Prados-rosales et al., 2011). Therefore, unique mechanisms of macrophage endocytosis may exist, such as lipid raft fusion, clathrin-, caveolin-, or dynamin-mediated entry (Kaparakis-Liaskos and Ferrero, 2015). Furthermore, unique PRR-mediated immunological responses exist for these modes of entry. For example, the nucleotide-binding oligomerization domain- containing protein 1 (NOD1), specifically initiates immune responses against these endosomes, so perhaps the anti-

inflammatory effect of 10(*Z*)-hexadecenoic acid resides more in its interactions with endosomal processes.

Given the diversity of fatty acid receptors in mammalian systems, and in order to take an unbiased approach to identifying potential mediators of the effects of 10(*Z*)-hexadecenoic acid, we conducted RNAseq analysis of LPS-stimulated, freshly isolated peritoneal macrophages in mice, with or without pre-exposure to 10(*Z*)-hexadecenoic acid. This approach identified a number of genes that were upregulated or downregulated following exposure to 10(*Z*)-hexadecenoic acid. We subsequently conducted pathway analysis to reveal potential signaling pathways involved in the anti-inflammatory effects of 10(*Z*)-hexadecenoic acid.

3.2 Materials and methods

3.2.1 Animals

Male BALB/c (BALB/cAnHsd; Cat. No. 047; Harlan, Indianapolis, IN, USA), C57BL/6J (Cat. No. 000664; Jackson Laboratory, Bar Harbor, ME, USA), and C57BL/6J PPARα$^{-/-}$ (Cat. No. 08154; Jackson Laboratory, Bar Harbor, ME, USA) mice aged 6-8 weeks old were housed 2-3 per cage under standard conditions with food and water available *ad libitum*.

3.2.2 10(*Z*)-hexadecenoic acid

Unless otherwise noted, reagents were obtained commercially and used without further purification. Dichloromethane (CH2Cl2) was distilled over calcium hydride (CaH2) under a nitrogen atmosphere. Tetrahydrofuran (THF; (CH2)4O) was distilled from sodium-benzophenone under a nitrogen atmosphere. Thin-layer chromatography analysis of reaction mixtures was performed on Dynamic Adsorbents, Inc., silica gel F-254 TLC plates. Flash chromatography was carried out on Zeoprep 60 ECO silica gel. 1H spectra were recorded with a Varian INOVA 500 spectrometer. Compounds were detected by monitoring UV absorbance at 254 nm.

To a 5 mL sealed tube containing 1-heptene (0.50 mL, 3.55 mmol), methyl 10-undecenoate (0.080 mL, 0.36 mmol) and 0.35 mL THF was added to a Grubbs Z-selective metathesis catalyst (2.2 mg, 3.48 µmol, Sigma-Aldrich, Cat. No. 771082). The reaction was stirred at 45 oC for 8 h before cooling to room temperature. The slurry was filtrated through a short plug of silica gel and concentrated. The obtained oil was dissolved in 1.0 mL THF. The solution was cooled to 0 oC, then 9-borabicyclo[3.3.1]nonane (9-BBN) solution in THF (1.28 mL, 0.50 M, 0.64 mmol)

was added. After 2 h stirring at 0 oC, the reaction was quenched with 60 µL EtOH, then 1.5 mL pH 7 potassium phosphate buffer and 1.5 mL 30% H2O2. The mixture was stirred at room temperature for 12 h, then extracted with 5 mL EtOAc three times. The combined organic layers were washed with 4 mL saturated Na2S2O3 and 3 mL brine, then dried over Na2SO4, filtered and concentrated. To the crude oil in 1.0 mL THF was added LiOH monohydrate (38 mg, 0.90 mmol) in 1.0 mL water. After 2 h, the reaction solution was cooled to 0 oC before addition of 0.91 mL 1.0 N HCl. After being concentrated under reduced pressure, the aqueous solution was saturated with NaCl and extracted with 3 mL dichloromethane three times. The combined organic layers were dried over Na2SO4, filtered and concentrated. Purification by flash chromatography (2:1:1 hexanes/dichloromethane/diethyl ether) provided (10Z)-hexadec-10-enoic acid (0.022 g, 90%) as a colorless oil. 1H NMR (500 MHz, CDCl3): δ 5.48 – 5.22 (m, 2H), 2.35 (t, J = 7.5 Hz, 2H), 2.01 (q, J = 6.6 Hz, 4H), 1.63 (p, J = 7.4 Hz, 2H), 1.35 – 1.15 (m, 16H), 0.88 (t, J = 6.9 Hz, 3H).

3.2.3 Macrophage stimulation assay

Murine peritoneal macrophages were isolated as previously described (Zhang et al., 2008) and used to determine the effects of 10(*Z*)-hexadecenoic acid on LPS-induced IL-6 secretion (Fig. 2.3G). Briefly, mice received one 1 ml i.p. injection of 3% thioglycollate medium (Cat. No. 9000-294, VWR, Radnor, PA, USA). Ninety-six hours later, macrophages were collected in DPBS (Cat. No. 14190136, Invitrogen, Carlsbad, CA, USA). Cells were centrifuged and resuspended in DMEM/F-12 (Cat. No. 10565018, Invitrogen) supplemented to be 10% (v/v) fetal bovine serum (Cat. No. 16000036, Invitrogen) and 1% penicillin/streptomycin (Cat.No. 15140148, Invitrogen). One mouse yielded enough cells for one experimental replicate. All

incubation occurred at 37°C and 5% CO_2. $1x10^5$ cells/well were allowed to adhere for 1.5 h before being washed with DPBS. 10(*Z*)-hexadecenoic acid was dissolved in DMEM/F-12 with 0.5% (v/v) dimethyl sulfoxide (Cat. No. D8418, Sigma-Aldrich). The macrophages were incubated with either 50 μM or 200 μM 10(*Z*)-hexadecenoic acid, as specified in the text, or DMEM/F-12 (0.2% DMSO) for 1 h before being stimulated with either 1 μg/ml lipopolysaccharide (serotype 0127:B8, Sigma-Aldrich, St. Louis, MO, USA) or DMEM/F-12. Culture supernatants were collected 12 h post-stimulation.

3.2.4 Cytokine ELISA

Cytokine concentrations in cell culture supernatants from freshly isolated peritoneal macrophages were measured using sandwiched ELISA (Cat. No. 431304, Biolegend, San Diego, CA, USA). Samples were diluted 1:200 for measurement of IL-6, and undiluted for measurement of IL-10. All samples were measured in duplicate.

3.2.5 RNA extraction and library preparation

Total RNA content of $1x10^5$ macrophages treated with 10(*Z*)-hexadecenoic acid (utilizing separate macrophage preparations from n = 3 mice) or vehicle (utilizing separate macrophage preparations from n = 3 mice) was extracted using TRI Reagent® (Cat. No. T9424, Sigma-Aldrich) according to manufacturer's instructions. The RNA input was quantified on a Qubit™ 3.0 Fluorometer (Cat. No. Q33216, Thermo Fisher) to ensure there was sufficient starting material. The RNA sequencing libraries were generated with the NEBNext rRNA Depletion Kit (Cat. No. E6310, New England BioLabs) in order to enrich the samples in mRNA, and NEBNext Ultra Directional RNA Library Prep Kit for Illumina (Cat. No. 7240, New England BioLabs). Briefly, mRNA was purified from 100 ng of total RNA, fragmented, and converted to double

stranded cDNA. Barcodes were ligated to the cDNA fragments, and prior to PCR enrichment of the library, the cDNA product was quantified on a Qubit 3.0 Fluorometer. The length distribution of the purified oligo libraries were evaluated on an Agilent Bioanalyzer 2100 (Cat. No. G2939BA, Agilent).

3.2.6 Sequencing

Libraries were sequenced at the Next Generation Sequencing Facility at the University of Colorado Boulder. The libraries were multiplexed and sequenced on an Illumina HiSeq 2000 Sequencing System (Cat. No. SY-401-1001, Illumina). For each sample, pair-end 100-bp reads were sequenced using V3 chemistry.

3.2.7 RNA read processing, mapping, and differential expression

Quality analysis of sequencing data was done using FastQC. The adaptors and low quality raw reads were cut with Trimmomatic (version 0.32) (Bolger et al., 2014). The reads were aligned to the mouse genome, mm10 (University of California, Santa Cruz, CA, USA), using the TopHat2 sequence aligner (version 2.0.6) (Kim et al., 2013). The Bowtie2 alignment option was set to ‘sensitive’, the expected inner distance was set to 200bp, the library type was specified as unstranded, and mm10 GTF (University of California, Santa Cruz) was provided for genome annotations. After mapping, alignment files were processed using SAMtools (version 0.1.16) (Li et al., 2009). Lastly, the reads mapping to exons were counted with HTseq (version 0.6.1) (Anders et al., 2015) using the options: reverse stranded and ‘intersection-nonempty’ mode. Differentially expressed genes were identified using the R package, DESeq (version 1.28.0) (Anders and Huber, 2010), using the default parameters.

3.2.8 Pathway analysis

The online resource DAVID (version 6.8) (Huang et al., 2007) and desktop version of GSEA (version 2.2.4) (Subramanian et al., 2005) were used to analyze the differential expression data. Brielfy, DAVID pathway analysis was performed separately with the gene IDs of the most significant upregulated and downregulated genes using the default parameters. For GSEA, the normalized gene counts were used and enrichment was calculated based on gene set permutations.

3.2.9 Transfections and reporter gene assays

Cells were transfected with the following receptor and reporter constructs: Gal4-PPARα-LBD, Gal4-PPARγ-LBD, Gal4-PPARδ-LBD, Gal4-RARα-LBD, pMH100-TK-luc, and pCMX-β-galactosidase (Chen and Evans, 1995). All transfection experiments were performed with COS1 cells using polyethylenimine (Sigma-Aldrich) reagent (Szatmari et al., 2006). After 6–8 h of the transfection, the medium was replaced with DMEM medium containing the indicated ligands or vehicle (as control) (Benko et al., 2003; Chen and Evans, 1995). Cells were lysed and assayed for reporter expression 18 h after transfection. The luciferase assay system (Promega, Madison, WI, USA) was used as described previously (Nagy et al., 1999). Measurements were carried out with a Wallac Victor-2, multilabel counter. Luciferase activity of each sample was normalized to the β-galactosidase activity.

3.2.10 Pharmacologic inhibition of PPARs

In the pharmacologic inhibition studies, macrophages were harvested and cultured as before, but after washing the cells, they were treated with either GW 6471 (PPARα antagonist, Cat. No. 4618, Tocris), GW 9662 (PPARγ antagonist, Cat. No. 1508, Tocris), GSK 0660 (PPARδ

antagonist, 3433, Tocris), or vehicle (DMEM/F-12, 0.2% DMSO). Antagonists were prepared to 5x or 20x their reported IC_{50}. After a 1 h incubation period, cells were treated with 200 μM 10(*Z*)-hexadecenoic acid, or a PPAR agonist corresponding to the PPAR antagonists listed above, WY 14643 (PPARα agonist, Cat. No. 1312, Tocris), rosiglitazone (PPARγ agonist, Cat. No. 5325, Tocris), GW 0742 (PPARδ agonist, Cat. No. 0742), or vehicle. Agonists were prepared to 1x, 2x, 5x, and 10x their respective EC_{50}. After a 1 h incubation period, cells were stimulated with either 1 μg/ml lipopolysaccharide (serotype 0127:B8, Sigma-Aldrich, St. Louis, MO, USA) or DMEM/F-12. Culture supernatants were collected 12 h post-stimulation.

3.2.11 Statistical analysis

Data are presented as means ± SEM or means + SEM. Data were subjected to a normality test and one-way, multifactor, and repeated measures ANOVA, followed by Fisher's least significant difference (LSD) tests were performed as appropriate. A two-tailed p value < 0.05 was considered significant.

3.3 Results

3.3.1 10(*Z*)-hexadecenoic acid suppresses LPS-induced inflammation

We had previously seen that the *M. vaccae* derived lipid, 10(*Z*)-hexadecenoic acid, suppressed secretion of IL-6 in a macrophage model of inflammation. Here we used RNA-Seq to identify potential receptors and pathways involved in the anti-inflammatory effect. Freshly isolated murine peritoneal macrophages were treated with 200 μM 10(*Z*)-hexadecenoic acid for 1 h, before being stimulated with 1 μg/ml LPS. IL-6 secretion was measured 12 h, and 24 h after LPS stimulation. There was a 49±12% and 36±6% inhibition of IL-6 after 12 h and 24 h,

respectively. For the RNA-Seq library preparation, the 12h time point was preferred over the 24h time point to identify earlier changes in steady-state mRNA levels.

For each treatment condition, vehicle with 1 μg/ml LPS or 200 μM 10(*Z*)-hexadecenoic acid with 1 μg/ml LPS, there was a sample size of 3 freshly isolated macrophage preparations, with each preparation from a different mouse. The sequencing libraries were prepared with an rRNA depletion protocol that also preserves mRNA directionality. The libraries were sequenced in a 100bp paired-end experiment on an Illumina HiSeq 2000 sequencing system. The number of raw sequences obtained from the prepared libraries ranged from 51.36 to 63.70 million reads. The average sequencing depth was 2.11 bases. After mapping the reads, the percentage of reads that were successfully paired and mapped ranged from 69.01% to 70.97%.

Differentially expressed transcripts were identified using the R package, DESeq (version 1.28.0) (Anders and Huber, 2010). Two hundred and three genes were found to be differentially expressed with an FDR-adjusted $p < 0.05$, and 719 with an unadjusted $p < 0.05$. Of the 203 differentially expressed genes, 109 were downregulated with 200 μM 10(*Z*)-hexadecenoic acid treatment and 94 were upregulated. The dispersion estimates and MA plot of mean gene counts are presented in Fig. 3.1. The top 10 most significant genes are reported in Table 5.1 (all 203 genes with $q < 0.05$ are listed in Appendix 3). Five of the top 10 most significant genes are related to inflammation, three of which were downregulated, and two of which were upregulated. The first downregulated gene was IL-6. Interestingly, there was ~4x less IL-6 mRNA in cells treated with 10(*Z*)-hexadecenoic acid compared to ~0.5x less IL-6 protein released from the cell, based on previous studies. The second downregulated inflammation-related mRNA was *ptgs2*, encoding prostaglandin-endoperoxide synthase 2 (i.e. Cox-2). Cox-2 is responsible for the

generation of many classes of prostaglandins, which are associated with initiating inflammation (Lee et al., 2001). The last downregulated inflammation-related gene was *socs1*, encoding cytokine inducible SH2-containing protein, which is unique from the previous two in the sense that it negatively regulates cytokine signaling (Kazi et al., 2014). It belongs to a family of proteins called suppressors of cytokine signaling (SOCS), of which Socs1, Socs2, and Socs3 are all downregulated. The last 2 of these 5 inflammation-related genes are associated with anti-inflammatory processes and were upregulated. *Tsc22d3* was upregulated and is known to be induced by glucocorticoids, hence the alias glucocorticoid-induced leucine zipper (Gilz). Tsc22d3 regulates inflammation through formation of heterodimers with proinflammatory transcription factors, like nuclear factor κB (NF-κB) (Riccardi, 2015). The second upregulated inflammation-related gene was *dusp1*, which has broad phosphatase activity primarily affecting downstream targets of TLR4, thus inhibiting inflammation (Hammer et al., 2006). Outside the context of inflammation, but relevant to lipid-mediated signaling, is the gene perilipin 2, which is a direct target of PPARα (McMullen et al., 2014). In order to recognize a broader pattern among the differentially expressed genes, we employed several pathway analysis tools.

Table 3.1. Proinflammatory cytokine and chemokine ligand mRNAs downregulated by preincubation of freshly isolated murine peritoneal macrophages with 10(*Z*)-hexadecenoic acid prior to stimulation with lipopolysaccharide (selected from 203 differentially expressed mRNAs; FDR-adjusted $p < 0.1$)

#	Ensembl ID	Mean #Reads LPS (n =3)	Mean #Reads s148.2ffa +LPS (n = 3)	Effect	Log2 Fold-change	*p* value	Adjusted *p* value	Gene
2	ENSMUSG00000025746	1302	305	↓	-2.09	4.19E-23	4.37E-19	Il6
13	ENSMUSG00000027398	15,957	5349	↓	-2.16	4.03E-15	6.48E-12	Il1b
21	ENSMUSG00000035373	1182	441	↓	-1.42	3.37E-12	3.35E-9	Ccl7
22	ENSMUSG00000035385	5656	2234	↓	-1.34	5.18E-12	4.91E-9	Ccl2
26	ENSMUSG00000027776	714	268	↓	-1.42	5.70E-11	4.57E-8	Il12a
33	ENSMUSG00000031779	327	117	↓	-1.48	5.15E-10	3.26E-7	Ccl22
47	ENSMUSG00000018927	810	368	↓	-1.14	5.31E-8	2.36E-5	Ccl6
59	ENSMUSG00000024401	2098	1023	↓	-1.04	2.95E-7	1.04E-4	Tnf
61	ENSMUSG00000031780	24	3	↓	-3.08	3.97E-7	1.34E-4	Ccl17
67	ENSMUSG00000027399	16533	8500	↓	-0.96	1.02E-6	3.19E-4	Il1a
72	ENSMUSG00000021356	87	30	↓	-1.53	2.27E-06	6.56E-4	Irf4
77	ENSMUSG00000018930	603	305	↓	-0.98	3.75E-6	1.02E-3	Ccl4
90	ENSMUSG00000038067	215	102	↓	-1.06	1.51E-05	3.5E-4	Csf3
91	ENSMUSG00000004371	26	5	↓	-2.35	1.59E-5	3.7E-3	Il11
99	ENSMUSG00000058427	4726	2680	↓	-0.82	3.01E-5	6.4E-3	Cxcl2[1]

138	ENSMUSG00000018916	26	6	↓	-2.12	1.54E-4	2.3E-2	Csf2
142	ENSMUSG00000000982	6693	4067	↓	-0.72	1.99E-4	2.9E-2	Ccl3
158	ENSMUSG00000025225	916	556	↓	-0.72	3.85E-4	5.1E-2	Nfkb2
163	ENSMUSG00000004296	78	36	↓	-1.11	4.05E-4	5.2E-2	Il12b
167	ENSMUSG00000041515	776	475	↓	-0.71	4.56E-4	5.7E-2	Irf8
174	ENSMUSG00000020826	5417	3382	↓	-0.68	5.5E-4	6.6E-2	Nos2
193	ENSMUSG00000029379	8342	5215	↓	-0.68	7.68E-4	8.3E-2	Cxcl3

[1]Cxcl2 is a functional homologue of human IL-8

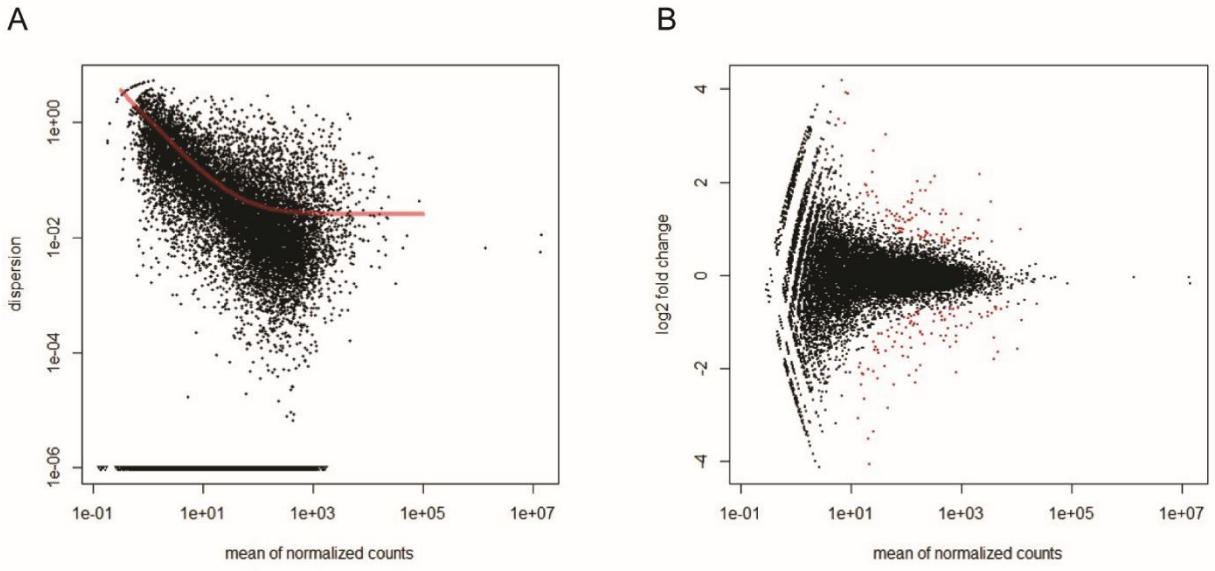

Figure 3.1 Differential expression of 10(*Z*)-hexadecenoic acid-treated and vehicle-treated cells in the presence of LPS.
Macrophage cultures were treated with either 10(*Z*)-hexadecenoic acid or vehicle (DMEM/F-12, 0.2% DMSO). After a1 h incubation, macrophages were stimulated with lipopolysaccharide (LPS; 0.1 μg/ml). (A) Dispersion estimates for all reads. The red line is the negative binomial estimator function. (B) MA plot of differentially expressed genes. Genes with an FDR-adjusted *p*-value, $q < 0.05$ are shown in red.

Table 3.2. Top 10 differentially expressed genes of freshly isolated murine peritoneal macrophages preincubated with 10(*Z*)-hexadecenoic acid prior to stimulation with lipopolysaccharide

Gene name	Gene symbol	Log2 fold change	FDR-adjusted *p*-value (*q*)
haptoglobin	Hp	2.155269	2.26E-21
interleukin 6	IL6	-2.09473	4.37E-19
TSC22 domain family, member 3	TSC22D3	2.132848	3.67E-17
prostaglandin-endoperoxide synthase 2	PTGS2	-1.81185	8.08E-16
cytokine inducible SH2-containing protein	CISH	-2.30575	4.38E-15
dual specificity phosphatase 1	DUSP1	1.986963	1.67E-14
ADAMTS-like 4	ADAMTSL4	2.012712	1.86E-12
Mir5105		-1.645503	1.98E-12
vanin 3	VNN3	-2.04621	2.63E-12
perilipin 2	PLIN2	1.578041	2.63E-12

Our first approach towards identifying cellular pathways significantly affected by treatment with200 200 µM 10(*Z*)-hexadecenoic acid in LPS-stimulated macrophages was to use the web-based platform DAVID (Huang et al., 2007, 2009). The list of 203 FDR-adjusted significant genes was used for the analysis. 40 KEGG pathways (Table A3.2) were enriched in the gene list. Twenty-nine of the 40 had an FDR < 10%—many of which were related to infection, but 6 of the most enriched pathways include broad, overlapping inflammatory processes. These included cytokine-cytokine receptor interaction (KEGG: mmu04060), TNF signaling pathway (KEGG: mmu04668), TLR signaling pathway (KEGG: mmu04620), Jak-STAT signaling pathway

(KEGG: mmu04630), chemokine signaling pathway (KEGG: mmu04062), and NF-κB signaling pathway (KEGG: mmu04064). Every gene identified in these pathways was downregulated with 10(*Z*)-hexadecenoic acid treatment.

Overall, there was clear downregulation of inflammatory pathways. Only two pathways were enriched with genes upregulated by 200 μM 10(*Z*)-hexadecenoic acid, PPAR and mitogen activated protein kinase (MAPK) signaling. Eight genes associated with MAPK signaling were downregulated with 10(*Z*)-hexadecenoic acid treatment, but 3 genes were upregulated, Fos, CACN (a calcium channel) and Dusp1. Dusp1 specifically inhibits activation of MAP kinases. Based on these findings from RNA-Seq analysis, PPARs are viable candidates for receptors for 10(*Z*)-hexadecenoic acid.

In this exploratory phase of analysis, we also used Gene Set Enrichment Analysis (GSEA) to identify Gene Ontologies (GO), pathways, and published gene sets that are enriched in our gene expression data (Subramanian et al., 2005). The normalized gene expression data from DESeq was queried against each of the GSEA gene set collections.

From the GSEA pathways database (c2.cp.kegg.v6.0), the top 5 enriched gene sets for the 10(*Z*)-hexadecenoic acid phenotype were: “peroxisome” (KEGG: hsa04146), “ppar_signaling_pathway” (KEGG: hsa03320), “citrate_cycle_tca_cycle” (KEGG: hsa00020), “fatty_acid_metabolism” (KEGG: hsa00071), and “propanoate_metabolism” (KEGG: hsa00640), a short chain fatty acid (Fig. 3.2A). All 5 gene sets were significant with an unadjusted p value < 0.05, but failed to reach significance using FDR-adjusted p values; nevertheless, there was a pattern of lipid metabolism. We also searched against the collection of transcription factor binding motifs (c3.tft.v6.0), which revealed enriched CREB, Gfi1, and

PPARα *cis*-regulatory motifs upstream of the genes upregulated with 10(*Z*)-hexadecenoic acid treatment in LPS-stimulated macrophages. Again, these were nominally significant (i.e. $p < 0.05$; $q > 0.05$), but these findings bolster PPARs, and specifically PPARα, as a potential receptor mediating anti-inflammatory effects of 10(*Z*)-hexadecenoic acid. Gfi1, is also an interesting result, as it has been shown to be an antagonist of NF-κB binding to NF-κB responsive elements in target gene promoters (Sharif-Askari et al., 2010). Lastly, we searched for gene set enrichments among the curated collection of immunologic signatures (c7.all.v6.0). This returned 40 gene sets that were significantly enriched at < 10% FDR, 11 of which involved macrophages as the model system. A common theme among the gene sets was cytokine signaling. Seven of these 11 came from a study exploring STAT3 activation. For example, there is significant enrichment for genes upregulated in *IL-6*$^{-/-}$ macrophages stimulated with IL-10 and LPS compared to an IL-10 KO with the same stimuli (Fig. 3.2) (GSE5589_3015_200_DN) (El Kasmi et al., 2006). While both IL-10 and IL-6 can activate STAT3 to produce an anti-inflammatory response, the authors suggest there are separate pathways towards that end. The pattern of genes upregulated during 10(*Z*)-hexadecenoic acid and LPS stimulation is more similar to IL-10 mediated STAT3 activation. Furthermore, this gene set significantly overlaps with the KEGG PPAR Signaling Pathway (hsa03320) ($q < 0.001$).

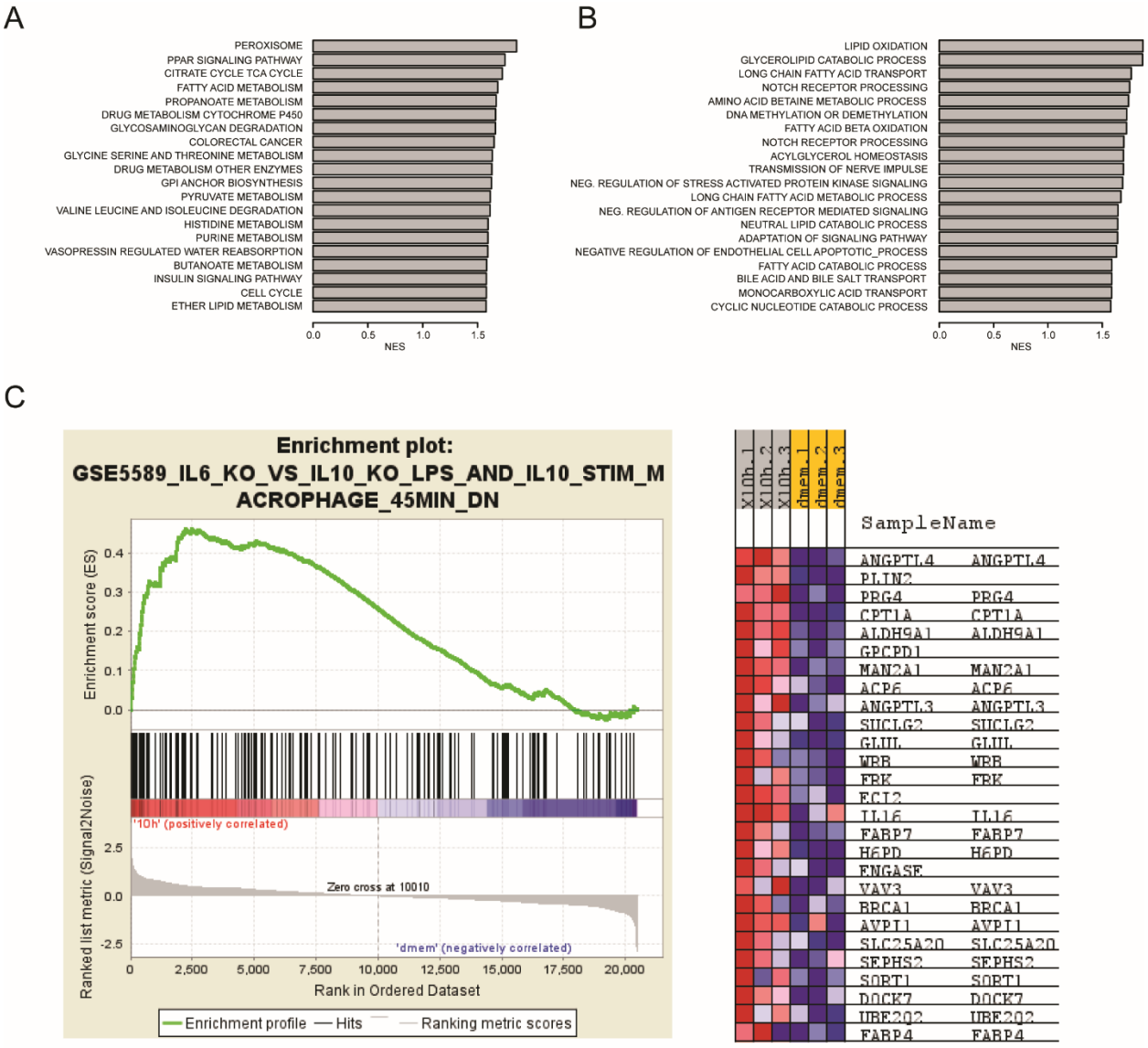

Figure 3.2 Summary of GSEA results enriched for LPS-stimulated macrophages pretreated with 10(*Z*)-hexadecenoic acid.
(A) Top 20 KEGG pathways enriched in LPS-stimulated macrophages pretreated with 10(*Z*)-hexadecenoic acid. (B) Top 20 GO "biological process" terms enriched in LPS-stimulated macrophages pretreated with 10(*Z*)-hexadecenoic acid. (C) Significant enrichment of an immunologic gene set in the 10(*Z*)-hexadecenoic acid pretreatment group. The vertical lines indicate genes represented in both gene sets. Shared genes with a positive fold change are shown more to the left and shared genes with the largest negative fold change are shown on the right. The top 27 shared genes with positive fold changes are shown in the heatmap.

We also searched the GSEA collections for gene sets enriched in the vehicle-pretreated, LPS-stimulated phenotype. From the KEGG pathways collection (c2.cp.kegg.v6.0) and

transcription factor binding motifs (c3.tft.v6.0) databases, similar trends to the DAVID analysis were revealed. There was enrichment for the NF-κB pathway as well enrichment for genes with NF-κB and IRF_Q6 transcription binding motifs at FDR < 25% (Fig. 3.3C). It was unclear whether the IRF-regulated genes are associated with type I, II, or III interferon response. We would expect a type I response, as the type I interferons are regulated by IRF3/7, which is activated downstream of TLR4. This was addressed by uploading the genes with the IRF_Q6 transcription factor binding site to Interferome (version 2.01), a database of type I, II, and III interferon regulated genes (Rusinova et al., 2013). All genes were found in the database, with 29% associated with a type I response, 23% associated with a type II response, and the plurality 45% associated with both type I and II responses (Fig. 3.3D). The ambiguity between the type I and type II response may be clarified by the significant upregulation ($p < 0.05$) of the type II interferon, IFNγ, and in the vehicle-treated phenotype and non-significant difference between expression of type I interferons. Furthermore, a gene set enrichment analysis for the canonical IFNα response revealed that many of the genes are found towards the middle of the ranked gene list (i.e. genes that are expressed at similar levels in both treatment groups)() (Fig. 3.3C). Together, this shows that the type II interferon response, which is activated downstream of the NF-κB target IL-12 is upregulated in the vehicle treated phenotype, and the type I response is relatively unchanged between vehicle and 10(*Z*)-hexadecenoic acid treatment (Ye et al., 1995). Lastly, we searched against the curated immunologic gene sets (c7.all.v6.0). The most significant enrichment was for genes upregulated in macrophages unstimulated vs. stimulated with LPS (Buxadé et al., 2012).

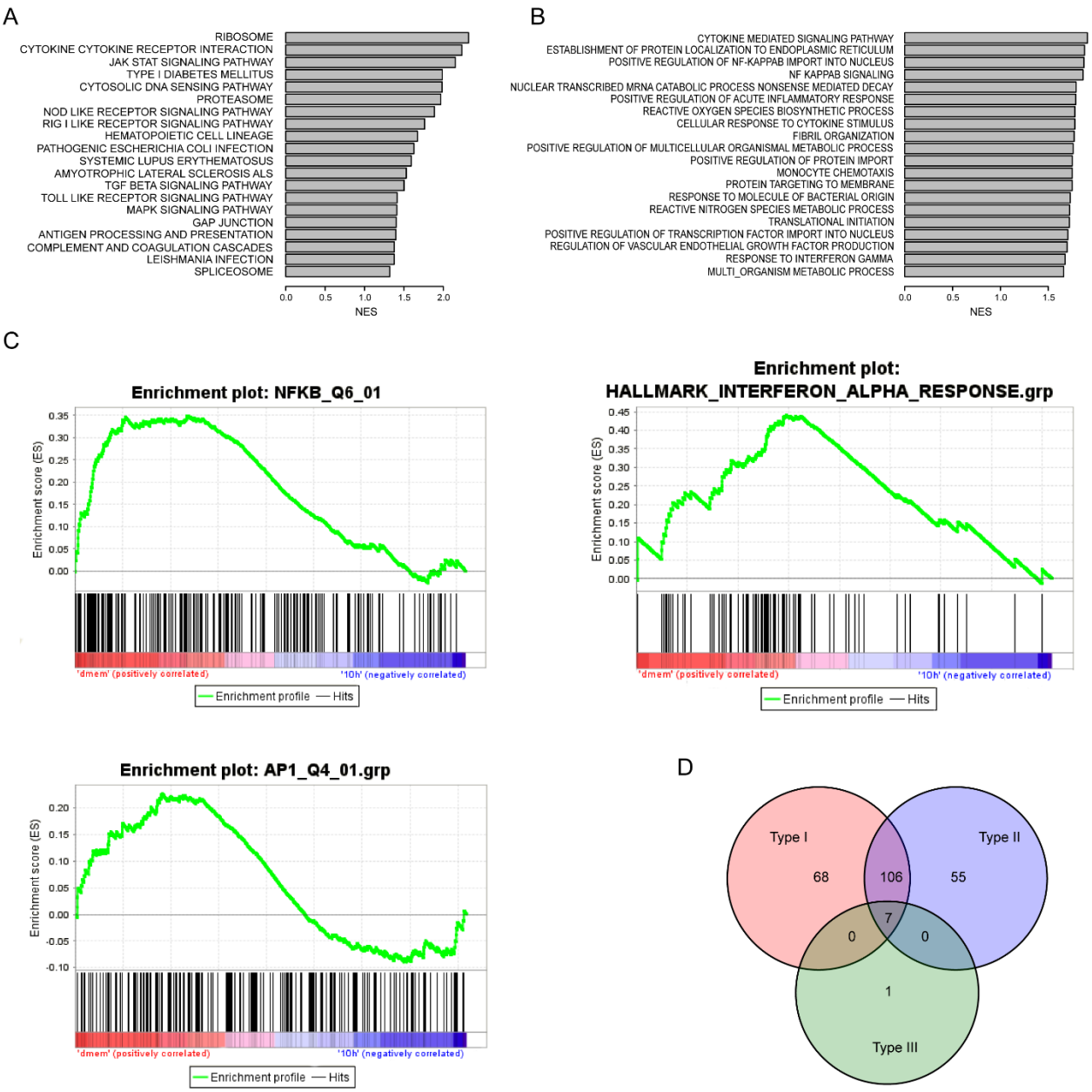

Figure 3.3 Summary of GSEA results enriched for vehicle ("DMEM") pretreatment of LPS-stimulated macrophages.

(A) Top 20 KEGG pathways enriched for the DMEM phenotype. (B) Top 20 GO "biological process" terms enriched for the DMEM phenotype. (C) Gene set enrichment for the three major downstream pathways of TLR4 activation: NF-κB, IRF, and AP-1. Vertical black lines indicate specific genes in the ranked gene list that are also found in indicated gene set. Enrichment profiles that skew to the left (red) are genes upregulated in vehicle-treated cells, skews to right represent genes upregulated in the 10(*Z*)-hexadecenoic acid treatment (blue), and enrichment profiles that peak in the center indicate genes that equally expressed in both treatment groups. (D) Venn diagram of genes enriched for the IRF_Q6

transcription factor binding site and their association with Type I, II, or III interferon response. Abbreviations: NES, normalized enrichment score.

As many of the GSEA gene sets involve similar experimental conditions and outcomes, we built gene set interaction networks to determine which of the enriched gene sets overlapped the most (Figure 3.3). From this macroscopic perspective, we observed broad downregulation of genes associated with cytokine signaling, as the central node of these gene sets is the JAK/STAT pathway (Figure 5.4A). In the network visualization of pathway gene sets upregulated with 10(*Z*)-hexadecenoic acid treatment, the central node is "Metabolism of lipids and lipoproteins". Many of the surrounding nodes involve the peroxisome and PPAR pathways. It is evident that upregulation of PPAR targets is correlated with downregulation of cytokine and NF-κB targets, but these data cannot explain how or if PPAR pathways affect inflammatory processes.

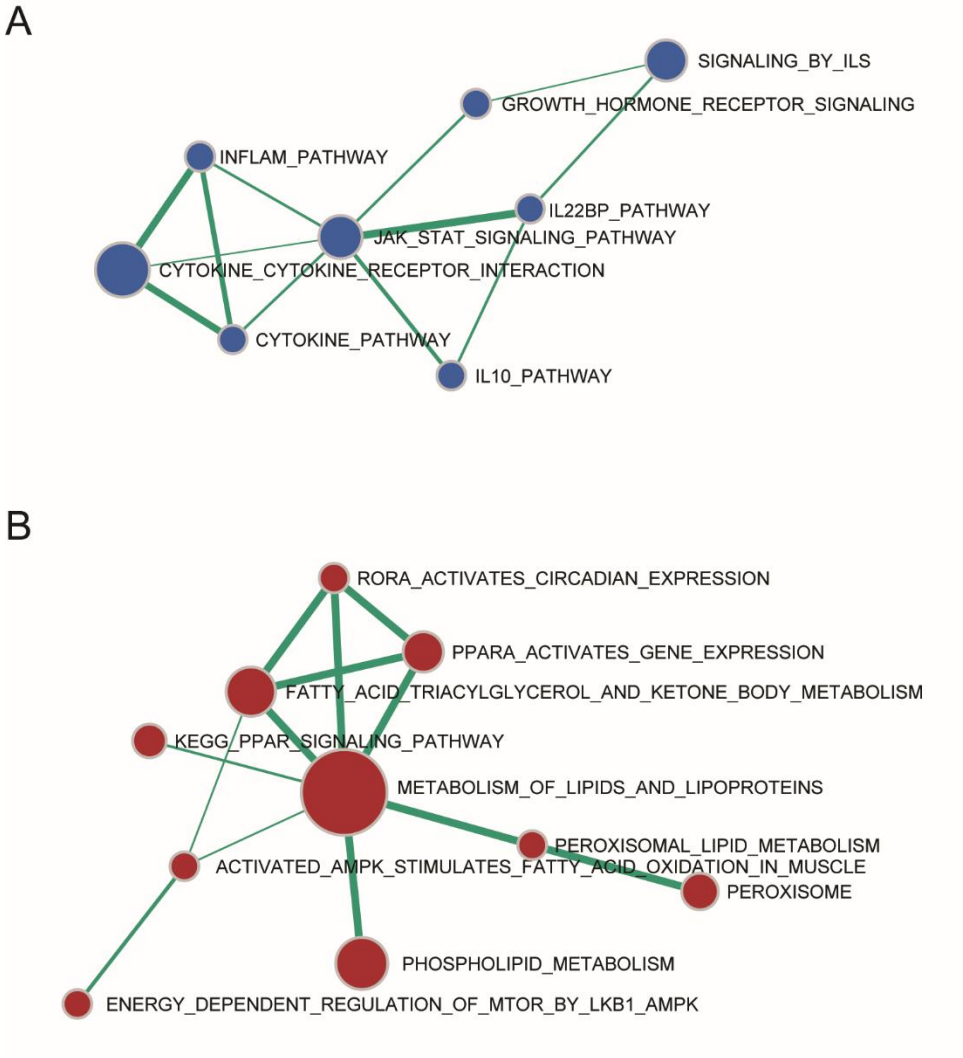

Figure 3.4 Network visualizations of related gene set enrichments.
Network visualizations of enriched gene sets were made with Cytoscape (Smoot et al., 2011). The sizes of the circles represent the number of genes in the gene set, and the thickness of the lines represents the number of genes two nodes share. (A) Overlapping KEGG pathways that are downregulated with treatment of 10(Z)-hexadecenoic acid. (B) Overlapping KEGG pathways upregulated with treatment of 10(Z)-hexadecenoic acid.

3.3.2 10(*Z*)-hexadecenoic acid activates PPARα

As described above, analysis of the effects of 10(*Z*)-hexadecenoic acid on LPS-induced transcriptional changes in freshly isolated murine peritoneal macrophages, using RNA-Seq, revealed PPAR signaling as a potential mediator of 10(*Z*)-hexadecenoic acid. Fatty acids can

modulate inflammation via the activation of nuclear hormone receptors. Therefore we assessed the nuclear receptor activation capacity of 10(*Z*)-hexadecenoic acid and its derivatives. We conducted reporter gene assays via the transfection of COS1 cells using GAL4-fusion ligand binding domains (LBDs) of various lipid-activated nuclear receptors (PPARα-LBD, PPARγ-LBD, PPARδ-LBD and RARα-LBD) along with a plasmid carrying MH100-TK-luciferase reporter (Chen and Evans, 1995). Transfected cells were incubated with 1-mono-[*Z*-10-hexadecenoyl]glycerol (PI-69), 1,2,3-tri[*Z*-10-hexadecenoyl]glycerol (PI-70), or 10(*Z*)-hexadecenoic acid (PI-71) for 18 h and relative luciferase activity, normalized to β-galactosidase activity, was measured. 10(*Z*)-hexadecenoic acid (PI-71), and 1-[*Z*-10-hexadecenoyl]glycerol (PI-69), at concentrations of 80 μM, reliably increased PPARα-, but not PPARγ-, PPARδ, or RARα-regulated reporter expression (Fig. 3.5). The triglyceride had no effect (Fig. 3.5). Together, these results demonstrate that 10(*Z*)-hexadecenoic acid and its monoacylglycerol form selectively activate the PPARα receptor signaling.

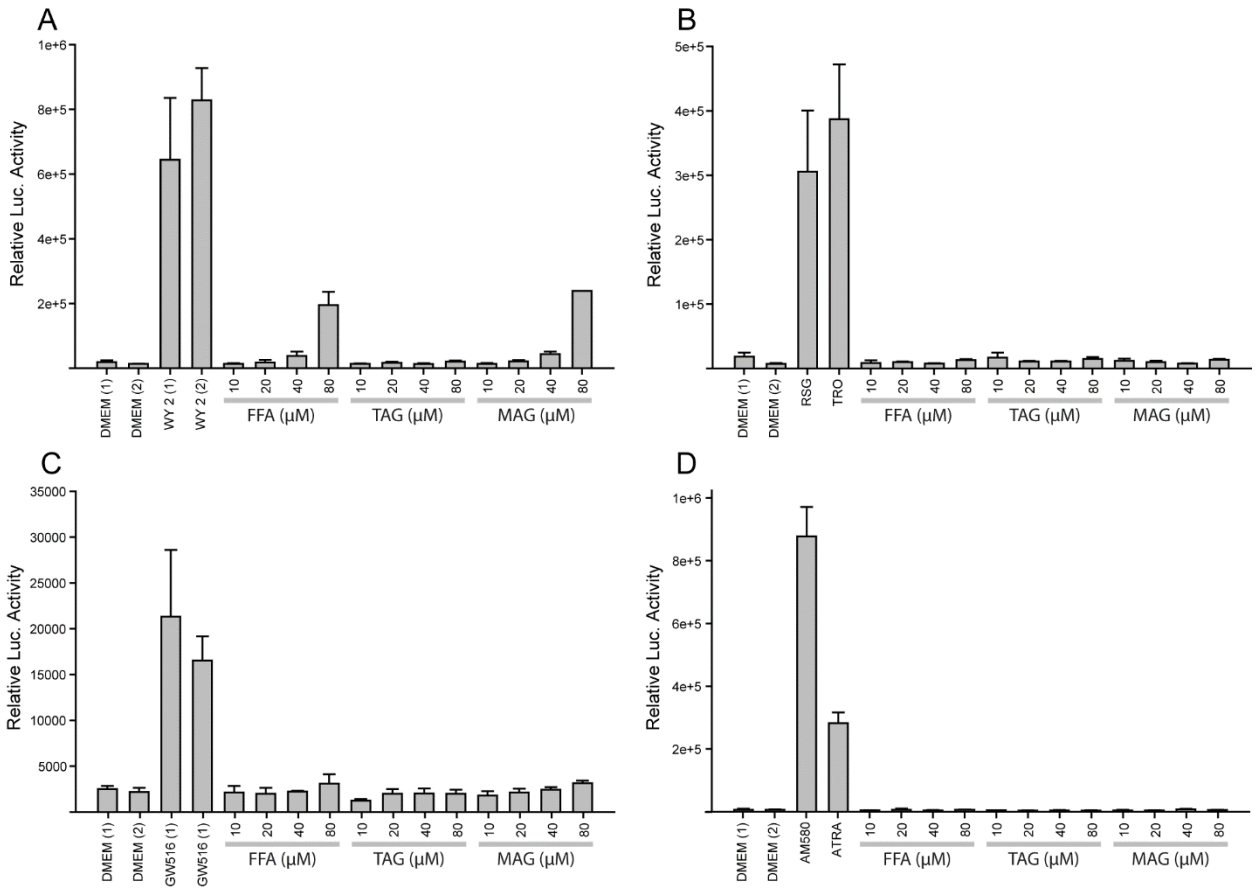

Figure 3.5 Analysis of the effects of *M. vaccae*-derived lipids on PPARα, PPARγ, PPARδ, and RARα signaling in transfection assays using COS-1 cells.
(A) Relative activity of PPARα following incubation with 1-[*Z*-10-hexadecenoyl]glycerol (PI-69; MAG), 1,2,3-tri[*Z*-10-hexadecenoyl]glycerol (PI-70; TAG), or 10(Z)-hexadecenoic acid (PI-71; FFA) for 18 h, expressed as relative luciferase activity, normalized to β-galactosidase activity. (B) Relative activity of PPARγ. (C) Relative activity of PPARδ. (D) Relative activity of RARα. Abbreviations: AM580 (RARα-specific agonist, 100 nM), ATRA, all-trans retinoic acid (RARα agonist, 100 nM), GW1516 (PPARδ agonist, 1 μM), RSG, rosiglitazone (PPARγ agonist, 2.5 μM), TRO, troglitazone (PPARγ agonist, 10 μM), WY, WY14643 (PPARα agonist, 2 μM). Data are representative of 2-3 replicates per experiment.

3.3.3 Anti-inflammatory effects of 10(*Z*)-hexadecenoic acid are dependent on PPARα

After determining 10(*Z*)-hexadecenoic acid to be a ligand of PPARα, we investigated if this interaction was necessary for inhibiting LPS-stimulated release of IL-6. Pharmacological agonists and antagonists of each PPAR were used to test if PPARα has a singular role in this process. The agonists and antagonists and their receptor specificities are listed in Table 5.2.

Macrophages were incubated with a single PPAR antagonist for 1 h prior to treatment with either 200 μM 10(*Z*)-hexadecenoic acid or a PPAR agonist corresponding to its respective PPAR antagonist. After another 1 h incubation period, the cells were stimulated with LPS, and IL-6 was measured 12 h later. Antagonists were assayed at 5x and 20x the IC_{50}. When tested in combination with 10(*Z*)-hexadecenoic acid, there was a main effect of antagonist using multifactor ANOVA ($F_{2,35} = 4.939$, $p < 0.05$). To test the effects of the selective PPAR agonists, the 20x concentration antagonist was used, and agonists were assayed at 1x, 2x, 5x, and 10x the EC_{50}. In an SRB cytotoxicity assay, none of the treatment combinations had a significant effect on cell viability. To test for an effect of agonist concentration, we used a multifactor repeated measures ANOVA with the repeated effect, concentration, measured on the three different agonist classes. Regardless of the agonist, concentration was not significant. To test for an effect of agonist, we used a multifactor repeated measures ANOVA, with the repeated effect, agonist class, measured on the four different concentrations. The agonist was significant at every level of agonist concentration (1x, $F_{(1.829,18.292)} = 13.183$, $p < 0.001$; 2x, $F_{(1.732,17.323)} = 10.702$, $p < 0.001$; 5x, $F_{(1.800,18.002)} = 27.817$, $p < 0.001$; 10x, $F_{(1.677,16.768)} = 27.374$, $p < 0.001$). The agonist*antagonist interaction term was also significant in this model at the 1x concentration ($F_{(1.829, 18.292)} = 3.941$, $p < 0.05$). From here, we used repeated measure ANOVAs to model each separate agonist class and found the effect of antagonist to be significant for the PPARα agonist, WY 14643. There was no effect of the PPARγ antagonist, GW9662, or the PPARδ antagonist, GSK0660.

Table 3.3. Selective PPAR antagonists and agonists.

	Antagonist		Agonist	
	Name	IC_{50}	Name	EC_{50}
PPARα	GW 6471 (Cat. No. 4618)	0.24 μM[1]	WY 14643 (Cat. No. 1312)	0.63 μM[1]
PPARγ	GW 9662 (Cat. No. 1508)	3.3 nM[1]	Rosiglitazone (Cat. No. 5325)	60 nM[1]
PPARδ	GSK 0660 (Cat. No. 3433)	0.16 μM[1]	GW 0742 (Cat. No. 2229)	1 nM[1]

[1]According to manufacturer information.

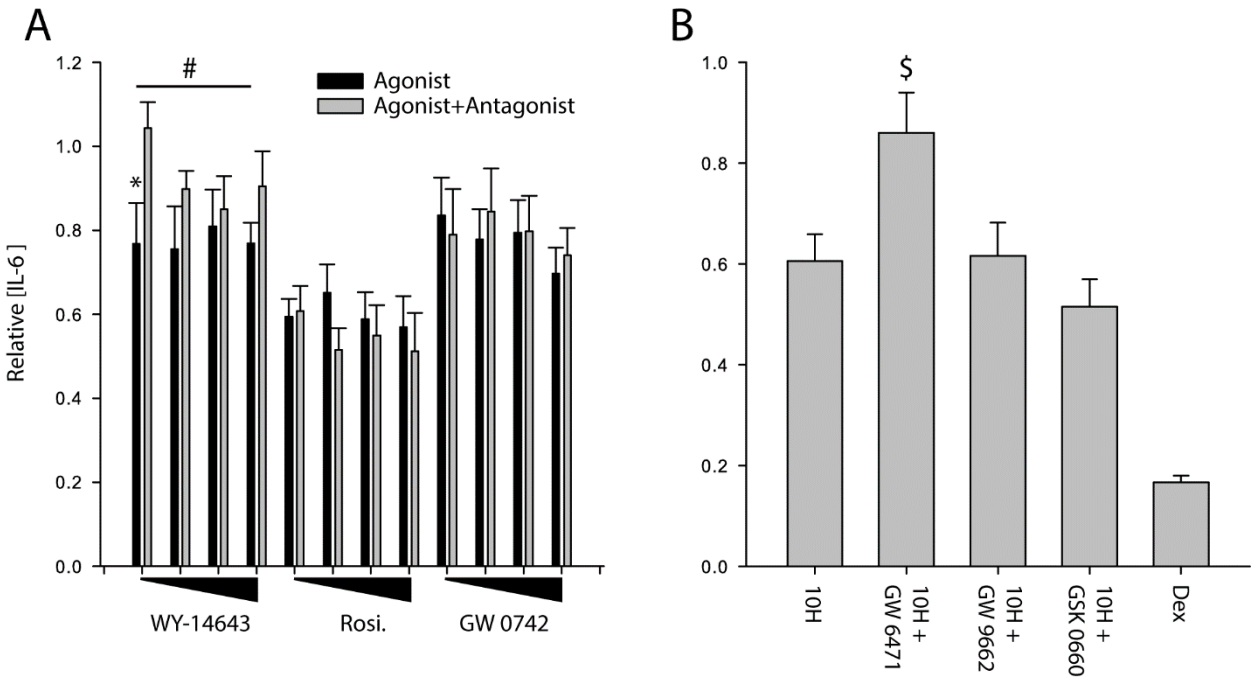

Figure 3.6 PPARα antagonist blocks anti-inflammatory effects of 10(Z)-hexadecenoic acid.
(A) Murine peritoneal macrophages were incubated with either PPARα antagonist (GW 6471), PPARγ antagonist (GW 9662), PPARδ antagonist (GSK 0660), or DMEM/F-12. After a 1h incubation, the cells were treated with the complementary agonist (PPARα: WY-14643, PPARγ: rosiglitazone; rosi., PPARδ: GW 0742). For each agonist, 4 concentrations were assayed, 1x, 2x, 5x, and 10x the EC_{50}. (B)

Alternatively, after incubation with the antagonists or DMEM/F-12, cells were treated with 200 μM 10(*Z*)-hexadecenoic acid. Dexamethasone ("Dex") was included as a positive anti-inflammatory control. Inflammation was reported as the concentration of IL-6 secreted relative to DMEM/F-12. #$p < 0.05$ main effect of agonist + antagonist condition relative to agonist alone condition in a multifactor ANOVA. *$p < 0.05$, Fisher's least significant difference (LSD), pair-wise comparison relative to antagonist-treated cells. \$$p < 0.05$, Fisher's LSD, relative to cells only treated with 10(*Z*)-hexadecenoic acid.

While 10(*Z*)-hexadecenoic acid had a significant anti-inflammatory effect ($p < 0.05$), the effect of higher concentrations of the PPARα agonist, WY-14643, could not be fully reversed with pretreatment of the PPARα antagonist (GW 6471).). To further explore the role of PPARα in the anti-inflammatory effects of 10(Z)-hexadecenoic acid, we repeated the assay in C57BL/6J PPARα$^{-/-}$ mice and used C57BL/6J as a genetic background control. There was a main effect of PPARα genotype on LPS-stimulated IL-6 release ($F_{(1,32)} = 9.639$, $p < 0.01$). Whereas 10(*Z*)-hexadecenoic acid was effective at suppressing LPS-stimulated IL-6 in wild type C57BL/6J mice, the mean LPS-stimulated IL-6 secretion of macrophages from the PPARα KO mice treated with 10(*Z*)-hexadecenoic acid relative to untreated macrophages was 0.99 ± 0.05. This indicated a full reversal of the anti-inflammatory effect of 10(*Z*)-hexadecenoic acid and the necessity of PPARα in mediating the effect.

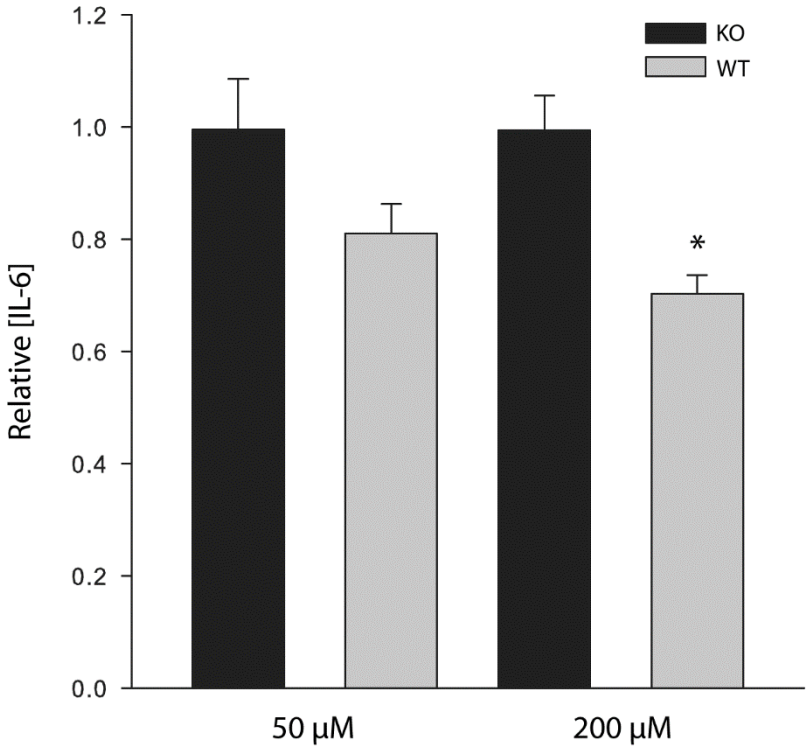

Figure 3.7 PPARα is necessary for anti-inflammatory effects of 10(*Z*)-hexadecenoic acid. Murine peritoneal macrophages from PPARα$^{-/-}$ or WT mice were harvested and cultured for inflammatory assay. Cells were incubated with DMEM/F-12. Subsequently, 10(*Z*)-hexadecenoic acid (50 µM or 200 µM) was added to the cells followed by stimulation with LPS (1 µg/ml). *$p < 0.05$ relative to KO.

3.4 Discussion

Here we show, using RNA-Seq analysis, that a novel lipid, 10(*Z*)-hexadecenoic acid, derived from the saprophytic, anti-inflammatory, immunoregulatory bacterium, *M. vaccae*, has anti-inflammatory effects in freshly isolated, LPS-stimulated murine macrophages. We further show using pathway analysis that PPARα, a murine fatty acid receptor, is a candidate receptor mediating effects of 10(*Z*)-hexadecenoic acid in macrophages. Receptor transfection studies demonstrated that 10(*Z*)-hexadecenoic acid activates PPARα signaling, but not PPARγ signaling, or PPARδ signaling, demonstrating that PPARα, but not PPARγ, or PPARδ, is sufficient to induce PPAR signaling. Pharmacologic studies support these findings, suggesting that PPARα is

both necessary and sufficient for anti-inflammatory effects in macrophages. Finally, studies using PPARα deficient mice confirm that PPARα is necessary for anti-inflammatory of 10(*Z*)-hexadecenoic acid.

Here we show, using RNA-Seq analysis, that a novel lipid, 10(*Z*)-hexadecenoic acid, derived from the saprophytic, anti-inflammatory, immunoregulatory bacterium, *M. vaccae*, has anti-inflammatory effects in LPS-stimulated murine macrophages. The effect had a broad transcriptional impact on inflammation as twenty-one of one hundred two significantly downregulated genes (FDR-adjusted p values, $q < 0.1$) were associated with the GO biological process: inflammatory process (GO:0006954). Using DAVID pathway analysis and GSEA, we demonstrated that the NF-κB pathway was significantly downregulated, including NF-κB. The pathway analyses also returned Jak-STAT pathways to be significantly downregulated. These pathways and associated genes are reported in Table A3.3. This result was not unexpected, as the proinflammatory cytokines regulated by NF-κB primarily signal through Jak-STAT pathways (Lawrence, 2009). These represent one of three pathways activated downstream of TLR4 stimulation; the other two common pathways are AP-1 and IRF3/7 (Fitzgerald et al., 2003). Interestingly, 10(*Z*)-hexadecenoic treatment had no effect on IRF3/7 mRNA levels, nor their gene targets, IFNα/β. Among all mapped reads, we identified 70 transcripts associated with interferons. Three (*ligp1*, *irf4*, and *irf8*) of the 70 were significantly downregulated, though they are not associated with canonical TLR4 activation, except *irf4*, which negatively regulates TLR4 induced proinflammatory cytokine production. The AP-1 arm of TLR4 activation regulates myriad cellular processes such as proliferation, apoptosis, and differentiation. The AP-1 pathways and target genes, like the IRFs, were not significantly enriched in downregulated

genes. The inverse may be true, as the protein constituents of the AP-1 heterodimer, fos and jun, were significantly upregulated in 10(*Z*)-hexadecenoic acid-treated macrophages. These data indicate that the anti-inflammatory effects of 10(*Z*)-hexadecenoic in LPS-stimulated macrophages are specifically achieved through suppression of NF-κB (Chinetti et al., 2000).

The principal findings from the upregulated genes were upregulation of fatty acid metabolic processes and an enrichment of PPAR signaling pathways, which regulate fatty acid metabolism. We further show using pathway analysis and GSEA that genes upregulated by 10(*Z*)-hexadecenoic acid are enriched with gene targets of PPARα. The only other receptor pathway enriched in the upregulated genes was notch receptor, which has also been associated with suppressing inflammation but requires specific protein ligands, and the receptor was inconsistently identified between pathway analysis methods. PPARα is a lipid sensing receptor and is activated by a wide variety of saturated and unsaturated fatty acids (Berger and Moller, 2002). These ligands include dietary fatty acids as well as endogenous lipid hormones. 8,9- and 11,12-epoxyeicosatrienoic acids are PPARα agonists and suppress NF-κB activation (Wray et al., 2009). A second class of anti-inflammatory lipid hormones that bind PPARα includes 12- and 15-hydroxyeicosatetraenoic acid (Murakami et al., 1999). Thus, PPARα is a candidate receptor mediating effects of 10(*Z*)-hexadecenoic acid in macrophages.

Receptor transfection studies demonstrated that 10(*Z*)-hexadecenoic acid activates PPARα, but not PPARγ, or PPARδ, demonstrating that PPARα, but not PPARγ, or PPARδ, is sufficient to induce PPAR signaling. Furthermore, pharmacologic inhibition of PPARα reversed the anti-inflammatory effects of 10(*Z*)-hexadecenoic acid and low concentrations of the PPARα agonist, WY-14643, which suggests that PPARα is necessary and sufficient for anti-inflammatory effects

in macrophages. Finally, studies using PPARα-deficient mice confirmed that PPARα was necessary for the anti-inflammatory effects of 10(*Z*)-hexadecenoic acid, as 10(Z)-hexadecenoic acid had no effect on LPS-stimulated secretion of IL-6 in PPARα KO mice.

Bacterially-derived agonists of PPARs have potential for modulation of host immunity; PPARs have been found to regulate T cell survival, activation, and $CD4^+$ T helper cell differentiation into the Th1, Th2, Th17, and Treg lineages (Choi and Bothwell, 2012). We have shown that 10(*Z*)-hexadecenoic acid originally isolated from *M. vaccae* can protect against allergic asthma, that the same molecule suppresses LPS-induced IL-6 in freshly isolated macrophages, and can activate PPARα, but not PPARβ/δ, PPARγ, or RARα nuclear hormone receptors. Together, these data support the hypothesis that 10(*Z*)-hexadecenoic acid may induce macrophage anergy through actions on PPARα. Peroxisome proliferator-activated receptors, PPARα, PPARβ/δ, and PPARγ are ligand-activated nuclear receptors, each of which acts as a heterodimer with retinoid X receptor (RXR), with potent anti-inflammatory properties, through interference with proinflammatory transcription factor pathways (Chinetti et al., 2003). Our data suggest that activation of PPARα in macrophages inhibits the production of proinflammatory response markers, including IL-6, IL-1β, TNF, and inducible nitric oxide synthase, however, it is unclear that the inhibition is achieved through activation of PPARα target genes or repression of NF-κB genes. In support of the latter mechanism, activated PPARγ represses NF-κB targets through direct interaction with the p50 subunit (Kleemann et al., 2003). The transcriptional program of NF-κB and PPARs is influenced by interactions with coactivators, so a second proposed mechanism of ligand-dependent PPAR transrepression is as an antagonist of NF-κB coactivators(Jepsen et al., 2000). Another, alternative, mechanism for PPARα-mediated

transrepression was shown to involve inhibition of protein kinase C, which is an upstream activator of NF-κB (Ricote and Glass, 2007). These mechanisms are not mutually exclusive nor necessarily specific for TLR4, so, the existence of multiple lines of immune suppression make PPARα ligands broadly appealing anti-inflammatory molecules. The role of PPARα in inflammation is underscored by its exploitation by endogenous molecules to manipulate inflammation. Endogenous host-derived agonists of PPARα include oleoylethanolamide, the monounsaturated analogue of the endocannabinoid anandamide (Fu et al., 2003, 2005), as well as a number of long-chain monocarboxylic acids, including linoleic, α-linolenic, γ-linolenic, arachidonic, docosahexaenoic, and eicosapentaenoic acids (Forman et al., 1997; Kliewer et al., 1997). In addition, oxygenated fatty acid derivatives and other products of lipoxygenase metabolism, such as 8(S)-hydroxyeicosatetraenoic acid (8(S)-HETE), and ±8-hydroxyeicosapentaenoic acid (±8-HEPE) are endogenous PPARα agonists (Forman et al., 1997; Kliewer et al., 1997). Other endogenous PPARα agonists include 15-deoxy-D12,14-prostaglandin J2 (Forman et al., 1997; Kota et al., 2005). Finally, the monounsaturated fatty acids, oleic ((9*Z*)-octadec-9-enoic acid), petroselenic ((6*Z*)-octadec-6-enoic acid), and palmitoleic acid ((9*Z*)-hexadec-9-enoic acid) are endogenous host-derived PPARα agonists (Kliewer et al., 1997; Kota et al., 2005). Palmitoleic acid is a lipokine, released from adipose cells, localizes predominantly to nuclear fractions, consistent with a nuclear mechanisms of action in host cells (Foryst-Ludwig et al., 2015), and is potently anti-inflammatory (Chan et al., 2015).

Mycobacteria are phagocytosed by macrophages and can persist within the macrophage as an intracellular parasite. This suggests that, following release of 10(*Z*)-hexadecenoic acid into the

cytoplasm of the cell, and following binding of 10(*Z*)-hexadecenoic acid to cytosolic PPARα, *M. vaccae* may co-opt the macrophage's own anti-inflammatory mechanisms to suppress inflammation. It is unclear if 10(*Z*)-hexadecenoic acid induces a shift toward an alternatively activated, anti-inflammatory M2 phenotype, or a novel phenotype.

The significance of PPARα in human health is largely explored in clinical trials for the treatment of obesity, dyslipidemia, and type 2 diabetes. PPARα is a logical and effective target for these conditions because of its role in lipid metabolism. In nondiabetic obese adults, PPARα is downregulated in adipose tissue (Martinelli et al., 2010; Mejía-Barradas et al., 2014). Interestingly, the opposite is true of type 2 diabetic people (Carey et al., 2006). A resolution to the discrepancy was sought by epidemiological sequencing of PPARα. Although the study was unable to identify a genetic background for type 2 diabetes, it did reveal a L162V missense mutation that was a risk factor for hyperapobetalipoproteinemia, which is associated with the development of coronary artery disease. To date, > 6,000 single nucleotide polymorphisms have been observed on or affect the PPARα gene, of which 49 have a global minor allele frequency > 0.01. In the context of inflammation, the genetic variants have been associated with allergic rhinitis (Krasznai et al., 2012), IBD (Di Narzo et al., 2016), and atherosclerosis (Lu et al., 2010). Furthermore, PPARα is downregulated in the skin of patients with psoriasis (Gudjonsson et al., 2009).

These studies raise the possibility that 10(*Z*)-hexadecenoic acid may have therapeutic value in acute or chronic inflammatory disease. The positive anti-inflammatory control in these studies, dexamethasone, was superior to 10(*Z*)-hexadecenoic acid in the context of inhibiting IL-6 release. In many instances, it was reduced to 5-10% of the untreated cells, but a complete

inhibition of inflammatory responses is not ideal for certain physiological states. Thus, 10(*Z*)-hexadecenoic acid may have therapeutic value in clinical conditions characterized by chronic inflammation, including allergic asthma, but with fewer side effects (Chinetti et al., 2003).

Bibliography

Abdallah, A.M., Gey van Pittius, N.C., Champion, P. a D., Cox, J., Luirink, J., Vandenbroucke-Grauls, C.M.J.E., Appelmelk, B.J., and Bitter, W. (2007). Type VII secretion--mycobacteria show the way. Nat. Rev. Microbiol. *5*, 883–891.

Abdelmohsen, U.R., Bayer, K., and Hentschel, U. (2014). Diversity, abundance and natural products of marine sponge-associated actinomycetes. Nat. Prod. Rep. *31*, 381.

Adams, V.C., Hunt, J.R.F., Martinelli, R., Palmer, R., Rook, G.A.W., and Brunet, L.R. (2004). *Mycobacterium vaccae* induces a population of pulmonary CD11c+ cells with regulatory potential in allergic mice. Eur. J. Immunol. *34*, 631–638.

Alvarez-Curto, E., and Milligan, G. (2016). Metabolism meets immunity: The role of free fatty acid receptors in the immune system. Biochem. Pharmacol. *114*, 3–13.

Anders, S., and Huber, W. (2010). Differential expression analysis for sequence count data. Genome Biol. *11*, R106.

Anders, S., Pyl, P.T., and Huber, W. (2015). HTSeq-A Python framework to work with high-throughput sequencing data. Bioinformatics *31*, 166–169.

Appelmelk, B.J., den Dunnen, J., Driessen, N.N., Ummels, R., Pak, M., Nigou, J., Larrouy-Maumus, G., Gurcha, S.S., Movahedzadeh, F., Geurtsen, J., et al. (2008). The mannose cap of mycobacterial lipoarabinomannan does not dominate the Mycobacterium-host interaction. Cell. Microbiol. *10*, 930–944.

Arnold, I.C., Dehzad, N., Reuter, S., Martin, H., Becher, B., Taube, C., and M\"uller, a. (2011). Helicobacter pylori infection prevents allergic asthma in mouse models through the induction of regulatory T cells. J Clin Invest *121*, 3088–3093.

Arnold, I.C., Hitzler, I., and Müller, A. (2012). The Immunomodulatory Properties of Helicobacter pylori Confer Protection Against Allergic and Chronic Inflammatory Disorders. Front. Cell. Infect. Microbiol. *2*, 1–11.

Arpaia, N., Campbell, C., Fan, X., Dikiy, S., van der Veeken, J., deRoos, P., Liu, H., Cross, J.R., Pfeffer, K., Coffer, P.J., et al. (2013). Metabolites produced by commensal bacteria promote peripheral regulatory T-cell generation. Nature *504*, 451–455.

Ashenafi, S., Aderaye, G., Bekele, A., Zewdie, M., Aseffa, G., Hoang, A.T.N., Carow, B., Habtamu, M., Wijkander, M., Rottenberg, M., et al. (2014). Progression of clinical tuberculosis is associated with a Th2 immune response signature in combination with elevated levels of SOCS3. Clin. Immunol. *151*, 84–99.

Bach, J. (2002a). The Effect of Susceptibility to Autoimmune and Allergic Diseases. N.

Engl. J. Med. *347*, 911–920.

Bach, J.-F. (2002b). SUSCEPTIBILITY TO AUTOIMMUNE AND ALLERGIC DISEASES. N Engl J Med *347*, 911–920.

Bansal-Mutalik, R., and Nikaido, H. (2014). Mycobacterial outer membrane is a lipid bilayer and the inner membrane is unusually rich in diacyl phosphatidylinositol dimannosides. Proc. Natl. Acad. Sci. U. S. A. *111*, 4958–4963.

Barton, G.M., and Medzhitov, R. (2004). Toll signaling: RIPping off the TNF pathway. Nat. Immunol. *5*, 472–474.

Beasley, R., Keil, U., Von Mutius, E., and Pearce, N. (1998). Worldwide variation in prevalence of symptoms of asthma, allergic rhinoconjunctivitis, and atopic eczema: ISAAC. Lancet *351*, 1225–1232.

Belkaid, Y., Piccirillo, C. a, and Mendez, S. (2002). CD4+CD25+ regulatory T cells control Leishmania major persistence and immunity. Nature *420*, 502–507.

Benko, S., Love, J.D., Beládi, M., Schwabe, J.W.R., and Nagy, L. (2003). Molecular determinants of the balance between co-repressor and co-activator recruitment to the retinoic acid receptor. J. Biol. Chem. *278*, 43797–43806.

Benn, C.S., Melbye, M., Wohlfahrt, J., Björkstén, B., and Aaby, P. (2004). Cohort study of sibling effect, infectious diseases, and risk of atopic dermatitis during first 18 months of life. BMJ *328*, 1223.

Berger, J., and Moller, D.E. (2002). T m a ppar.

Bergman, M.P., Engering, A., Smits, H.H., van Vliet, S.J., van Bodegraven, A. a, Wirth, H.-P., Kapsenberg, M.L., Vandenbroucke-Grauls, C.M.J.E., van Kooyk, Y., and Appelmelk, B.J. (2004). Helicobacter pylori modulates the T helper cell 1/T helper cell 2 balance through phase-variable interaction between lipopolysaccharide and DC-SIGN. J. Exp. Med. *200*, 979–990.

Le Bert, N., Chain, B.M., Rook, G., and Noursadeghi, M. (2011a). DC priming by M. vaccae inhibits Th2 responses in contrast to specific TLR2 priming and is associated with selective activation of the CREB pathway. PLoS One *6*, e18346.

Le Bert, N., Chain, B.M., Rook, G., and Noursadeghi, M. (2011b). DC priming by *M. vaccae* inhibits Th2 responses in contrast to specific TLR2 priming and is associated with selective activation of the CREB pathway. PLoS One *6*, e18346.

Bertelli, C., Laird, M.R., Williams, K.P., Lau, B.Y., Hoad, G., Winsor, G.L., and Brinkman, F.S. (2017). IslandViewer 4: expanded prediction of genomic islands for larger-scale datasets. Nucleic Acids Res. *17*, 132.

Besra, G.S., Minnikin, D.E., Wheeler, P.R., and Ratledge, C. (1993). Synthesis of methyl

(Z)-tetracos-5-enoate and both enantiomers of ethyl (E)-6-methyltetracos-4-enoate: possible intermediates in the biosynthesis of mycolic acids in mycobacteria. Chem. Phys. Lipids *66*, 23–34.

Bjorksten, B., Naaber, P., Sepp, E., and Mikelsaar, M. (1999). The intestinal microflora in allergic Estonian and Swedish 2-year-old children. Clin. Exp. Allergy *29*, 342–346.

Bligh, E.G., and Dyer, W.J. (1959). A rapid method of total lipid extraction and purification. Can. J. Biochem. Physiol. *37*, 911–917.

Bloomfield, S.F., Rook, G.A., Scott, E.A., Shanahan, F., Stanwell-Smith, R., and Turner, P. (2016). Time to abandon the hygiene hypothesis: new perspectives on allergic disease, the human microbiome, infectious disease prevention and the role of targeted hygiene. Perspect. Public Health *136*, 213–224.

Bolger, A.M., Lohse, M., and Usadel, B. (2014). Trimmomatic: A flexible trimmer for Illumina sequence data. Bioinformatics *30*, 2114–2120.

Braibant, M., Gilot, P., and Content, J. (2000). The ATP binding cassette (ABC) transport systems of Mycobacterium tuberculosis. FEMS Microbiol. Rev. *24*, 449–467.

Braun-Fahrländer, C., Riedler, J., Herz, U., Eder, W., Waser, M., Grize, L., Maisch, S., Carr, D., Gerlach, F., Bufe, A., et al. (2002). Environmental Exposure to Endotoxin and Its Relation to Asthma in School-Age Children. N. Engl. J. Med. *347*, 869–877.

Bremner, S.A., Carey, I.M., DeWilde, S., Richards, N., Maier, W.C., Hilton, S.R., Strachan, D.P., and Cook, D.G. (2008). Infections presenting for clinical care in early life and later risk of hay fever in two UK birth cohorts. Allergy Eur. J. Allergy Clin. Immunol. *63*, 274–283.

Brennan, P.J. (2003). Structure, function, and biogenesis of the cell wall of *Mycobacterium tuberculosis*. In Tuberculosis (Edinb), pp. 91–97.

Butler, M.S. (2004). The role of natural product chemistry in drug discovery. J. Nat. Prod. *67*, 2141–2153.

Buxadé, M., Lunazzi, G., Minguillón, J., Iborra, S., Berga-Bolaños, R., del Val, M., Aramburu, J., and López-Rodríguez, C. (2012). Gene expression induced by Toll-like receptors in macrophages requires the transcription factor NFAT5. J. Exp. Med. *209*, 379–393.

Cahenzli, J., Köller, Y., Wyss, M., Geuking, M.B., and McCoy, K.D. (2013). Intestinal microbial diversity during early-life colonization shapes long-term IgE levels. Cell Host Microbe *14*, 559–570.

Carey, A.L., Petersen, E.W., Bruce, C.R., Southgate, R.J., Pilegaard, H., Hawley, J.A., Pedersen, B.K., and Febbraio, M.A. (2006). Discordant gene expression in skeletal muscle and adipose tissue of patients with type 2 diabetes: Effect of interleukin-6 infusion. Diabetologia *49*, 1000–1007.

Cavaglieri, C.R., Nishiyama, A., Fernandes, L.C., Curi, R., Miles, E.A., and Calder, P.C. (2003). Differential effects of short-chain fatty acids on proliferation and production of pro- and anti-inflammatory cytokines by cultured lymphocytes. Life Sci. *73*, 1683–1690.

Chan, K.L., Pillon, N.J., Sivaloganathan, D.M., Costford, S.R., Liu, Z., Théret, M., Chazaud, B., and Klip, A. (2015). Palmitoleate reverses high fat-induced proinflammatory macrophage polarization via AMP-activated protein kinase (AMPK). J. Biol. Chem. *290*, 16979–16988.

Chawla, A. (2010). Control of macrophage activation and function by PPARs. Circ. Res. *106*, 1559–1569.

Chen, J.D., and Evans, R.M. (1995). A transcriptional co-repressor that interacts with nuclear hormone receptors. Nature *377*, 454–457.

Chinetti, G., Fruchart, J.C., and Staels, B. (2000). Peroxisome proliferator-activated receptors (PPARs): Nuclear receptors at the crossroads between lipid metabolism and inflammation. Inflamm. Res. *49*, 497–505.

Chinetti, G., Fruchart, J.C., and Staels, B. (2003). Peroxisome proliferator-activated receptors: new targets for the pharmacological modulation of macrophage gene expression and function. Curr Opin Lipidol *14*, 459–468.

Choi, J.M., and Bothwell, A.L.M. (2012). The nuclear receptor PPARs as important regulators of T-cell functions and autoimmune diseases. Mol. Cells *33*, 217–222.

Collins, S.M., and Bercik, P. (2009). The relationship between intestinal microbiota and the central nervous system in normal gastrointestinal function and disease. Gastroenterology *136*, 2003–2014.

D'Auria, G., Jiménez-Hernández, N., Peris-Bondia, F., Moya, A., and Latorre, A. (2010). Legionella pneumophila pangenome reveals strain-specific virulence factors. BMC Genomics *11*, 181.

Demain, A.L. (2014). Importance of microbial natural products and the need to revitalize their discovery. J. Ind. Microbiol. Biotechnol. *41*, 185–201.

Dennis, E.A., and Norris, P.C. (2015). Eicosanoid storm in infection and inflammation. Nat. Rev. Immunol. *15*, 724–724.

Dhanasekaran, A.R., Pearson, J.L., Ganesan, B., and Weimer, B.C. (2015). Metabolome searcher: a high throughput tool for metabolite identification and metabolic pathway mapping directly from mass spectrometry and using genome restriction. BMC Bioinformatics *16*, 62.

Doetze, A., Satoguina, J., Burchard, G., Rau, T., Loliger, C., Fleischer, B., and Hoerauf, A. (2000). Antigen-specific cellular hyporesponsiveness in a chronic human helminth infection is mediated by T(h)3/T(r)1-type cytokines IL-10 and transforming growth factor-beta but not by a T(h)1 to T(h)2 shift. Int. Immunol. *12*, 623–630.

Draper, E., DeCourcey, J., Higgins, S.C., Canavan, M., McEvoy, F., Lynch, M., Keogh, B., Reynolds, C., Roche, H.M., Mills, K.H.G., et al. (2014). Conjugated linoleic acid suppresses dendritic cell activation and subsequent Th17 responses. J. Nutr. Biochem. *25*, 741–749.

Duan, W., and Croft, M. (2014). Control of regulatory T Cells and airway tolerance by lung macrophages and dendritic cells. Ann. Am. Thorac. Soc. *11*, S306–S313.

Eder, W., Ege, M.J., and von Mutius, E. (2006). The Asthma Epidemic. N. Engl. J. Med. *355*, 2226–2235.

Evans, N.P., Misyak, S. a, Schmelz, E.M., Guri, A.J., Hontecillas, R., and Bassaganya-riera, J. (2010). Conjugated linoleic acid ameliorates inflammation-induced colorectal cancer in mice through activation of PPARγ. J. Nutr. *140*, 515–521.

Ferrao, R., Li, J., Bergamin, E., and Wu, H. (2012). Structural insights into the assembly of large oligomeric signalosomes in the Toll-like receptor-interleukin-1 receptor superfamily. Sci. Signal. *5*, re3.

Fitzgerald, K.A., Rowe, D.C., Barnes, B.J., Caffrey, D.R., Visintin, A., Latz, E., Monks, B., Pitha, P.M., and Golenbock, D.T. (2003). LPS-TLR4 Signaling to IRF-3/7 and NF-κB Involves the Toll Adapters TRAM and TRIF. J. Exp. Med. *198*, 1043–1055.

Forman, B.M., Chen, J., and Evans, R.M. (1997). Hypolipidemic drugs, polyunsaturated fatty acids, and eicosanoids are ligands for peroxisome proliferator-activated receptors alpha and delta. Proc. Natl. Acad. Sci. United States Am. Sci. *94*, 4312–4317.

Foryst-Ludwig, A., Kreissl, M.C., Benz, V., Brix, S., Smeir, E., Ban, Z., Januszewicz, E., Salatzki, J., Grune, J., Schwanstecher, A.K., et al. (2015). Adipose tissue lipolysis promotes exercise-induced cardiac hypertrophy involving the lipokine C16: 1n7-palmitoleate. J. Biol. Chem. *290*, 23603–23615.

Francis, G.W. (1981). Alkylthiolation for the determination of double-bond position in unsaturated fatty acid esters. Chem. Phys. Lipids *29*, 369–374.

Fu, J., Gaetani, S., Oveisi, F., Lo Verme, J., Serrano, A., Rodriguez De Fonseca, F., Rosengarth, A., Luecke, H., Di Giacomo, B., Tarzia, G., et al. (2003). Oleylethanolamide regulates feeding and body weight through activation of the nuclear receptor PPAR-α. Nature *425*, 90–93.

Fu, J., Oveisi, F., Gaetani, S., Lin, E., and Piomelli, D. (2005). Oleoylethanolamide, an endogenous PPAR-α agonist, lowers body weight and hyperlipidemia in obese rats. Neuropharmacology *48*, 1147–1153.

Fujimura, Y. (1986). Functional morphology of microfold cells (M cells) in Peyer's patches--phagocytosis and transport of BCG by M cells into rabbit Peyer's patches. Gastroenterol. Jpn. *21*, 325–335.

Furukawa, S., Ito, S., Nitta, Y., Fukumitsu, H., Soumiya, H., Ikeno, K., and Nakamura, T. (2012). Antidepressant-like activity of 10-hydroxy-trans-2-decenoic acid, a unique unsaturated fatty acid of royal jelly, in stress-inducible depression-like mouse model. Evidence-Based Complement. Altern. Med. *2012*.

Garn, H., Bahn, S., Baune, B.T., Binder, E.B., Bisgaard, H., Chatila, T.A., Chavakis, T., Culmsee, C., Dannlowski, U., Gay, S., et al. (2016). Current concepts in chronic inflammatory diseases: Interactions between microbes, cellular metabolism, and inflammation. J. Allergy Clin. Immunol. *138*, 47–56.

Garton, N.J., Christensen, H., Minnikin, D.E., Adegbola, R.A., and Barer, M.R. (2002). Intracellular lipophilic inclusions of mycobacteria *in vitro* and in sputum. Microbiology *148*, 2951–2958.

Gautam, R., and Jachak, S.M. (2009). Recent developments in anti-inflammatory natural products. Med. Res. Rev. *29*, 767–820.

Geffner, L., Yokobori, N., Basile, J., Schierloh, P., Balboa, L., Romero, M.M., Ritacco, V., Vescovo, M., Montaner, P.G., Lopez, B., et al. (2009). Patients with multidrug-resistant tuberculosis display impaired Th1 responses and enhanced regulatory T-cell levels in response to an outbreak of multidrug-resistant Mycobacterium tuberculosis M and Ra strains. Infect. Immun. *77*, 5025–5034.

Gillespie, K.M., Bain, S.C., Barnett, P.A.H., Bingley, P.P.J., Christie, M.R., Gill, G. V., and Gale, P.E.A.M. (2004). The rising incidence of childhood type 1 diabetes and reduced contribution of high-risk HLA haplotypes. Lancet *364*, 1699–1700.

Gröschel, M.I., Sayes, F., Simeone, R., Majlessi, L., and Brosch, R. (2016). ESX secretion systems: mycobacterial evolution to counter host immunity. Nat. Rev. Microbiol. *14*, 677–691.

Guarner, F., Bourdet-Sicard, R., Brandtzaeg, P., Gill, H.S., McGuirk, P., van Eden, W., Versalovic, J., Weinstock, J. V, and Rook, G. a W. (2006). Mechanisms of disease: the hygiene hypothesis revisited. Nat. Clin. Pract. Gastroenterol. Hepatol. *3*, 275–284.

Gudjonsson, J.E., Ding, J., Li, X., Nair, R.P., Tejasvi, T., Qin, Z.S., Ghosh, D., Aphale, A., Gumucio, D.L., Voorhees, J.J., et al. (2009). Global gene expression analysis reveals evidence for decreased lipid biosynthesis and increased innate immunity in uninvolved psoriatic skin. J. Invest. Dermatol. *129*, 2795–2804.

Gutzwiller, M.E.R., Reist, M., Peel, J.E., Seewald, W., Brunet, L.R., and Roosje, P.J. (2007). Intradermal injection of heat-killed *Mycobacterium vaccae* in dogs with atopic dermatitis: A multicentre pilot study. Vet. Dermatol. *18*, 87–93.

Hammer, M., Mages, J., Dietrich, H., Servatius, A., Howells, N., Cato, A.C.B., and Lang, R. (2006). Dual specificity phosphatase 1 (DUSP1) regulates a subset of LPS-induced genes and protects mice from lethal endotoxin shock. J. Exp. Med. *203*, 15–20.

Han, K.J., Su, X., Xu, L.G., Bin, L.H., Zhang, J., and Shu, H.B. (2004). Mechanisms of the TRIF-induced Interferon-stimulated Response Element and NF-κB Activation and Apoptosis Pathways. J. Biol. Chem. *279*, 15652–15661.

Herbst, T., Sichelstiel, A., Schär, C., Yadava, K., Bürki, K., Cahenzli, J., McCoy, K., Marsland, B.J., and Harris, N.L. (2011). Dysregulation of allergic airway inflammation in the absence of microbial colonization. Am. J. Respir. Crit. Care Med. *184*, 198–205.

Herker, E., and Ott, M. (2012). Emerging role of lipid droplets in host/pathogen interactions. J. Biol. Chem. *287*, 2280–2287.

Hernandez-Pando, R., Pavön, L., Arriaga, K., Orozco, H., Madrid-Marina, V., and Rook, G. (1997). Pathogenesis of tuberculosis in mice exposed to low and high doses of an environmental mycobacterial saprophyte before infection. Infect. Immun. *65*, 3317–3327.

Hoisington, A.J., Brenner, L.A., Kinney, K.A., Postolache, T.T., and Lowry, C.A. (2015). The microbiome of the built environment and mental health. Microbiome *3*, 60.

Horai, H., Arita, M., Kanaya, S., Nihei, Y., Ikeda, T., Suwa, K., Ojima, Y., Tanaka, K., Tanaka, S., Aoshima, K., et al. (2010). MassBank: A public repository for sharing mass spectral data for life sciences. J. Mass Spectrom. *45*, 703–714.

Hu, W., Jain, A., Gao, Y., Dozmorov, I.M., Mandraju, R., Wakeland, E.K., and Pasare, C. (2015). Differential outcome of TRIF-mediated signaling in TLR4 and TLR3 induced DC maturation. Proc. Natl. Acad. Sci. *112*, 13994–13999.

Huang, D.W., Sherman, B.T., Tan, Q., Kir, J., Liu, D., Bryant, D., Guo, Y., Stephens, R., Baseler, M.W., Lane, H.C., et al. (2007). DAVID Bioinformatics Resources: Expanded annotation database and novel algorithms to better extract biology from large gene lists. Nucleic Acids Res. *35*.

Huang, D.W., Sherman, B.T., Lempicki, R.A., Huang, D., Sherman, B., Lempicki, R., Huang, D., Sherman, B., Lempicki, R., Maere, S., et al. (2009). Bioinformatics enrichment tools: paths toward the comprehensive functional analysis of large gene lists. Nucleic Acids Res. *37*, 1–13.

Hunt, J.R.F., Martinelli, R., Adams, V.C., Rook, G., and Brunet, L.R. (2005). Intragastric administration of *Mycobacterium vaccae* inhibits severe pulmonary allergic inflammation in a mouse model. Clin. Exp. Allergy *35*, 685–690.

Jackson, M. (2014). The mycobacterial cell envelope-lipids. Cold Spring Harb. Perspect. Med. *4*.

Janeway, C. a, and Medzhitov, R. (2002). Innate immune recognition. Annu. Rev. Immunol. *20*, 197–216.

Jepsen, K., Hermanson, O., Onami, T.M., Gleiberman, A.S., Lunyak, V., McEvilly, R.J.,

Kurokawa, R., Kumar, V., Liu, F., Seto, E., et al. (2000). Combinatorial roles of the nuclear receptor corepressor in transcription and development. Cell *102*, 753–763.

Jüngling, E., and Kammermeier, H. (1988). A one-vial method for routine extraction and quantification of free fatty acids in blood and tissue by HPLC. Anal. Biochem. *171*, 150–157.

Kaparakis-Liaskos, M., and Ferrero, R.L. (2015). Immune modulation by bacterial outer membrane vesicles. Nat. Rev. Immunol. *15*, 375–387.

El Kasmi, K.C., Holst, J., Coffre, M., Mielke, L., de Pauw, A., Lhocine, N., Smith, A.M., Rutschman, R., Kaushal, D., Shen, Y., et al. (2006). General nature of the STAT3-activated anti-inflammatory response. J. Immunol. *177*, 7880–7888.

Kawai, T., Adachi, O., Ogawa, T., Takeda, K., and Akira, S. (1999). Unresponsiveness of MyD88-deficient mice to endotoxin. Immunity *11*, 115–122.

Kazi, J.U., Kabir, N.N., Flores-Morales, A., and Rönnstrand, L. (2014). SOCS proteins in regulation of receptor tyrosine kinase signaling. Cell. Mol. Life Sci. *71*, 3297–3310.

Kieser, K.J., and Rubin, E.J. (2014a). How sisters grow apart: mycobacterial growth and division. Nat Rev Microbiol *12*, 550–562.

Kieser, K.J., and Rubin, E.J. (2014b). How sisters grow apart: mycobacterial growth and division. Nat Rev Microbiol *12*, 550–562.

Kim, D., Pertea, G., Trapnell, C., Pimentel, H., Kelley, R., and Salzberg, S.L. (2013). TopHat2: accurate alignment of transcriptomes in the presence of insertions, deletions and gene fusions. Genome Biol. *14*, R36.

Kim, D.-I., Kim, K.-H., Kang, J.-H., Jung, E.-M., Kim, S.-S., Jeung, E.-B., and Yang, M.-P. (2011). Trans-10, cis-12-conjugated linoleic acid modulates NF-κB activation and TNF-α production in porcine peripheral blood mononuclear cells via a PPARγ-dependent pathway. Br. J. Nutr. *105*, 1329–1336.

King, C.L., Mahanty, S., Kumaraswami, V., Abrams, J.S., Regunathan, J., Jayaraman, K., Ottesen, E.A., and Nutman, T.B. (1993). Cytokine control of parasite-specific anergy in human lymphatic filariasis. Preferential induction of a regulatory T helper type 2 lymphocyte subset. J. Clin. Invest. *92*, 1667–1673.

Kino, T., Hatanaka, H., Hashimoto, M., Nishiyama, M., Goto, T., Okuhara, M., Kohsaka, M., Aoki, H., and Imanaka, H. (1987). FK-506, a novel immunosuppressant isolated from a Streptomyces. I. Fermentation, isolation, and physico-chemical and biological characteristics. J. Antibiot. (Tokyo). *40*, 1249–1255.

Kishino, S., Takeuchi, M., Park, S.-B., Hirata, A., Kitamura, N., Kunisawa, J., Kiyono, H., Iwamoto, R., Isobe, Y., Arita, M., et al. (2013). Polyunsaturated fatty acid saturation by gut lactic acid bacteria affecting host lipid composition. Proc. Natl. Acad. Sci. U. S. A. *110*.

Kleemann, R., Gervois, P.P., Verschuren, L., Staels, B., Princen, H.M.G., and Kooistra, T. (2003). Fibrates down-regulate IL-1-stimulated C-reactive protein gene expression in hepatocytes by reducing nuclear p50-NFκB-C/EBP-β complex formation. Blood *101*, 545–551.

van der Kleij, D., and Yazdanbakhsh, M. (2003). Control of inflammatory diseases by pathogens: Lipids and the immune system. Eur. J. Immunol. *33*, 2953–2963.

van der Kleij, D., Latz, E., Brouwers, J.F.H.M., Kruize, Y.C.M., Schmitz, M., Kurt-Jones, E.A., Espevik, T., de Jong, E.C., Kapsenberg, M.L., Golenbock, D.T., et al. (2002). A novel host-parasite lipid cross-talk. Schistosomal lyso-phosphatidylserine activates toll-like receptor 2 and affects immune polarization. J. Biol. Chem. *277*, 48122–48129.

Kliewer, S.A., Sundseth, S.S., Jones, S.A., Brown, P.J., Wisely, G.B., Koble, C.S., Devchand, P., Wahli, W., Willson, T.M., Lenhard, J.M., et al. (1997). Fatty acids and eicosanoids regulate gene expression through direct interactions with peroxisome proliferator-activated receptors alpha and gamma. Proc. Natl. Acad. Sci. U. S. A. *94*, 4318–4323.

Kónya, A., Szabó, Z., Láng, I., Barta, I., and Salát, J. (2008). Production of FK520 by Streptomyces tubercidicus. Microbiol. Res. *163*, 624–632.

van Kooyk, Y., and Geijtenbeek, T.B.H. (2003). DC-SIGN: escape mechanism for pathogens. Nat. Rev. Immunol. *3*, 697–709.

Kota, B.P., Huang, T.H.W., and Roufogalis, B.D. (2005). An overview on biological mechanisms of PPARs. Pharmacol. Res. *51*, 85–94.

Krasznai, M., Szaniszlo, K., Kraxner, H., Vargha, E., Kovacs, M., Kaszas, E., Mezei, G., Cserhati, E., Borocz, Z., and Cseh, K. (2012). Association of PPAR polymorphisms with cytokine levels in allergic rhinitis. Eur. Arch. Oto-Rhino-Laryngology *269*, 513–521.

Lawrence, T. (2009). The Nuclear Factor NF-κB Pathway in Inflammation. About Cold Spring Harb. Perspect. Biol. *1*, 1–10.

Lee, J.Y., Sohn, K.H., Rhee, S.H., and Hwang, D. (2001). Saturated Fatty Acids, but Not Unsaturated Fatty Acids, Induce the Expression of Cyclooxygenase-2 Mediated through Toll-like Receptor 4. J. Biol. Chem. *276*, 16683–16689.

Lee, S.O., Kim, C.S., Cho, S.K., Choi, H.J., Ji, G.E., and Oh, D.K. (2003a). Bioconversion of linoleic acid into conjugated linoleic acid during fermentation and by washed cells of Lactobacillus reuteri. Biotechnol. Lett. *25*, 935–938.

Lee, S.O., Hong, G.W., and Oh, D.K. (2003b). Bioconversion of linoleic acid into conjugated linoleic acid by immobilized *Lactobacillus reuteri*. Biotechnol. Prog. *19*, 1081–1084.

Li, H., Handsaker, B., Wysoker, A., Fennell, T., Ruan, J., Homer, N., Marth, G., Abecasis, G., and Durbin, R. (2009). The Sequence Alignment/Map format and SAMtools. Bioinformatics *25*, 2078–2079.

van Liempt, E., Bank, C.M.C., Mehta, P., García-Vallejo, J.J., Kawar, Z.S., Geyer, R., Alvarez, R.A., Cummings, R.D., Kooyk, Y. van, and van Die, I. (2006). Specificity of DC-SIGN for mannose- and fucose-containing glycans. FEBS Lett. *580*, 6123–6131.

de Lima Procópio, R.E., da Silva, I.R., Martins, M.K., de Azevedo, J.L., and de Araújo, J.M. (2012). Antibiotics produced by Streptomyces. Brazilian J. Infect. Dis. *16*, 466–471.

Lin, S.-C., Lo, Y.-C., and Wu, H. (2010). Helical assembly in the MyD88-IRAK4-IRAK2 complex in TLR/IL-1R signalling. Nature *465*, 885–890.

Loscher, C.E., Draper, E., Leavy, O., Kelleher, D., Mills, K.H.G., and Roche, H.M. (2005). Conjugated linoleic acid suppresses NF-κB activation and IL-12 production in dendritic cells through ERK-mediated IL-10 induction. J. Immunol. *175*, 4990–4998.

Lowry, C.A., Smith, D.G., Siebler, P.H., Schmidt, D., Stamper, C.E., Hassell, J.E., Yamashita, P.S., Fox, J.H., Reber, S.O., Brenner, L.A., et al. (2016). The microbiota, immunoregulation, and mental health: implications for public health. Curr. Environ. Health. Rep *3*, 270–286.

Lu, Y., Feskens, E.J.M., Doll??, M.E.T., Imholz, S., Verschuren, W.M.M., M??ller, M., and Boer, J.M.A. (2010). Dietary n-3 and n-6 polyunsaturated fatty acid intake interacts with FADS1 genetic variation to affect total and HDL-cholesterol concentrations in the Doetinchem Cohort Study. Am. J. Clin. Nutr. *92*, 258–265.

Lyte, M., and Cryan, J.F. (2014). Microbial Endocrinology: The Microbiota- Gut-Brain Axis in Health and Disease.

Marrakchi, H., Lanéelle, M.-A., and Daffé, M. (2014). Mycolic acids: structures, biosynthesis, and beyond. Chem. Biol. *21*, 67–85.

Martinelli, R., Nardelli, C., Pilone, V., Buonomo, T., Liguori, R., Castanò, I., Buono, P., Masone, S., Persico, G., Forestieri, P., et al. (2010). miR-519d Overexpression Is Associated With Human Obesity. Obesity *18*, 2170–2176.

Matricardi, P.M., and Ronchetti, R. (2001). Are infections protecting from atopy? Curr Opin Allergy Clin Immunol *1*, 413–419.

McCoy, K.D., Harris, N.L., Diener, P., Hatak, S., Odermatt, B., Hangartner, L., Senn, B.M., Marsland, B.J., Geuking, M.B., Hengartner, H., et al. (2006). Natural IgE production in the absence of MHC class II cognate help. Immunity *24*, 329–339.

McMullen, P.D., Bhattacharya, S., Woods, C.G., Sun, B., Yarborough, K., Ross, S.M., Miller, M.E., McBride, M.T., Lecluyse, E.L., Clewell, R.A., et al. (2014). A map of the PPAR?? transcription regulatory network for primary human hepatocytes. Chem. Biol. Interact. *209*, 14–24.

Meijerink, M., van Hemert, S., Taverne, N., Wels, M., de Vos, P., Bron, P. a., Savelkoul,

H.F., van Bilsen, J., Kleerebezem, M., and Wells, J.M. (2010). Identification of genetic loci in Lactobacillus plantarum that modulate the immune response of dendritic cells using comparative genome hybridization. PLoS One *5*.

Mejía-Barradas, C.M., Del-Río-Navarro, B.E., Domínguez-López, A., Campos-Rodríguez, R., Martínez-Godínez, M.D.L.Á., Rojas-Hernández, S., Lara-Padilla, E., Abarca-Rojano, E., and Miliar-García, Á. (2014). The consumption of n-3 polyunsaturated fatty acids differentially modulates gene expression of peroxisome proliferator-activated receptor alpha and gamma and hypoxia-inducible factor 1 alpha in subcutaneous adipose tissue of obese adolescents. Endocrine *45*, 98–105.

Mezrich, J.D., Fechner, J.H., Zhang, X., Johnson, B.P., Burlingham, W.J., and Bradfield, C.A. (2010). An Interaction between Kynurenine and the Aryl Hydrocarbon Receptor Can Generate Regulatory T Cells. J. Immunol. *185*, 3190–3198.

Minikkin, D. (1982). Lipids: Complex lipids, their chemistry, biosynthesis and roles (London: Academic).

Miyamoto, J., Mizukure, T., Park, S.B., Kishino, S., Kimura, I., Hirano, K., Bergamo, P., Rossi, M., Suzuki, T., Arita, M., et al. (2015). A gut microbial metabolite of linoleic acid, 10-hydroxy-cis-12-octadecenoic acid, ameliorates intestinal epithelial barrier impairment partially via GPR40-MEK-ERK pathway. J. Biol. Chem. *290*, 2902–2918.

Murakami, K., Ide, T., Suzuki, M., Mochizuki, T., and Kadowaki, T. (1999). Evidence for direct binding of fatty acids and eicosanoids to human peroxisome proliferators-activated receptor alpha. Biochem. Biophys. Res. Commun. *260*, 609–613.

Muzzi, A., Masignani, V., and Rappuoli, R. (2007). The pan-genome: towards a knowledge-based discovery of novel targets for vaccines and antibacterials. Drug Discov. Today *12*, 429–439.

Nagy, L., Kao, H.Y., Love, J.D., Li, C., Banayo, E., Gooch, J.T., Krishna, V., Chatterjee, K., Evans, R.M., and Schwabe, J.W.R. (1999). Mechanism of corepressor binding and release from nuclear hormone receptors. Genes Dev. *13*, 3209–3216.

Nandedkar, A.K. (1983). Comparative Study of the Lipid Composition of Particular Pathogenic And Nonpathogenic Species of Mycobacterium. J. Natl. Med. Assoc. *75*, 69–74.

Napetschnig, J., and Wu, H. (2013). Molecular basis of NF-κB signaling. Annu. Rev. Biophys. *42*, 443–468.

Di Narzo, A.F., Peters, L.A., Argmann, C., Stojmirovic, A., Perrigoue, J., Li, K., Telesco, S., Kidd, B., Walker, J., Dudley, J., et al. (2016). Blood and Intestine eQTLs from an Anti-TNF-Resistant Crohn's Disease Cohort Inform IBD Genetic Association Loci. Clin. Transl. Gastroenterol. *7*, e177.

Newman, D.J., and Cragg, G.M. (2016). Natural Products as Sources of New Drugs from

1981 to 2014. J. Nat. Prod. *79*, 629–661.

O'Neill, L. a J., and Bowie, A.G. (2007). The family of five: TIR-domain-containing adaptors in Toll-like receptor signalling. Nat. Rev. Immunol. *7*, 353–364.

Ogawa, J., Kishino, S., Ando, A., Sugimoto, S., Mihara, K., and Shimizu, S. (2005). Production of conjugated fatty acids by lactic acid bacteria. J. Biosci. Bioeng. *100*, 355–364.

Oh, D.Y., Talukdar, S., Bae, E.J., Imamura, T., Morinaga, H., Fan, W., Li, P., Lu, W.J., Watkins, S.M., and Olefsky, J.M. (2010). GPR120 Is an Omega-3 Fatty Acid Receptor Mediating Potent Anti-inflammatory and Insulin-Sensitizing Effects. Cell *142*, 687–698.

Okada, H., Kuhn, C., Feillet, H., and Bach, J.-F. (2010). The "hygiene hypothesis" for autoimmune and allergic diseases: an update. Clin. Exp. Immunol. *160*, 1–9.

Osborne, J., and Devaney, E. (1999). Interleukin-10 and Antigen-Presenting Cells Actively Suppress Th1 Cells in BALB/c Mice Infected with the Filarial Parasite *Brugia pahangi*. Infect. Immun. *67*, 1599–1605.

Peters, N., and Sacks, D. (2006). Immune privilege in sites of chronic infection: *Leishmania* and regulatory T cells. Immunol. Rev. *213*, 159–179.

Prados-rosales, R., Baena, A., Martinez, L.R., Luque-garcia, J., Kalscheuer, R., Veeraraghavan, U., Camara, C., Nosanchuk, J.D., Besra, G.S., Chen, B., et al. (2011). Mycobacteria release active membrane vesicles that modulate immune responses in a TLR2-dependent manner in mice. *121*, 1471–1483.

Prince, A., Alvarez, F.S., and Young, J. (1973). Preparation of prostaglandins A2, E2 and 11-epi-E2 from their 15 acetates methyl esters using an endogenous enzyme system present in plexaura Homomalla (Esper). Prostaglandins *3*, 531–535.

Quintana, F., Basso, a, Iglesias, a, Korn, T., Farez, M., Bettelli, E., Caccamo, M., Oukka, M., and Weiner, H. (2008). Control of T(reg) and T(H)17 cell differentiation by the aryl hydrocarbon receptor. Nature *453*, 65–71.

Ragnarsdottir, B., Lutay, N., Gronberg-Hernandez, J., Koves, B., and Svanborg, C. (2011). Genetics of innate immunity and UTI susceptibility. Nat Rev Urol *8*, 449–468.

Reber, S.O., Siebler, P.H., Donner, N.C., Morton, J.T., Smith, D.G., Kopelman, J.M., Lowe, K.R., Wheeler, K.J., Fox, J.H., Hassell, J.E., et al. (2016). Immunization with a heat-killed preparation of the environmental bacterium *Mycobacterium vaccae* promotes stress resilience in mice. Proc. Natl. Acad. Sci. *113*, 3130–3139.

Reed, M.B., Gagneux, S., DeRiemer, K., Small, P.M., and Barry, C.E. (2007). The W-Beijing lineage of Mycobacterium tuberculosis overproduces triglycerides and has the DosR dormancy regulon constitutively upregulated. J. Bacteriol. *189*, 2583–2589.

Reina, E., Ramos, F.A., Castellanos, L., Aragõn, M., and Ospina, L.F. (2013). Anti-inflammatory R-prostaglandins from Caribbean Colombian soft coral Plexaura homomalla. J. Pharm. Pharmacol. *65*, 1643–1652.

Riccardi, C. (2015). GILZ as a mediator of the anti-inflammatory effects of glucocorticoids. Front. Endocrinol. (Lausanne). *6*, 1–6.

Ricote, M., and Glass, C.K. (2007). PPARs and molecular mechanisms of transrepression. Biochim. Biophys. Acta - Mol. Cell Biol. Lipids *1771*, 926–935.

Riedler, J., Braun-Fahrländer, C., Eder, W., Schreuer, M., Waser, M., Maisch, S., Carr, D., Schierl, R., Nowak, D., von Mutius, E., et al. (2001). Exposure to farming in early life and development of asthma and\rallergy: a cross-sectional survey. Lancet *358*, 1129–1133.

Roman-Nunez, M., Cuesta-Alonso, E.P., and Gilliland, S.E. (2007). Influence of sodium glycocholate on production of conjugated linoleic acid by cells of *Lactobacillus reuteri* ATCC 55739. J. Food Sci. *72*, 140–143.

Rook, G.A.W. (2009). Review series on helminths, immune modulation and the hygiene hypothesis: The broader implications of the hygiene hypothesis. Immunology *126*, 3–11.

Rook, G.A.W. (2010). 99th Dahlem Conference on Infection, Inflammation and Chronic Inflammatory Disorders: Darwinian medicine and the “hygiene” or “old friends” hypothesis. Clin. Exp. Immunol. *160*, 70–79.

Rook, G.A.W., and Lowry, C.A. (2009). The hygiene hypothesis and affective and anxiety disorders. In The Hygiene Hypothesis and Darwinian Medicine, pp. 189–220.

Rook, G.A.W., and Rosa Brunet, L. (2002). Give us this day our daily germs. Biologist (London). *49*, 145–149.

Rook, G.A.W., Raison, C.L., and Lowry, C.A. MICROBIAL “ OLD FRIENDS ”, IMMUNOREGULATION AND PSYCHIATRIC DISORDERS. 1–31.

Rook, G.A.W., Hamelmann, E., and Rosa Brunet, L. (2007). Mycobacteria and allergies. Immunobiology *212*, 461–473.

Rook, G. a W., Adams, V., Hunt, J., Palmer, R., Martinelli, R., and Brunet, L.R. (2004). Mycobacteria and other environmental organisms as immunomodulators for immunoregulatory disorders. Springer Semin. Immunopathol. *25*, 237–255.

Rusinova, I., Forster, S., Yu, S., Kannan, A., Masse, M., Cumming, H., Chapman, R., and Hertzog, P.J. (2013). INTERFEROME v2.0: An updated database of annotated interferon-regulated genes. Nucleic Acids Res. *41*.

Sartain, M.J., Dick, D.L., Rithner, C.D., Crick, D.C., and Belisle, J.T. (2011). Lipidomic analyses of Mycobacterium tuberculosis based on accurate mass measurements and the novel

"Mtb LipidDB". J. Lipid Res. *52*, 861–872.

Sawczenko, A., Sandhu, B., Logan, R., Jenkins, H., Taylor, C., Mian, S., and Lynn, R. (2001). Prospective survey of childhood inflammatory bowel disease in the British Isles. Lancet *357*, 1093–1094.

Schnoeller, C., Rausch, S., Pillai, S., Avagyan, A., Wittig, B.M., Loddenkemper, C., Hamann, A., Hamelmann, E., Lucius, R., and Hartmann, S. (2008). A helminth immunomodulator reduces allergic and inflammatory responses by induction of IL-10-producing macrophages. J. Immunol. *180*, 4265–4272.

Schreber, S.L. (1991). The Immunophilins Their Immunosuppressive Ligands Molecular Recognition by the Immunophilins. Sci. Artic. *251*, 283–287.

Sharif-Askari, E., Vassen, L., Kosan, C., Khandanpour, C., Gaudreau, M.-C., Heyd, F., Okayama, T., Jin, J., Rojas, M.E.B., Grimes, H.L., et al. (2010). Zinc finger protein Gfi1 controls the endotoxin-mediated Toll-like receptor inflammatory response by antagonizing NF-kappaB p65. Mol. Cell. Biol. *30*, 3929–3942.

Shibolet, O., and Podolsky, D.K. (2007). TLRs in the Gut. IV. Negative regulation of Toll-like receptors and intestinal homeostasis: addition by subtraction. Am J Physiol Gastrointest Liver Physiol *292*, G1469-73.

Smith, P.D., Ochsenbauer-Jambor, C., and Smythies, L.E. (2005). Intestinal macrophages: unique effector cells of the innate immune system. Immunol. Rev. *206*, 149–159.

Smith, P.M., Howitt, M.R., Panikov, N., Michaud, M., Gallini, C.A., Bohlooly-Y, M., Glickman, J.N., and Garrett, W.S. (2013). The microbial metabolites, short chain fatty acids, regulate colonic Treg cell homeostasis. Science *341*, 10.1126/science.1241165.

Smits, H.H., Engering, A., Van Der Kleij, D., De Jong, E.C., Schipper, K., Van Capel, T.M.M., Zaat, B. a J., Yazdanbakhsh, M., Wierenga, E. a., Van Kooyk, Y., et al. (2005). Selective probiotic bacteria induce IL-10-producing regulatory T cells in vitro by modulating dendritic cell function through dendritic cell-specific intercellular adhesion molecule 3-grabbing nonintegrin. J. Allergy Clin. Immunol. *115*, 1260–1267.

Smoot, M.E., Ono, K., Ruscheinski, J., Wang, P.L., and Ideker, T. (2011). Cytoscape 2.8: New features for data integration and network visualization. Bioinformatics *27*, 431–432.

Smythies, L.E., Sellers, M., Clements, R.H., Mosteller-Barnum, M., Meng, G., Benjamin, W.H., Orenstein, J.M., and Smith, P.D. (2005). Human intestinal macrophages display profound inflammatory anergy despite avid phagocytic and bacteriocidal activity. J. Clin. Invest. *115*, 66–75.

Smythies, L.E., Shen, R., Bimczok, D., Novak, L., Clements, R.H., Eckhoff, D.E., Bouchard, P., George, M.D., Hu, W.K., Dandekar, S., et al. (2010). Inflammation anergy in human intestinal macrophages is due to Smad-induced IκBα expression and NF-κB inactivation.

J. Biol. Chem. *285*, 19593–19604.

Sonnenburg, E.D., Sonnenburg, J.L., Adler, C.J., Dobney, K., Weyrich, L.S., Kaidonis, J., Walker, A.W., Haak, W., Bradshaw, C.J., Townsend, G., et al. (2014). Starving our microbial self: the deleterious consequences of a diet deficient in microbiota-accessible carbohydrates. Cell Metab. *20*, 779–786.

Soroosh, P., Doherty, T.A., Duan, W., Mehta, A.K., Choi, H., Adams, Y.F., Mikulski, Z., Khorram, N., Rosenthal, P., Broide, D.H., et al. (2013). Lung-resident tissue macrophages generate Foxp3+ regulatory T cells and promote airway tolerance. J. Exp. Med. *210*, 775–788.

Stamper, C.E., Hoisington, A.J., Gomez, O.M., Halweg-Edwards, A.L., Smith, D.G., Bates, K.L., Kinney, K.A., Postolache, T.T., Brenner, L.A., Rook, G.A.W., et al. (2016). The microbiome of the built environment and human behavior: implications for emotional health and well-being in postmodern western societies. Int Rev Neurobiol *131*, 289–323.

Stanford, J.L. (1999). Immunotherapy with Mycobacterium vaccae in the treatment of mycobacterial disease . J.Infect. *39*, 179–182.

Strachan, D.P. (2000). Family size , infection and atopy : the first decade of the " hygiene hypothesis ." *55*, 2–10.

Strickland, D., Kees, U.R., and Holt, P.G. (1996). Regulation of T-cell activation in the lung: isolated lung T cells exhibit surface phenotypic characteristics of recent activation including down-modulated T-cell receptors, but are locked into the G0/G1 phase of the cell cycle. Immunology *87*, 242–249.

Subramanian, A., Tamayo, P., Mootha, V.K., Mukherjee, S., Ebert, B.L., Gillette, M.A., Paulovich, A., Pomeroy, S.L., Golub, T.R., Lander, E.S., et al. (2005). Gene set enrichment analysis: a knowledge-based approach for interpreting genome-wide expression profiles. Proc. Natl. Acad. Sci. U. S. A. *102*, 15545–15550.

Sud, M., Fahy, E., Cotter, D., Brown, A., Dennis, E.A., Glass, C.K., Merrill, A.H., Murphy, R.C., Raetz, C.R.H., Russell, D.W., et al. (2007). LMSD: LIPID MAPS structure database. Nucleic Acids Res. *35*.

Summers, R.W. (2005). Trichuris suis therapy in Crohn's disease. Gut *54*, 87–90.

Tamokou, J. de D., Simo Mpetga, D.J., Keilah Lunga, P., Tene, M., Tane, P., and Kuiate, J.R. (2012). Antioxidant and antimicrobial activities of ethyl acetate extract, fractions and compounds from stem bark of Albizia adianthifolia (Mimosoideae). BMC Complement. Altern. Med. *12*, 1074.

Tedelind, S., Westberg, F., Kjerrulf, M., and Vidal, A. (2007). Anti-inflammatory properties of the short-chain fatty acids acetate and propionate: A study with relevance to inflammatory bowel disease. World J. Gastroenterol. *13*, 2826–2832.

Teitelbaum, R., Schubert, W., Gunther, L., Kress, Y., Macaluso, F., Pollard, J.W., McMurray, D.N., and Bloom, B.R. (1999). The M cell as a portal of entry to the lung for the bacterial pathogen Mycobacterium tuberculosis. Immunity *10*, 641–650.

Upton, M.N. (2000). Intergenerational 20 year trends in the prevalence of asthma and hay fever in adults: the Midspan family study surveys of parents and offspring. BMJ *321*, 88–92.

Vandevenne, P., Sadzot-Delvaux, C., and Piette, J. (2010). Innate immune response and viral interference strategies developed by Human Herpesviruses. Biochem. Pharmacol. *80*, 1955–1972.

Vergne, I., Gilleron, M., and Nigou, J. (2014). Manipulation of the endocytic pathway and phagocyte functions by Mycobacterium tuberculosis lipoarabinomannan. Front. Cell. Infect. Microbiol. *4*, 187.

Vichai, V., and Kirtikara, K. (2006). Sulforhodamine B colorimetric assay for cytotoxicity screening. Nat. Protoc. *1*, 1112–1116.

Wheeler, P.R., and Ratledge, C. (1988). Use of carbon sources for lipid biosynthesis in Mycobacterium leprae: a comparison with other pathogenic mycobacteria. J. Gen. Microbiol. *134*, 2111–2121.

Wilson, M.S., Taylor, M.D., Balic, A., Finney, C.A., Lamb, J.R., and Maizels, R.M. (2005). Suppression of allergic airway inflammation by helminth-induced regulatory T cells. J Exp Med *202*, 1199–1212.

Wilson, M.S., Mentink-Kane, M.M., Pesce, J.T., Ramalingam, T.R., Thompson, R., and Wynn, T. a (2007). Immunopathology of schistosomiasis. Immunol. Cell Biol. *85*, 148–154.

Van Der Woude, A.D., Sarkar, D., Bhatt, A., Sparrius, M., Raadsen, S.A., Boon, L., Geurtsen, J., Van Der Sar, A.M., Luirink, J., Houben, E.N.G., et al. (2012). Unexpected link between lipooligosaccharide biosynthesis and surface protein release in Mycobacterium marinum. J. Biol. Chem. *287*, 20417–20429.

Wray, J.A., Sugden, M.C., Zeldin, D.C., Greenwood, G.K., Samsuddin, S., Miller-Degraff, L., Bradbury, J.A., Holness, M.J., Warner, T.D., and Bishop-Bailey, D. (2009). The epoxygenases CYP2J2 activates the nuclear receptor PPARα in vitro and in vivo. PLoS One *4*, 4–10.

Xu, J., Racke, M.K., and Drew, P.D. (2007). Peroxisome proliferator-activated receptor-α agonist fenofibrate regulates IL-12 family cytokine expression in the CNS: Relevance to multiple sclerosis. J. Neurochem. *103*, 1801–1810.

Yazdanbakhsh, M., Kremsner, P.G., and van Ree, R. (2002). Allergy, parasites, and the hygiene hypothesis. Science *296*, 490–494.

Ye, J., Ortaldo, J.R., Conlon, K., Winkler-Pickett, R., and Young, H. a (1995). Cellular and

molecular mechanisms of IFN-gamma production induced by IL-2 and IL-12 in a human NK cell line. J. Leukoc. Biol. *58*, 225–233.

Zaccone, P., Burton, O., Miller, N., Jones, F.M., Dunne, D.W., and Cooke, A. (2009). Schistosoma mansoni egg antigens induce Treg that participate in diabetes prevention in NOD mice. Eur. J. Immunol. *39*, 1098–1107.

Zelante, T., Iannitti, R.G., Cunha, C., DeLuca, A., Giovannini, G., Pieraccini, G., Zecchi, R., D'Angelo, C., Massi-Benedetti, C., Fallarino, F., et al. (2013). Tryptophan catabolites from microbiota engage aryl hydrocarbon receptor and balance mucosal reactivity via interleukin-22. Immunity *39*, 372–385.

Zeng, H., and Chi, H. (2015). Metabolic control of regulatory T cell development and function. Trends Immunol. *36*, 3–12.

Zhang, Y., and Sievert, S.M. (2014). Pan-genome analyses identify lineage- and niche-specific markers of evolution and adaptation in Epsilonproteobacteria. Front. Microbiol. *5*, 1–13.

Zhang, X., Goncalves, R., and Mosser, D.M. (2008). The Isolation and Characterization of Murine Macrophages. Curr. Protoc. Immunol. *CHAPTER 14*.

Zuany-Amorim, C., Sawicka, E., Manlius, C., Le Moine, A., Brunet, L.R., Kemeny, D.M., Bowen, G., Rook, G., and Walker, C. (2002a). Suppression of airway eosinophilia by killed *Mycobacterium vaccae*-induced allergen-specific regulatory T-cells. Nat. Med. *8*, 625–629.

Zuany-Amorim, C., Manlius, C., Trifilieff, A., Brunet, L.R., Rook, G., Bowen, G., Pay, G., and Walker, C. (2002b). Long-term protective and antigen-specific effect of heat-killed Mycobacterium vaccae in a murine model of allergic pulmonary inflammation. J. Immunol. *169*, 1492–1499.

Appendix 1. *In vitro* cell-based assay for identification of anti-inflammatory *M. vaccae*-derived small molecules

Acknowledgments: This work was completed in collaboration with Alexandra Cantley and Jon Clardy. Alexandra Cantley grew *Mycobacterium vaccae* and performed all of the extraction and fractionation procedures. Jon Clardy assisted with experimental design.

A1.1 **Introduction**

A1.1.1 Natural product chemistry

There is an extremely diverse array of small molecules produced across all domains of life. In particular, eubacteria constitute one of the largest sources of novel chemical structures, which has attracted the attention of many natural chemists. The diverse environments in which bacteria thrive have led them to evolve an arsenal of defensive molecules. Many of the patented antibiotics, antivirals, antifungals, and cancer therapies are, or were, derived from bacteria (Butler, 2004; Newman and Cragg, 2016) . Beyond the individual molecules isolated from the bacteria, through bioengineering, *in silico* design, or combinatorial chemistry, their structures are often derived to create new and more powerful drugs.

The use of microbial natural products in prevention and treatment of disease has a substantial history. In spite of massive advances in chemical libraries and high throughput screening, natural products continue to populate pharmacological patents. From 1981 to 2014, natural products, natural product mimics, and natural product botanicals have accounted for 33% of all drugs approved by the FDA (Newman and Cragg, 2016). In particular, natural product research has focused on the refractory issue of immune system regulation.

One of the largest resources for drug development is the Actinobacteria phylum. Among the most remarkable genera of Actinobacteria is the *Streptomyces* genus, the species of which

produce antifungals, antivirals, antitumorals, anti-hypertensives, antibiotics, and immunosuppressants (de Lima Procópio et al., 2012). Of particular interest to this research are the immunosuppressants. Two of the most prevalent immunosuppressants today are rapamycin (sirolimus) and FK506 (tacrolimus) (Demain, 2014; Kino et al., 1987). At the time of their discovery, they were 100 times more powerful than the closest market competitor (Demain, 2014). Both of these molecules were discovered from *Streptomyces* species and share the common macrolide structure, but, interestingly, do not share a common mechanism of suppression (Schreber, 1991). Identifying more of such molecules may not only lead to improved health care, but also may advance our understanding of the biology.

A1.1.2 *M. vaccae*

For this particular study we chose to use the *M. vaccae* type strain (*Mycobacterium vaccae* Bonicke and Juhasz (ATCC® 15483™). The type strain was the only strain with a publicly available genome, which would be potentially useful for future experiments, and it had the most extensive background of cell culture methodology. Furthermore, this nonpathogenic organism is closely related to many pathogenic mycobacteria, which are notorious for both immune evasion (Geffner et al., 2009). *M. vaccae* is an ideal system to screen for immunoregulatory molecules because the shared, or perhaps unique, genetic machinery of immune suppression may be present but without the virulence components.

One method of intercellular communication between a bacterium and other cells is through secreted molecules. Mycobacteria are equipped with various ATP binding cassette (ABC) transporters, unique type-VII secretion systems (T7SSs) (also referred to as ESX secretion systems), and the ability to shed exosomes(Abdallah et al., 2007; Braibant et al., 2000; Gröschel

et al., 2016; Prados-rosales et al., 2011). Secreted molecules may play an important role in interactions between mycobacteria and the mammalian host, for example, to promote immune evasion or symbiosis. In this study, we extracted and fractionated the supernatants of *M. vaccae* cultures and performed a bioassay to test the anti-inflammatory properties of the fractions in a macrophage model of inflammation.

A1.2 Materials and methods

A1.2.1 Animals

For all studies involving *ex vivo* assays using freshly isolated peritoneal macrophages, 6-8 week-old male BALB/c (BALB/c; Cat. No. 047; Harlan, Indianapolis, IN, USA) were used and housed under standard conditions with food and water available *ad libitum*. Both food (Cat No. 2018, Teklad Global 18% Protein Rodent Diet, Harlan, Madison, WI, USA) and tap water were provided *ad libitum* for the duration of the experiment. Mice were kept on a standard 12 h:12 h light/dark cycle (lights on 0600). The experiments were conducted in accordance with the *Guide for the Care and Use of Laboratory Animals*, Eighth Edition (Institute for Laboratory Animal Research, The National Academies Press, Washington, D.C., 2011) and were approved by the University of Colorado Boulder Institutional Animal Care and Use Committee. All possible efforts were made to minimize the number of animals used and their suffering.

A1.2.2 Growing *M. vaccae*

M. vaccae (ATCC 15483) was grown in 2L baffled flasks. 7H9 Middlebrook media (BD Biosciences) was prepared according to manufacturer's instructions. After autoclaving the media, it was supplemented with ADC (10 g bovine albumin fraction V (Fisher Scientific), 4 g dextrose (Sigma-Aldrich), 0.006 g catalase (Sigma-Aldrich)). The media was inoculated with a

single colony of *M. vaccae* grown on 7H11 plates (BD Biosciences). Cells were grown at 37°C until the stationary phase was achieved (OD600 ~0.5).

A1.2.3 Extraction and separation of culture supernatants

Cultures were centrifuged (4000g, 10 min), and the supernatants were sterile filtered (0.2 μm). Crude extractions of the supernatant were performed with hexanes (1:1) and then ethyl acetate (1:1). The aqueous phase was also retained for the bioassay. The cell pellet was extracted with chloroform—methanol (3:1). The crude extracts were evaporated under rotovap and, for immediate assay, were resuspended in Dulbecco's Modified Eagle Medium (DMEM; ThermoFisher), or for further fractionation, were resuspended in 15% methanol. For the second fractionation, the crude extracts were then fractionated on a C18 Sep-Pak® column (Waters) and eluted on a gradient of acetonitrile. Five fractions, consisting of the flow-through, 15% acetonitrile, 50% acetonitrile, 100% acetonitrile, and acetone wash were collected for the bioassay. The third fractionation was also performed on a C18 column and eluted on an acetonitrile gradient.

A1.2.4 Macrophage bioassay

Murine peritoneal macrophages were isolated and cultured as previously described(Zhang et al., 2008) and used to determine the effects of crude extracts and fractionated material on lipopolysaccharide-induced IL-6 secretion. Briefly, mice received one 1 ml i.p. injection of 3% thioglycollate medium (Cat. No. 9000-294, VWR, Radnor, PA, USA). Ninety-six hours later, macrophages were collected in Dulbecco's phosphate-buffered saline (DPBS; Cat. No. 14190136, Invitrogen, Carlsbad, CA, USA). Cells were centrifuged and resuspended in DMEM/F-12 (Cat. No. 10565018, Invitrogen) supplemented to be 10% (v/v) fetal bovine serum

(Cat. No. 16000036, Invitrogen) and 1% penicillin/streptomycin (Cat.No. 15140148, Invitrogen). One mouse yielded enough cells for one experimental replicate (n = 1). $1x10^5$ cells/well were allowed to adhere for 1.5 h before being washed with DPBS. The dried extracts and fractionated material of *M. vaccae* broth were resuspended in DMEM/F-12, 0.2% DMSO for a final concentration of 100 μg/ml. The macrophages were incubated with the extracts/fractionated material or vehicle (DMEM/F-12, 0.2% DMSO for 1 h before being stimulated with LPS (serotype 0127:B8, Sigma-Aldrich, St. Louis, MO, USA). Cell culture supernatants were collected 6 h and 24 h after stimulation and diluted 1:200. IL-6 in the supernatant was measured using sandwiched ELISA (Cat. No. 431304, Biolegend, San Diego, CA, USA). All samples were measured in duplicate. Cytotoxicity was determined using the sulforhodamine B (SRB) colorimetric assay, as previously described(Vichai and Kirtikara, 2006).

A1.3 **Results**

A1.3.1 Advanced screening

Initial ethyl acetate and hexanes extractions were fractionated on a C18 column. The flow through, 15%, 50%, 100% acetonitrile, and acetone wash were collected for assay. The anti-inflammatory activity of the fractions was determined from the relative IL-6 secretion of LPS-stimulated macrophages. There was no significant activity in the hexanes fractions or the *M. vaccae* pellet fractions (Fig. A1.1). The 50% acetonitrile elution of the ethyl acetate extraction had profound anti-inflammatory effects 6 h and 24 h after LPS stimulation (Fig. A1.1). To ensure these results were not artefactual, the LC/MS spectra ofthe *M. vaccae* E3 fraction and fractions of the growth media ethyl acetate extract were compared, and we were able to identify unique masses in the *M. vaccae* E3 fraction. A second round of separation was performed on a C18

column. Forty-three fractions, defined by time on column, were collected, and fractions 4-43 were screened for potential anti-inflammatory activity,

Several candidate fractions were observed in the second separation of the ethyl acetate extraction (Fig. A1.2). The most potent fractions were 25, 28, and 30, which almost completely abrogated LPS-induced IL-6 release. The 12 most abundant masses from the LC/MS trace of these three fractions are reported in Table 3.1. Simply based on mass alone, there is an enormous number of possible structures, but we were able to infer some information about the general nature of these molecules. All of the peaks belonged to *M. vaccae*, as none of the peaks matched growth media components. Secondly, most apolar, neutral molecules would have been extracted into the hexanes, and heavily charged molecules, like nucleic acids and most polypeptides, are not soluble in ethyl acetate. Lastly, the masses range from 100-600 Da, which is consistent with small molecule metabolites, lipids, or lipid conjugates.

Each of the masses was queried against 4 metabolomics databases: the LIPID Metabolites and Pathway Strategy (LIPID MAPS) database(Sud et al., 2007), a lipidomic profile of *Mycobacterium tuberculosis*(Sartain et al., 2011), the online tool Metabolome Searcher(Dhanasekaran et al., 2015), and MassBank(Horai et al., 2010). The number of hits from each database is reported in Table 3.1. Two of the 12 masses only hit on the lipid databases and they each had only one hit in the *M. tuberculosis* dataset. From these results we gain confidence that fatty acids or lipid molecules are in the most bioactive E3 fraction of *M. vaccae*, under the conditions of these assays.

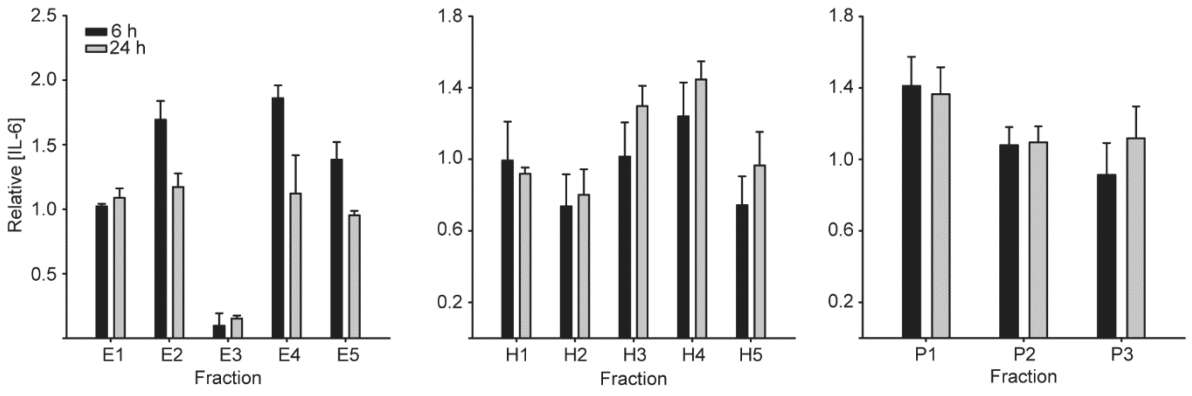

Figure A1.1 Anti-inflammatory activity of fractionated *M. vaccae* extractions.
Anti-inflammatory activity was assessed as lipopolysaccharide (LPS)-stimulated interleukin (IL) 6 secretion from freshly isolated murine peritoneal macrophages. Data are reported as IL-6 concentration in culture supernatant relative to DMEM controls. Data are expressed as means + standard error of the mean (SEM). Abbreviations: E* refers to ethyl acetate extracts, H* refers to hexanes extract, and P* refers to the pellet. 1-5 correspond to FT, 10%, 50%, 100% ACN, and acetone wash, respectively. P1 is the FT, P2 is 100% CAN, and P3 is 100% acetone.

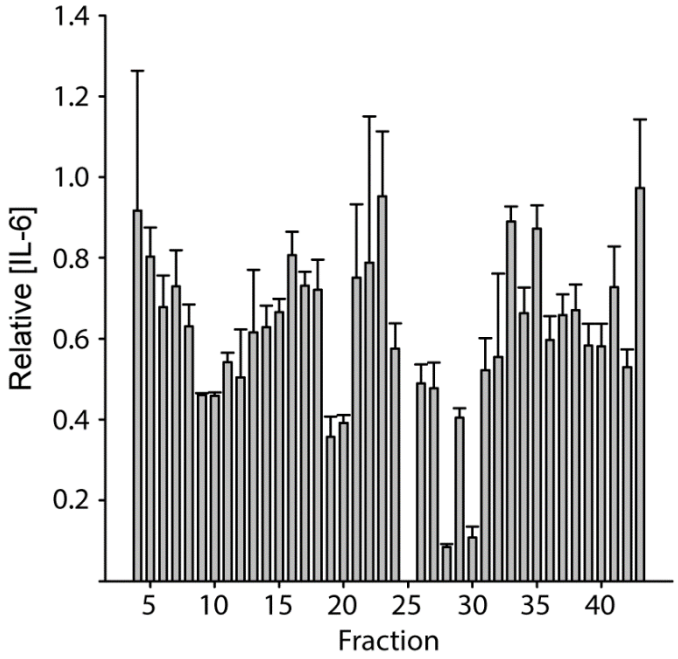

Figure A1.2 Anti-inflammatory activity of fractionated *M. vaccae* E3 fraction.
Anti-inflammatory activity was assessed as lipopolysaccharide (LPS)-stimulated interleukin (IL)-6 secretion from macrophages. Data are reported as IL-6 concentration in culture supernatant relative to DMEM controls. Data are expressed as means ± standard error of the mean.

Table A1.1. Masses and possible structures of fractions 25, 28, and 30 of EtOAc 3

Mass (M+H)	# lipid maps hits	# MtdDB hits	# metabolome searcher hits	# massbank hits	Lipid Maps main classes	Likely molecule
223.1681	37	0	4	15	Fatty acid and conjugates, fatty aldehydes, fatty esters, isoprenoids	
295.1865	61	0	5	10	Fatty Acids and Conjugates, Octadecanoids, Flavonoids, Isoprenoids	
353.1545	195	0	2	12	Fatty Acids and Conjugates, Eicosanoids, Flavonoids, Aromatic polyketides	
674.4999	15	1	0	0	Glycerophosphocholines, Glycerophosphoethanolamines, Ceramides	Diacylglycerolphosphoethanolamines (PE) PE (R1CO2H+R2CO2H=31:1)
215.0902	48	0	4	13	Fatty Acids and Conjugates, Aromatic polyketides, Isoprenoids, Fatty esters	
239.0516	62	0	0	8	Flavonoids	
313.1607	118	0	1	15	Fatty Acids and Conjugates, Octadecanoids, Aflatoxins and related substances, Steroids, Sterols	
353.1549	195	0	3	10	Fatty Acids and Conjugates, Eicosanoids, Flavonoids, Aromatic polyketides, Isoprenoids, Steroid conjugates	
381.1496	73	1	0	1	Eicosanoids, Glycerophosphates, Flavonoids, Aromatic polyketides, Isoprenoids, Steroids, Steroid conjugates	Mycolipenic acid (C25), C25H48O2
283.153	112	0	0	4	Fatty Acids and Conjugates, Flavonoids, Aromatic polyketides, Isoprenoids	
365.1555	43	0	0	7	Fatty Acids and Conjugates, Eicosanoids, Flavonoids, Isoprenoids, Steroids	
157.0853	72	0	14	5	Fatty Acids and Conjugates, Oxygenated hydrocarbons, Polyether antibiotics, Isoprenoids	

A1.4 **Discussion**

Specific fractions of ethyl acetate extracts of supernatants from cultures of *M. vaccae* NCTC 11659 were effective at suppressing LPS-stimulated release of IL-6, suggesting that *M. vaccae* secretes a number of polar anti-inflammatory compounds. In contrast, we were unable to identify fractions of hexane extracts, or fractions derived from the cell pellet, with potent anti-inflammatory activity. Overall, since the final E3 ethyl acetate fractions are likely to contain many compounds, the effects of some individual extracts on IL-6 secretion in freshly isolated macrophages may be a composite of both proinflammatory and anti-inflammatory molecules; nevertheless, some fractions were clearly dominated by anti-inflammatory effects.

Specific fractions of ethyl acetate extracts of supernatants from cultures of *M. vaccae* NCTC 11659 were effective at suppressing LPS-stimulated release of IL-6, suggesting that *M. vaccae* secretes a number of polar anti-inflammatory compounds. The specific source(s) of the anti-inflammatory molecules is unknown. Because the ethyl acetate extracts were derived from the cell culture supernatant, it is possible that the bioactive compounds represent secreted compounds that are used for intercellular signaling, either to other bacteria (i.e. quorum sensing), or to host organisms. Secreted anti-inflammatory compounds may play a role in maintaining a symbiotic relationship with other organisms, including mammalian hosts. Alternatively, these compounds may be metabolic byproducts, surface molecules liberated from the outer cell wall during sample preparation, or active membrane vesicles, which have been shown to be released by mycobacteria and to modulate immune responses in a TLR2-dependent manner in mice (Prados-rosales et al., 2011).

Interest in mycobacterial natural products was stimulated by the success of many natural products discovered from *Streptomyces*, which produce a variety of molecules relevant to human health(de Lima Procópio et al., 2012) and also belong to the same phylum, Actinobacteria, as *Mycobacterium*. Many of the antibiotics, antifungals, and immunosuppressants discovered from *Streptomyces* are polyketides, which are often found in the ethyl acetate extracts (Kónya et al., 2008). In support of this, there are several polyketide synthases in the *M. vaccae* genome. However, from the three most bioactive fractions we surveyed on the lipidomic and metabolomic databases, there were 5 known polyketides with equivalent masses, and they were produced by either plants or fungi. This does not preclude the possibility that the bioactive fractions contain a polyketide, because the objective was to discover a molecule.

Two of the 12 most abundant masses identified may contain an unsaturated acyl chain, one of which is a diacylglycerolphosphoethanolamine and the other being a C25 mycolipenic acid. Both of these molecules have been identified in lipidomic studies of *Mycobacterium tuberculosis* H37Rv (Sartain et al., 2011). There is also is a high degree of conservation of lipid metabolism-associated enzymes between *M. vaccae* and *M. tuberculosis* H37Rv (see Appendix 1). Bioactive fatty acids (FAs) or FA derivatives are less common than polyketides, but not unheard of from ethyl acetate extracts. The lipid catabolite, prostaglandin A2, which has anti-inflammatory properties, was discovered in the ethyl acetate extract of a coral (Prince et al., 1973; Reina et al., 2013). Another bioactive lipid, n-hexadecanoic acid, with antioxidant and antimicrobial properties, was found in the ethyl acetate extract of stem bark (Tamokou et al., 2012). Anti-inflammatory lipids can be found across all domains of life, including bacteria, as reviewed here (Abdelmohsen et al., 2014; Furukawa et al., 2012; Gautam and Jachak, 2009). Overall, few

immunosuppressive fatty acyl molecules have been discovered from Actinobacteria, although some virulence factors of pathogenic mycobacteria, like ManLAM, have lipid components.

From what we have observed, 2 of 12 molecules detected in the most anti-inflammatory fractions are likely to be fatty acids. That conclusion was based on known molecules of phylogenetically-related species, and we have not validated any structural information. Furthermore, at this point, we cannot be certain whether the anti-inflammatory effects are due to a single molecule or a combination of molecules. Further research on the functional and structural roles of *M. vaccae*-derived molecules is needed.

Appendix 2: Evolution of nonpathogenic *Mycobacterium*: A Pan-genomic study

Screening extracts of bacteria in order to identify immunsuppressive molecules is a lengthy and high-risk process, so, to better understand the molecules produced *M. vaccae*, we looked towards the genome. This approach is also high risk, but it is more economical. The initial idea was to compare the *M. vaccae* genome to 29 other mycobacteria to identify the genes unique to *M. vaccae* followed by sequence alignments to discern biosynthetic clusters or particular genes. This approach, known as pangenomics or comparative genomics, has been applied to understanding environmental-niche adaptions, virulence factors, and vaccine development (D'Auria et al., 2010; Muzzi et al., 2007; Zhang and Sievert, 2014). This approach is unlikely to aid small molecule discovery, but it does provide a platform to better understand the many nonpathogenic mycobacteria left out of the research spotlight.

The peptide sequences of all coding DNA sequences (CDS) from 30 genomes (29 mycobacterial genomes and *Akkermansia muciniphila*) were downloaded. Genomes were selected to include the various pathogenic groups, nonpathogenic, slow growing, rapid growing, and ecological niches.

Table A2.1. Summary of the 30 genomes used in the analysis

Species	Status	Length	plasmids	GC %	Genes	NCBI	ecosystem	eco. Cat.	phenotype
Akkermansia muciniphila	complete	2664102	0	55.80 %	2319	NC_010655.1	host-associated	human	Not known to be pathogenic
Mycobacterium abscessus	complete	5270527	2	64.19 %	5235	NC_021282.1	host-associated	human	pathogen

bolletii 50594									
Mycobacterium abscessus ATCC 19977	complete	5090490	1	64.12%	4942	NC_010397.1	host-associated	human	pathogen
Mycobacterium africanum GM041182	complete	4389314	0	65.59%	3880	NC_015758.1	host-associated	mammal	pathogen
Mycobacterium avium subsp. paratuberculosis K-10	complete	4829781	0	69.30%	4415	NC_002944.2	host-associated	mammal	pathogen
Mycobacterium avium 104	complete	5475491	0	68.99%	5305	NC_008595.1	host-associated	human	pathogen
Mycobacterium bovis BCG str. Korea 1168P	complete	4304386	0	65.63%	4120	NC_020245.2	host-associated	mammal	pathogen
Mycobacterium bovis AF2122/97	complete	4345492	0	65.63%	4014	NC_002945.3	host-associated	mammal	pathogen
Mycobacterium canettii CIPT 140010059	complete	4482059	0	65.62%	3909	NC_015848.1	host-associated	human	pathogen
Mycobacterium chubuense NBB4	complete	6342624	2	68.29%	6069	NC_018027.1	environmental	terrestrial	not known to be pathogenic
Mycobacterium gilvum PYR-GCK	complete	5982829	3	67.74%	5683	NC_009338.1	environmental	aquatic	not known to be pathogenic
Mycobacterium intracellula	complete	5402402	0	68.10%	5193	NC_016946.1	Host-associated	human	pathogen

re ATCC 13950									
Mycobacterium kansasii ATCC 12478	complete	6577228	1	66.23%	5928	NC_022663.1	host-associated	human	pathogen
Mycobacterium leprae TN	complete	3268203	0	57.80%	2750	NC_002677.1	host-associated	mammal	pathogen
Mycobacterium liflandii 128FXT	complete	6399543	1	65.53%	5570	NC_020133.1	host-associated	amphibia	pathogen
Mycobacterium marinum M	complete	6660144	1	65.73%	5501	NC_010612.1	host-associated	human	pathogen
Mycobacterium neoaurum VKM Ac-1815D	complete	5400604	0	66.91%	5212	NC_023036.2	environmental	terrestrial	not known to be pathogenic
Mycobacterium rhodesiae NBB3	complete	6415739	0	65.49%	6342	NC_016604.1	environmental	aquatic	not known to be pathogenic
Mycobacterium smegmatis str. MC2 155	complete	6988209	0	67.40%	6941	NC_008596.1	engineered	lab	pathogen
Mycobacterium smegmatis NCTC8159	complete	6983267	0	67.33%	6728	NZ_LN831039.1	environmental	terrestrial	not known to be pathogenic
Mycobacterium sinense	complete	4643668	0	68.37%	4398	NC_015576.1	host-associated	human	pathogen
Mycobacterium sp. JLS	complete	6048425	0	68.36%	5855	NC_009077.1	environmental	terrestrial	not known to be

									pathogenic
Mycobacterium sp. KMS	complete	6256079	2	68.23%	6089	NC_008705.1	environmental	terrestrial	not known to be pathogenic
Mycobacterium sp. MCS	complete	5920523	1	68.39%	5704	NC_008146.1	environmental	terrestrial	not known to be pathogenic
Mycobacterium tuberculosis H37Rv	complete	4411708	0	65.62%	4170	NC_018143.2	host-associated	human	pathogen
Mycobacterium tuberculosis Haarlem	complete	4347292	0	65.34%	4376	NC_022350.1	host-associated	human	pathogen
Mycobacterium ulcerans Agy99	complete	5805761	1	65.39%	4306	CP000325.1	host-associated	human	pathogen
Mycobacterium vaccae ATCC 25954	draft	6223660	?	68.60%	5678	NZ_ALQA00000000.1	environmental	terrestrial	not known to be pathogenic
Mycobacterium vanbaalenii PYR-1	complete	6491865	0	67.79%	6047	NC_008726.1	environmental	terrestrial	not known to be pathogenic
Mycobacterium obuense UC 1	draft	6381766	?	67.62%	6342	NZ_LAUZ00000000.2	environmental	terrestrial	not known to be pathogenic

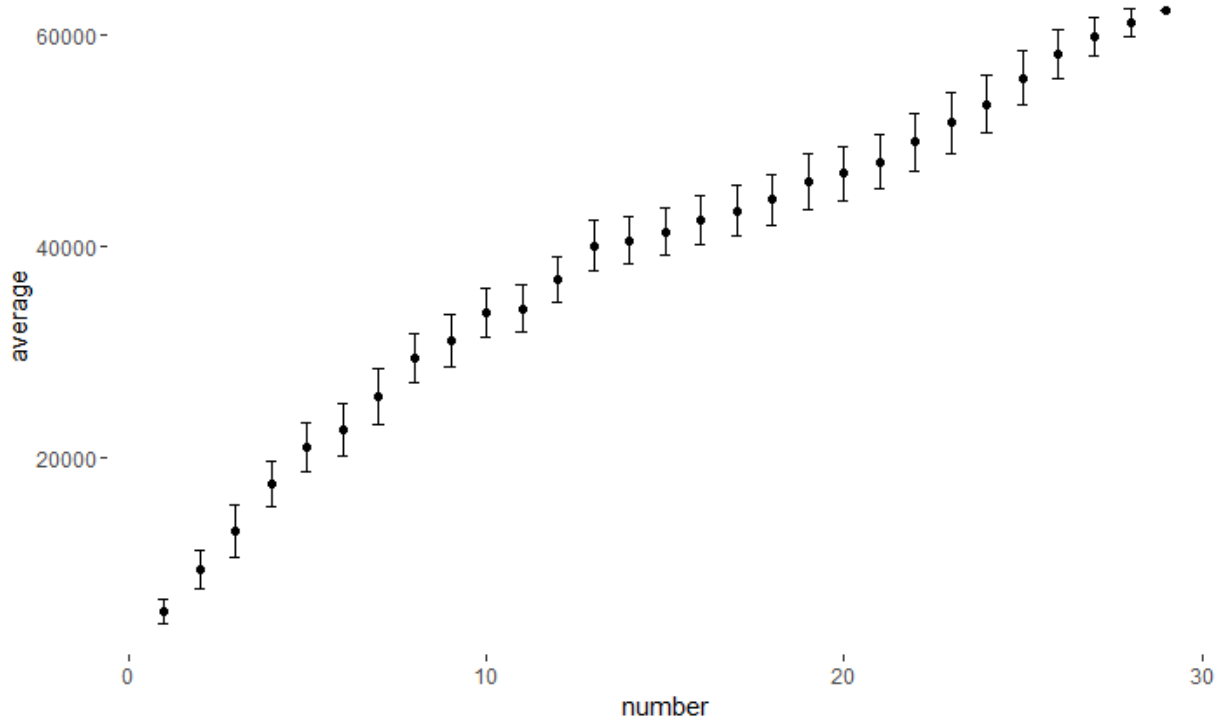

Figure A2.1 Pangenome size.
The total count of all unique genes for every genome added to the analysis.

2.1.1 Proteome-based phylogeny

One of the underlying missions of this study was to identify proteins or functions that are unique to nonpathogenic mycobacteria, *M. vaccae* in particular, relative to pathogenic mycobacteria. To understand how the 29 mycobacterial species and the *Akkermansia muciniphila* outgroup are related, we used all known or expected protein coding regions to build the phylogeny. This approach would also give the set of genes unique to a particular species or set of species. Before building the phylogenetic tree, we were interested to know how all homologous genes were distributed across subsets of mycobacterial species. To accomplish this task, each gene in a proteome was aligned using BLAST against a database of the other 29 genomes. The alignments were scored using a bit-score ratio (BSR), as opposed to the E-value.

The bit-score ratio is the alignment score of the target gene divided by the alignment score of the query to itself. In order for a gene to be considered homologous it had to have a BSR of at least 0.8 and 70% coverage. From the alignments, lists of homologous and non-homologous genes could be created, the presence or absence of the homologs was scored to create a dissimilarity matrix, which was then clustered using Unweighted Pair Group Method with Arithmetic Mean (UPGMA) (Fig A2.2) The process was a variation on defining clusters of orthologous genes (COG) within the 30 genomes. From 153201 proteins in all species, we identified 64701 homologous and nonhomologous protein sets. In the all vs all BLAST, nonpathogens on average, have more unique genes (3095) than the pathogen core genome (1505), which contained more genes than the unique gene sets of individual pathogens (620).

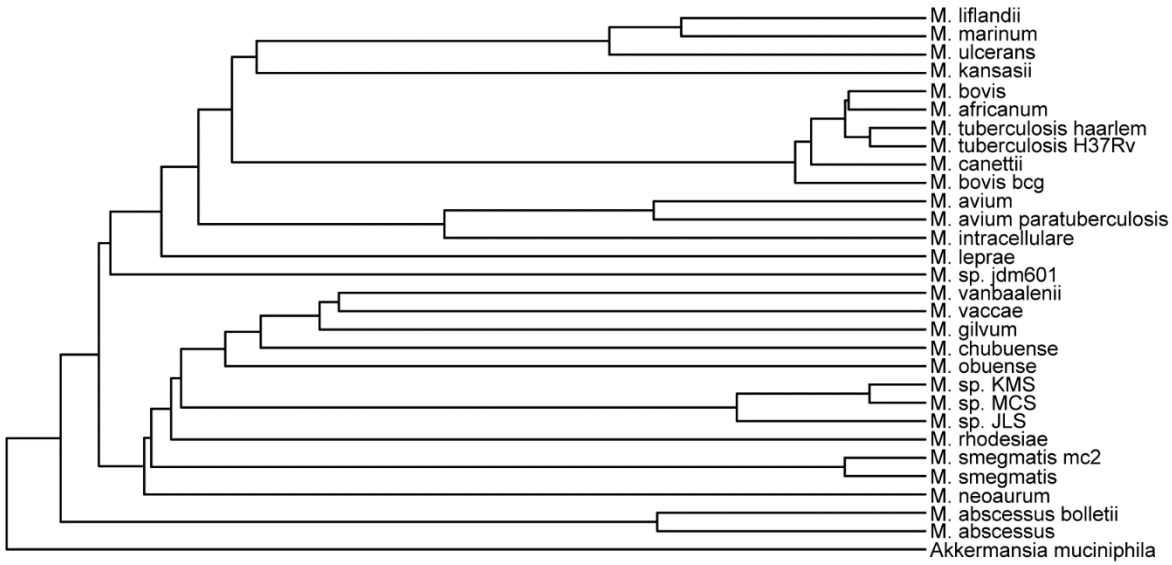

Figure A2.2 Phylogenetic clustering of *Mycobacterium* genomes based on proteome. Clusters of homologous genes were identified and counted for each genome. The distance was determined from the canberra distance, and the tree was built using UPGMA clustering. *Akkermansia muciniphila* is the outgroup.

The genomes naturally clustered with their known phenotypes. The *bovis* spp*, tuberculosis* spp., *canettii,* and *africanum* are all considered to be part of the *Mycobacterium tuberculosis*

complex. *Liflandii*, *marinum*, and *ulcerans* are all pathogens associated with water ecosystems. The *avium* spp. and *intracellulare* are associated with the *Mycobacterium avium* complex. All of the nonpathogens clustered together, though there is not enough information about them to determine unifying themes. Among the pathogens there is a conserved core of 1877 homolgous genes. Among the nonpathogens, there is a conserved core of 1205 genes.

In the *M. vaccae* genome there are 227 unique genes, which was a typical number of unique genes among the other genomes. Using an in-house script, gene ontologies (GO) were mined for each of the genes. The gene set was predominantly associated with molecular functions with 175 of 271 total GO terms. The top two molecular function terms were oxidoreductase activity and transferase activity. Furthermore, many of the nonhomologous genes were proximal to each other, which is an indication that the genes may be coexpressed, and based on the GO terms, likely involved in novel metabolic functions. The clustering of unique genes could also be an indication of transposable elements.

There is a large gap between the metabolic profiling of nonpathogenic and pathogenic mycobacterial species. These small molecules or polymers may underlie a critical separation between the two phenotypes. To test for such differences *in silico*, we curated all known enzymes to be involved in tryptophan (Trp) metabolism, and the biosynthesis of mycolic acid, lipoarabinomannan polymers, phthiocerol dimycocerosates, phenolic glycolipids, mycolactones, lipooligosaccharides, triacyl glycerides, and all genes associated with virulence and the *Mtb* cell wall.

Briefly, to assess the pathway conservation among mycobacteria, we built a web crawler to collect gene IDs from the KEGG pathway database, or a gene list provided by the user, which

then searches Uniprot for a *Mycobacterium* FASTA sequence, which is aligned to the 29 genomes using BLAST. All the mycobacterial species studied can synthesize Trp, however, non-pathogenic species lack chorismate mutase and are not able to convert Trp to phenylalanine or tyrosine. Otherwise, all but two genes in the KEGG tryptophan biosynthesis pathway (map00400) are conserved among mycobacteria. Conversely, there is scattered conservation of the KEGG tryptophan metabolism pathway (map00380). Among all 29 mycobacterial genomes, 41±10% of the pathway genes are present. The ability to degrade L-kynurenine is unique to non-pathogenic species, whereas none of the mycobacteria can convert Trp to serotonin. Manually curated lists for the biosynthesis of triacyal glycerols (TAGs), mycolic acids, phthiocerol dimycoserosates, and phenolic glycolipids revealed a high degree of conservation among all mycobacterial species, except for 3 of 54 genes related to TAG biosynthesis are only present in the *Mtb*-complex. We next looked at mannosylated lipoarabinomannan (ManLAM) biosynthesis, which is an important immunosuppressive molecule. The mannose capping of LAM is critical for the immunosuppressive effects, and the capping enzymes are only present in pathogenic species. Based on the BLAST scores, nonpathogenic species can only produce phosphate capped LAM. Mycolic acid, which is a principal component of the outer cell wall, biosynthesis is strongly conserved in all 29 genomes. We also examined the biosynthesis of lipooligosaccharides (LOSs) and found that nonpathogenic bacteria are incapable of extending the oligosaccharide beyond two sugar monomers (LOS-II). LOS are important virulence factors, which contribute to the secretion of virulent PE_PGRS proteins (Van Der Woude et al., 2012). Lastly, among a list of 771 *M. tuberculosis* genes associated with cell wall processes, only 5 genes were uniquely missing from nonpathogenic species: Rv1037c, Rv1038c, Rv3619c, Rv3620c, Rv3779. We also curated a list of *Mtb* complex virulence factors. Based on these results, which are primarily based

on gene lists compiled from pathogenic bacteria, the composition and structure of the nonpathogenic bacteria cell wall is very similar to pathogenic bacteria. Similar to the cell wall processes, the same genes conserved in other in pathogen groups (e.g. the *Mav*-complex) are also conserved in the nonpathogens, though they account for less than 50% of the *Mtb* virulence factors.

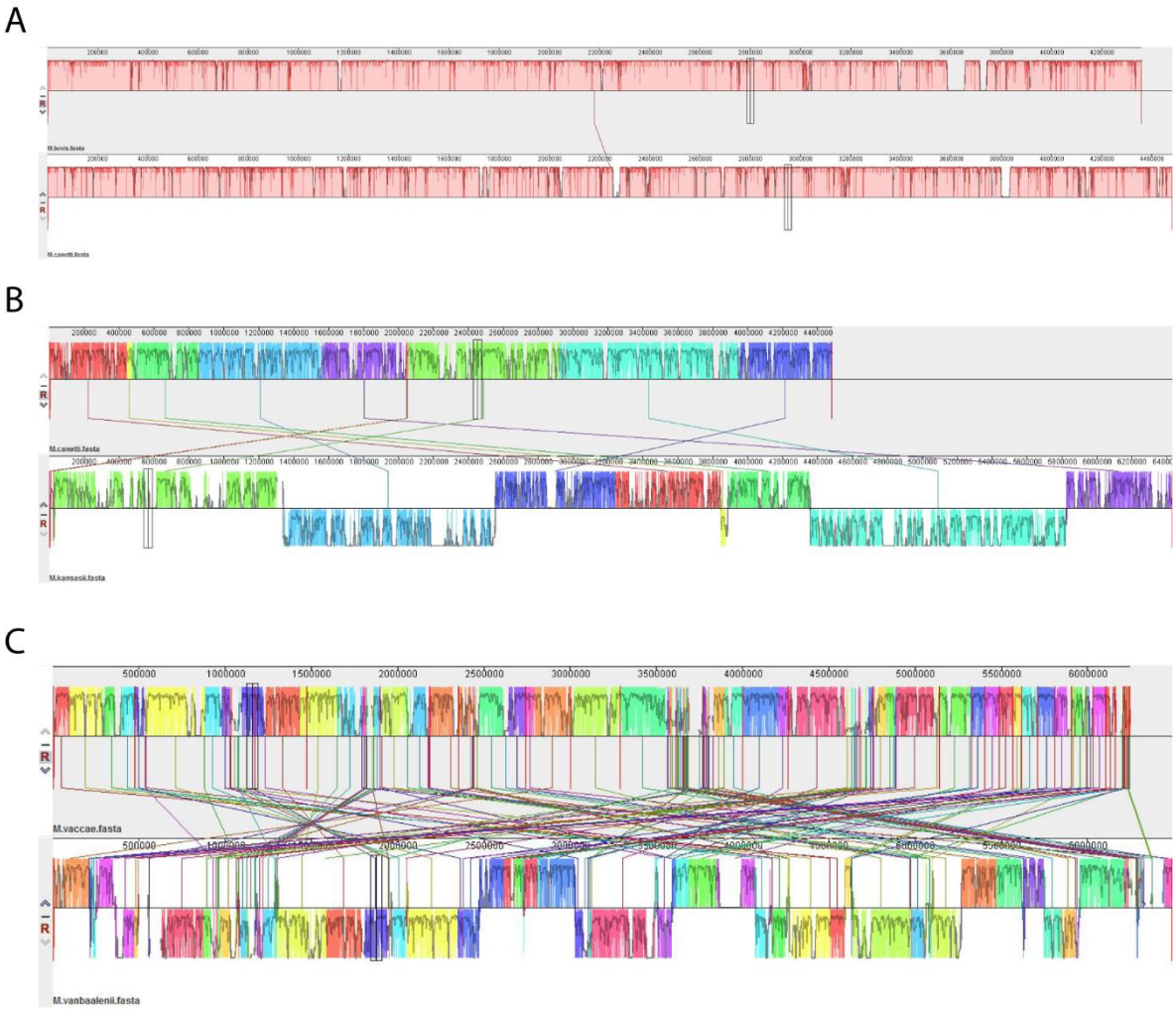

Figure A2.3 Genome synteny among mycobacteria.
(A) *M. canettii* aligned with *M. bovis*. (B) *M. canettii* aligned with *M. kansasii*. (C) *M. vaccae* aligned with *M. vanbaalenii*

Transposition is a powerful evolutionary force, so we performed whole genome alignments of the mycobacterial genomes. Looking at genome rearrangements of the most disparate genomes of the *Mtb* complex, there is no evidence of transposition (Fig. A2.3, top). When we compared genomes between pathogen groups, we identifed at least 9 transposition events (Fig. A2.3, middle). .hen we compared the genomes of *M. vaccae* and the closest related genome, *M. vanbaalenii*, there were 50 transposition events that separated them. With the exception of *M. sp. KMS* and *M. sp. MCS*, this is similar for all of the nonpathogenic species.

Despite rampant transposition events, the nonpathogenic species share a core pangenome of 1205 genes. The list of nonpathogenic genes was uploaded to the DAVID pipeline to understand common functionalities. The most enriched pathways included the TCA cycle, amino acid metabolism, and purine metabolism, however these pathways were also enriched in the core genome of all 29 mycobactria genomes. Unique to the nonpathogens, was an enrichment for ABC transporter pathways, nicotinate and nicotinamide metabolism, and amino sugar and nucleotide sugar metabolism. We also explored and annotated the 227 genes unique to *M. vaccae*. Six acyl transferases, 27 transporters (16 of 27 unique transporters were ABC transporters), as well as 12 other transerfase enzymes, like glycosyl transferases or SAM-dependent methyltransferases, were identified. Furthermore, oxidoreductase activity was the most common GO biological process term, followed by sequence-specific DNA binding. Interestingly, there were 15 clusters of at least 4 continugous genes, which may be artefactual or horizontal gene transfer events. The combination of unique transcription factors and oxidoreductases seems indicative of unique anabolic processes, but it’s outside the scope of this work to determine what sort of molecule is synthesized. We analyzed all 29 genomes using the

IslandViewer to identify genomic regions with unusual G+C content or codon usage—indicitative of a gene transfer event.

Only three of twentyo-one *M. vaccae* clusters aligned with other genomes (E-value = 0.0, coverage > 80%). One of the three is *Streptomyces silaceus*, with the other two clusters aligned with *Mycobacterium* spp. Most of the unique genes in other .28 *Mycobacterium* genomes reside in these genomic islands.

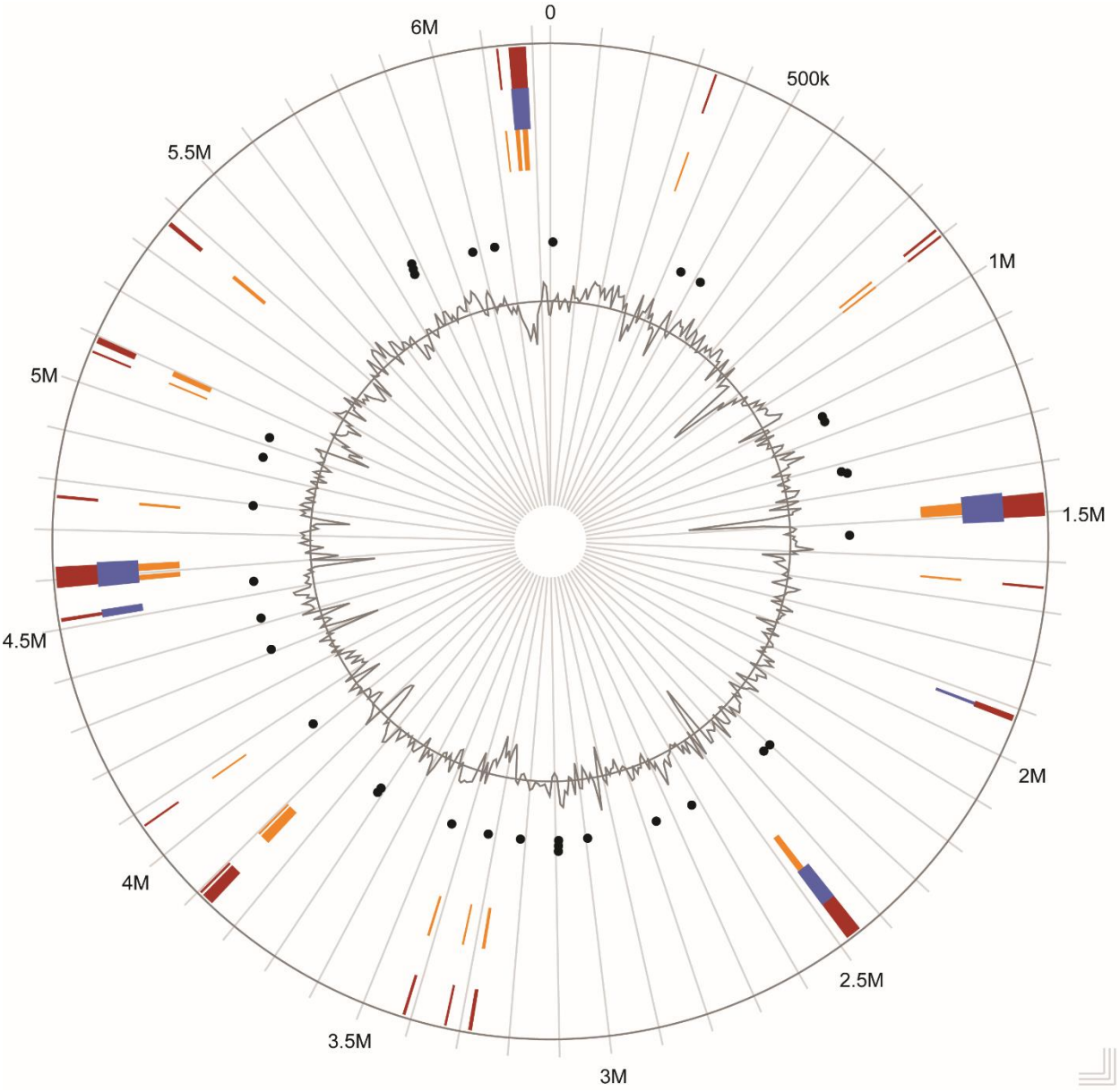

Figure A2.4 Circular plot of genomic islands in *M. vaccae*.
Genomic islands, which are often indicative of horizontal gene transfer events, were identified using IslandViewer 3.0 (Bertelli et al., 2017).

Appendix 3: RNA-Seq supplemental material

Table A3.1. Rank ordered list of most significant ($q < 0.1$) differentially expressed genes.

Log2Fold Change	padj	gene	Ensembl ID	Log2Fold Change	padj	gene	
2.155269	2.26E-21	Hp	ENSMUSG00000031722	4.175519	0.006465	Gm807	ENSMUSG00000097848
-2.09473	4.37E-19	Il6	ENSMUSG00000025746	0.866752	0.006465	Cpt1a	ENSMUSG00000024900
2.132848	3.67E-17	Tsc22d3	ENSMUSG00000031431	1.201891	0.006658	Havcr2	ENSMUSG00000020399
-1.81185	8.08E-16	Ptgs2	ENSMUSG00000032487	-0.84047	0.006831	Zyx	ENSMUSG00000029860
-2.30575	4.38E-15	Cish	ENSMUSG00000032578	1.679239	0.006937	Wee1	ENSMUSG00000031016
1.986963	1.67E-14	Dusp1	ENSMUSG00000024190	1.318917	0.007903	Adrb2	ENSMUSG00000045730
2.012712	1.86E-12	Adamtsl4	ENSMUSG00000015850	-1.02689	0.008108	Timp1	ENSMUSG00000001131
-1.6455	1.98E-12	Mir5105	ENSMUSG00000093077	1.166393	0.008496	Foxred2	ENSMUSG00000016552
-2.04621	2.63E-12	Vnn3	ENSMUSG00000020010	1.245321	0.009034	Jdp2	ENSMUSG00000034271
1.578041	2.63E-12	Plin2	ENSMUSG00000028494	-0.8805	0.009042	Pim1	ENSMUSG00000024014
-1.93629	5.09E-12	F3	ENSMUSG00000028128	0.881662	0.009058	Sgms1	ENSMUSG00000040451
-2.8558	5.31E-12	Hdc	ENSMUSG00000027360	1.272806	0.00933	Rims3	ENSMUSG00000032890
-1.5767	6.48E-12	Il1b	ENSMUSG00000027398	0.915219	0.009572	Prkar2b	ENSMUSG00000002997
-2.15506	7.97E-12	Flrt3	ENSMUSG00000051379	-1.60497	0.009607	Rnf180	ENSMUSG00000021720
3.024984	2.40E-11	Ctla2b	ENSMUSG00000074874	-2.14325	0.009652	Syt7	ENSMUSG00000024743
1.811323	4.79E-11	Tns1	ENSMUSG00000055322	-1.6082	0.009895	Hspa1a	ENSMUSG00000091971
1.82332	1.45E-10	Klhl6	ENSMUSG00000043008	-1.02922	0.010112	Tfec	ENSMUSG00000029553
-1.53809	2.78E-10	Plbd1	ENSMUSG00000030214	-1.32561	0.010112	Zfp558	ENSMUSG00000074500
-4.06225	4.95E-10	Cyp26b1	ENSMUSG00000063415	-0.78966	0.010112	Il1rn	ENSMUSG00000026981
-2.35715	5.70E-10	Ch25h	ENSMUSG00000050370	0.801393	0.010902	Dock10	ENSMUSG00000038608
-1.4212	3.35E-09	Ccl7	ENSMUSG00000035373	0.858932	0.010902	Tgfbi	ENSMUSG00000035493
-1.34039	4.91E-09	Ccl2	ENSMUSG00000035385	0.788151	0.010902	Pla2g7	ENSMUSG00000023913
-3.35822	6.81E-09	Car4	ENSMUSG00000000805	1.794042	0.010902	Srgap3	ENSMUSG00000030257
1.750436	1.16E-08	Susd2	ENSMUSG00000006342	0.983421	0.010993	Abcc3	ENSMUSG00000020865

-3.51502	2.92E-08	Adm	ENSMUSG00000030790	-1.03832	0.012028	Dennd3	ENSMUSG00000036661
-1.41666	4.57E-08	Il12a	ENSMUSG00000027776	0.78379	0.013193	Man2a1	ENSMUSG00000024085
1.394626	5.98E-08	Ppp1r12b	ENSMUSG00000073557	1.561095	0.013193	Frmd4b	ENSMUSG00000030064
1.317669	7.23E-08	Dennd4c	ENSMUSG00000038024	1.181418	0.013404	Per2	ENSMUSG00000055866
-1.56573	7.86E-08	Gm10499	ENSMUSG00000073403	1.920189	0.013773	Kcnk13	ENSMUSG00000045404
-1.76168	1.01E-07	Hbegf	ENSMUSG00000024486	-0.80185	0.014517	Plk2	ENSMUSG00000021701
1.619779	2.04E-07	Ms4a8a	ENSMUSG00000024730	1.39729	0.014584	Nrg4	ENSMUSG00000032311
-1.29736	2.22E-07	Itgax	ENSMUSG00000030789	1.946616	0.016015	Fabp4	ENSMUSG00000062515
-1.48148	3.26E-07	Ccl22	ENSMUSG00000031779	0.814942	0.018239	Adam8	ENSMUSG00000025473
1.312963	5.18E-07	Glul	ENSMUSG00000026473	-0.99463	0.018957	Slamf1	ENSMUSG00000015316
-1.29094	6.75E-07	Iigp1	ENSMUSG00000054072	0.896952	0.01948	Plpp1	ENSMUSG00000021759
1.426376	7.14E-07	Lpxn	ENSMUSG00000024696	0.778795	0.01948	Cd47	ENSMUSG00000055447
-1.30554	8.49E-07	Slc1a2	ENSMUSG00000005089	3.257959	0.019865	Saxo1	ENSMUSG00000028492
1.555412	8.59E-07	Fos	ENSMUSG00000021250	-2.11589	0.023245	Csf2	ENSMUSG00000018916
-1.73463	1.06E-06	Scimp	ENSMUSG00000057135	-0.83357	0.024354	Gm14023	ENSMUSG00000085498
1.307021	1.18E-06	Slc43a2	ENSMUSG00000038178	1.256371	0.026556	Cdo1	ENSMUSG00000033022
2.671207	1.26E-06	Ly6c2	ENSMUSG00000022584	-0.81499	0.027117	Ier3	ENSMUSG00000003541
1.168314	2.02E-06	Lcn2	ENSMUSG00000026822	0.806704	0.029122	Dock5	ENSMUSG00000044447
1.578367	2.97E-06	Fkbp5	ENSMUSG00000024222	-0.71877	0.029122	Ccl3	ENSMUSG00000000982
1.370214	4.86E-06	Sepp1	ENSMUSG00000064373	0.851011	0.03319	Rassf2	ENSMUSG00000027339
1.299991	5.32E-06	Sort1	ENSMUSG00000068747	-1.53448	0.03319	Schip1	ENSMUSG00000027777
-1.24524	1.79E-05	Upp1	ENSMUSG00000020407	0.943748	0.034299	Alox5ap	ENSMUSG00000060063
-1.1367	2.36E-05	Ccl6	ENSMUSG00000018927	0.738488	0.039546	Sdc4	ENSMUSG00000017009
-1.35404	2.68E-05	Cnn3	ENSMUSG00000053931	-1.05575	0.043357	Olfm1	ENSMUSG00000026833
-2.22194	2.86E-05	Gm5483	ENSMUSG00000079597	0.734737	0.044388	Mt2	ENSMUSG00000031762
1.131171	3.65E-05	Ecm1	ENSMUSG00000028108	-0.71991	0.044388	Inhba	ENSMUSG00000041324
1.297072	3.65E-05	Cacna1d	ENSMUSG00000015968	0.833112	0.044388	Ift57	ENSMUSG00000032965
-1.28314	3.90E-05	Olr1	ENSMUSG00000030162	1.775472	0.044388	Fabp7	ENSMUSG00000019874
-1.54507	4.24E-05	Ahr	ENSMUSG00000019256	-0.78572	0.044388	Trim30c	ENSMUSG00000078616

-1.96156	4.34E-05	Car2	ENSMUSG00000027562	-0.68344	0.044485	Rpph1	ENSMUSG00000092837
-2.66361	5.55E-05	Hspa1b	ENSMUSG00000090877	0.75981	0.047915	Ezr	ENSMUSG00000052397
-1.0926	6.25E-05	Plaur	ENSMUSG00000046223	-0.87194	0.048952	Cd83	ENSMUSG00000015396
-1.22776	7.12E-05	Procr	ENSMUSG00000027611	0.802102	0.048952	Gpcpd1	ENSMUSG00000027346
1.463418	8.54E-05	Nav2	ENSMUSG00000052512	-0.72003	0.050936	Nfkb2	ENSMUSG00000025225
-1.03592	0.000104	Tnf	ENSMUSG00000024401	-1.8997	0.050936	Lrrc32	ENSMUSG00000090958
-1.12432	0.000105	Serpinb2	ENSMUSG00000062345	0.746734	0.051435	Itga4	ENSMUSG00000027009
-1.08005	0.000134	Clec7a	ENSMUSG00000079293	-0.92303	0.051789	Cd86	ENSMUSG00000022901
-3.0819	0.000134	Ccl17	ENSMUSG00000031780	-0.73811	0.051789	Cmklr1	ENSMUSG00000042190
2.207158	0.000208	Orm1	ENSMUSG00000039196	-1.11436	0.051885	Il12b	ENSMUSG00000004296
1.323308	0.000232	Cd300a	ENSMUSG00000034652	-1.98017	0.053401	Gm13872	ENSMUSG00000087185
0.972281	0.00028	Saa3	ENSMUSG00000040026	0.784546	0.056288	Gm12840	ENSMUSG00000086320
-1.20636	0.000281	Egr2	ENSMUSG00000037868	-0.70065	0.05698	Oasl1	ENSMUSG00000041827
-0.95987	0.000319	Il1a	ENSMUSG00000027399	-0.70774	0.05698	Irf8	ENSMUSG00000041515
-1.62852	0.00032	Tnc	ENSMUSG00000028364	-1.19175	0.058415	Frmd6	ENSMUSG00000048285
1.004165	0.000329	Xdh	ENSMUSG00000024066	0.849896	0.058415	Per1	ENSMUSG00000020893
-0.97547	0.000451	Cmpk2	ENSMUSG00000020638	0.735235	0.059193	Hal	ENSMUSG00000020017
1.213513	0.000585	Htra1	ENSMUSG00000006205	-0.72158	0.059548	Wars	ENSMUSG00000021266
-1.53878	0.000656	Irf4	ENSMUSG00000021356	1.006913	0.062477	Mmp19	ENSMUSG00000025355
-1.42269	0.000656	AA467197	ENSMUSG00000033213	-0.57969	0.062658	Gm10800	ENSMUSG00000075014
-2.07631	0.000696	Kazn	ENSMUSG00000040606	-0.67963	0.065954	Nos2	ENSMUSG00000020826
0.956982	0.000867	Cd24a	ENSMUSG00000047139	-0.83535	0.066479	Csrnp1	ENSMUSG00000032515
-0.89122	0.000958	Rmrp	ENSMUSG00000088088	0.712094	0.068155	Gm26809	ENSMUSG00000097815
-0.9802	0.001016	Ccl4	ENSMUSG00000018930	-0.78044	0.068155	Insig1	ENSMUSG00000045294
3.903311	0.001194	Dnah12	ENSMUSG00000021879	-0.61444	0.070733		ENSMUSG00000045999
1.169473	0.001524	Rin3	ENSMUSG00000044456	1.704424	0.071129	Bpifc	ENSMUSG00000050108
1.169244	0.001741	F13a1	ENSMUSG00000039109	0.701972	0.071129	Pdxk	ENSMUSG00000032788
-0.949	0.002022	Chst11	ENSMUSG00000034612	0.994597	0.071577	Trim29	ENSMUSG00000032013
-0.9961	0.002166	Casp7	ENSMUSG00000025076	-0.8871	0.076468	Mmp13	ENSMUSG00000050578

3.931076	0.002435	Bach2os	ENSMUSG00000086150	0.991755	0.078103	Wipi1	ENSMUSG00000041895
0.885144	0.002435	Lox	ENSMUSG00000024529	1.00311	0.079388	Serinc5	ENSMUSG00000021703
-1.66375	0.002486	Rhoh	ENSMUSG00000029204	-1.25174	0.079543	Il1f9	ENSMUSG00000044103
-1.24964	0.002515		ENSMUSG00000092773	-0.67556	0.080434	Nfkb1	ENSMUSG00000028163
-1.08726	0.002887	Socs1	ENSMUSG00000038037	0.942972	0.080838	Syt11	ENSMUSG00000068923
1.302178	0.003251	Paqr7	ENSMUSG00000037348	1.324205	0.080838	Klra2	ENSMUSG00000030187
-0.90079	0.003254	Mmp12	ENSMUSG00000049723	-0.71767	0.082101	Tmem2	ENSMUSG00000024754
-1.06355	0.003509	Csf3	ENSMUSG00000038067	0.734669	0.082101	Ergic1	ENSMUSG00000001576
-2.35111	0.003653	Il11	ENSMUSG00000004371	-0.80694	0.08253	Wfs1	ENSMUSG00000039474
-0.84287	0.003941	Rsad2	ENSMUSG00000020641	-0.68387	0.082531	Isg15	ENSMUSG00000035692
-1.12922	0.004208	Timp3	ENSMUSG00000020044	-0.67778	0.083148	Cxcl3	ENSMUSG00000029379
-2.03218	0.004208	Dcstamp	ENSMUSG00000022303	-0.90013	0.086117	Fst	ENSMUSG00000021765
1.386263	0.00424	Mgll	ENSMUSG00000033174	1.157447	0.087469	Apoc2	ENSMUSG00000002992
-0.89309	0.004485	Dab2	ENSMUSG00000022150	0.80021	0.090822	Cyth3	ENSMUSG00000018001
1.14163	0.005073	Mafb	ENSMUSG00000028874	1.07939	0.090822	Col18a1	ENSMUSG00000001435
0.940402	0.005073	Fgr	ENSMUSG00000074622	-1.25793	0.091248	Osmr	ENSMUSG00000022146
-0.81843	0.006355	Cxcl2	ENSMUSG00000058427	-1.42935	0.091568	Alpk2	ENSMUSG00000032845
-1.24059	0.006465	Ptgs2os2	ENSMUSG00000097754	-0.72425	0.09327	Axl	ENSMUSG00000002602
				0.815505	0.095702	Aldh9a1	ENSMUSG00000026687
				0.925759	0.095702	Cav1	ENSMUSG00000007655
				3.350338	0.099786	Glyctk	ENSMUSG00000020258

Table A3.2. Top scoring KEGG pathways enriched for differential expressed genes ($q < 0.1$).

Term	Count	% genes in pathway	Fold Enrichment	Benjamini	FDR
mmu05134:Legionellosis	12	6.185567	15.33267	3.36E-08	2.33E-07
mmu05133:Pertussis	11	5.670103	10.82611	4.33E-06	6.01E-05
mmu05132:Salmonella infection	11	5.670103	10.27092	4.83E-06	1.01E-04
mmu05140:Leishmaniasis	10	5.154639	11.37972	7.38E-06	2.05E-04

mmu05323:Rheumatoid arthritis	10	5.154639	8.88173	5.13E-05	0.001779
mmu04668:TNF signaling pathway	11	5.670103	7.349836	5.77E-05	0.002402
mmu04620:Toll-like receptor signaling pathway	10	5.154639	7.21091	2.11E-04	0.010234
mmu05142:Chagas disease (American trypanosomiasis)	10	5.154639	7.070892	2.17E-04	0.012025
mmu04640:Hematopoietic cell lineage	9	4.639175	7.803235	3.27E-04	0.020396
mmu04060:Cytokine-cytokine receptor interaction	14	7.216495	4.161725	4.43E-04	0.030737
mmu05164:Influenza A	11	5.670103	4.684983	0.001651	0.126043
mmu05321:Inflammatory bowel disease (IBD)	7	3.608247	8.64087	0.00203	0.169085
mmu04630:Jak-STAT signaling pathway	10	5.154639	5.022772	0.002005	0.180893
mmu05146:Amoebiasis	9	4.639175	5.602322	0.002267	0.220249
mmu04062:Chemokine signaling pathway	11	5.670103	4.087409	0.003697	0.384834
mmu05144:Malaria	6	3.092784	9.103774	0.005023	0.557603
mmu05162:Measles	9	4.639175	4.819645	0.005203	0.613481
mmu05152:Tuberculosis	10	5.154639	4.138079	0.006105	0.761997
mmu05145:Toxoplasmosis	8	4.123711	5.15612	0.007753	1.021024
mmu05143:African trypanosomiasis	5	2.57732	10.40431	0.010775	1.492265
mmu04940:Type I diabetes mellitus	6	3.092784	7.048083	0.012405	1.802632
mmu05168:Herpes simplex infection	10	5.154639	3.501451	0.016134	2.452592
mmu05332:Graft-versus-host disease	5	2.57732	7.002903	0.040085	6.321057
mmu05205:Proteoglycans in cancer	9	4.639175	3.228925	0.045359	7.439826
mmu04621:NOD-like receptor signaling pathway	5	2.57732	6.502695	0.047851	8.154999
mmu04380:Osteoclast differentiation	7	3.608247	4.046122	0.048295	8.543908
mmu04010:MAPK signaling pathway	10	5.154639	2.878664	0.047148	8.651597
mmu04064:NF-kappa B signaling pathway	6	3.092784	4.50496	0.062425	11.772
mmu04622:RIG-I-like receptor signaling pathway	5	2.57732	5.355161	0.079744	15.40049
mmu00910:Nitrogen metabolism	3	1.546392	12.85239	0.122031	23.7337
mmu05330:Allograft rejection	4	2.061856	5.202156	0.209372	39.67281
mmu00340:Histidine metabolism	3	1.546392	9.103774	0.209628	40.6909
mmu04923:Regulation of lipolysis in adipocytes	4	2.061856	5.11089	0.206209	41.0717

mmu04915:Estrogen signaling pathway	5	2.57732	3.715826	0.209529	42.5792
mmu04623:Cytosolic DNA-sensing pathway	4	2.061856	4.551887	0.253222	50.79551
mmu04932:Non-alcoholic fatty liver disease (NAFLD)	6	3.092784	2.783319	0.271611	54.69423
mmu05020:Prion diseases	3	1.546392	6.82783	0.29259	58.88365
mmu04917:Prolactin signaling pathway	4	2.061856	3.990695	0.310953	62.54923
mmu05410:Hypertrophic cardiomyopathy (HCM)	4	2.061856	3.687604	0.355616	69.55837
mmu03320:PPAR signaling pathway	4	2.061856	3.641509	0.357001	70.64847

Table A3.3. KEGG pathways and GO biological process with associated genes that are significantly downregulated in LPS-stimulated murine macrophages preincubated with 10(*Z*)-hexadecenoic acid.

NF-κB (KEGG PATHWAY: mmu04064)	**Jak-STAT (KEGG PATHWAY: mmu04630)**	**Inflammatory response (GO:0006954)**	
chemokine (C-C motif) ligand 4 (Ccl4)	colony stimulating factor 2 (granulocyte-macrophage)(Csf2)	AXL receptor tyrosine kinase (Axl)	chemokine (C-X-C motif) ligand 3 (Cxcl3)
interleukin 1 beta (Il1b)	colony stimulating factor 3 (granulocyte) (Csf3)	C-type lectin domain family 7, member a (Clec7a)	cytochrome P450, family 26, subfamily b, polypeptide 1 (Cyp26b1)
nuclear factor of kappa light polypeptide gene enhancer in B cells 1, p105 (Nfkb1)	cytokine inducible SH2-containing protein (Cish)	chemokine (C-C motif) ligand 17 (Ccl17)	interleukin 1 alpha (Il1a)
nuclear factor of kappa light polypeptide gene enhancer in B cells 2, p49/p100 (Nfkb2)	interleukin 11 (Il11)	chemokine (C-C motif) ligand 2 (Ccl2)	interleukin 1 beta (Il1b)
prostaglandin-endoperoxide synthase 2 (Ptgs2)	interleukin 12a (Il12a)	chemokine (C-C motif) ligand 22 (Ccl22)	interleukin 1 family, member 9 (Il1f9)
tumor necrosis factor (Tnf)	interleukin 12b (Il12b)	chemokine (C-C motif) ligand 3 (Ccl3)	interleukin 6 (Il6)
	interleukin 6 (Il6)	chemokine (C-C motif) ligand 4 (Ccl4)	nitric oxide synthase 2, inducible (Nos2)
	oncostatin M receptor (Osmr)	chemokine (C-C motif) ligand 6 (Ccl6)	nuclear factor of kappa light polypeptide gene enhancer in B cells 2, p49/p100 (Nfkb2)
	proviral integration site 1 (Pim1)	chemokine (C-C motif) ligand 7 (Ccl7)	oxidized low density lipoprotein (lectin-like) receptor 1 (Olr1)

	suppressor of cytokine signaling 1(Socs1)	chemokine (C-X-C motif) ligand 2(Cxcl2)	prostaglandin-endoperoxide synthase 2 (Ptgs2)
			tumor necrosis factor (Tnf)